ARTU ÜLIKOOLI
TOIMETISED
CTA ET COMMENTATIONES UNIVERSITATIS TARTUENSIS

973

NON-ELASTIC STRUCTURES

MITTEELASTSED KONSTRUKTSIOONID

Mehaanika-alaseid töid

TARTU 1994

TARTU ÜLIKOOLI TOIMETISED
ACTA ET COMMENTATIONES UNIVERSITATIS TARTUENSIS
ALUSTATUD 1893. a. VIHIK 973

NON-ELASTIC STRUCTURES

MITTEELASTSED KONSTRUKTSIOONID

Mehaanika-alaseid töid

TARTU 1994

Tartu Ülikooli Kirjastuse trükikoda
Tiigi 78, EE2400 Tartu
Tellimus nr. 417.

On the higher modal dynamic response of elastic-plastic beams

ÜLO LEPIK

Tartu University

Abstract The problem of higher modal response of rigid-plastic beams was treated in [2-4]. In this paper a solution for elastic-plastic beams is proposed. This solution depends only on one parameter γ; it is shown that by increasing this parameter the solution continuously transfers to that which is predicted by the rigid-plastic model. The problem of using higher modes in the energy absorbing devices is discussed.

1 Introduction

The problem of dynamic response of rigid-plastic beams has been treated in many papers. Essential simplifications for solving this problem were made possible by the method of mode form solutions, which was proposed by Martin and Symonds [1] in 1966. Among the publications in 1976-78 were published the papers by Jones and Wierzbicki [2] and by Jones and Soares [3] who studied higher mode responses produced by an initial velocity distribution. The idea of these papers is that in the case of higher modes we have more plastic hinges and the kinetic energy absorbed in these hinges should be greater as in the case of the fundamental mode. So excitation of higher modal deformations could find practical application in the development of energy absorbing devices.

In a paper by Lepik [4] it was shown that in the case of rigid-plastic material the second mode is unstable in the sense that slight deviations in the initial velosity distribution induce a motion which steadiely goes over to the fundamental mode. This circumstance might complicate the application

of higher modes in the energy-absorbing devices. Hereby it should be noted that in papers [2-3] a beam with clamped ends was considered, but in [4] calculations for a beam with simply supported ends were carried out.

The main purpose of this paper is to investigate the response of elastic-plastic beams in the case where higher modal motions are excited. Both undisturbed and perturbed motions are discussed.

2 Basic equations and method of solution

We shall consider a simply supported beam, which at the initial instant attains a transverse velocity; the subsequent motion is due to inertia. For simplicity we shall confine ourselves to the case where the cross-section of the beam is of rectangular form and has a constant area. The equation of motion is

$$\frac{\partial^2 M_*}{\partial x_*^2} = \rho B h \frac{\partial^2 w_*}{\partial t_*^2}. \tag{1}$$

Here w, ρ, B, h stand correspondingly for the deflection, density, beam width and height; M_* is the bending moment, t_* - time. The beam coordinate is x_*, the origin of this axis is taken in the left support of the beam. In order to reduce the number of beam and material parameters to a minimum, we shall go over to the following nondimensional quantities:

$$w = \frac{w_*}{\beta v_0^*}, \qquad t = \frac{t_*}{\beta}, \qquad (\beta = \frac{L^2}{h}\sqrt{\frac{\rho}{E}}) \tag{2}$$

$$x = \frac{x_*}{L}, \qquad M = \frac{4M_*}{\sigma_s B h^2}.$$

In these formula σ_s is the yield stress, E - Young's modulus, v_0^* is the initial velocity in a characteristic section of the beam $x = x_0$.

The equation of motion obtains now the form

$$M'' = \gamma \ddot{w}, \tag{3}$$

where

$$\gamma = 4\frac{v_0^*}{\sigma_s}\sqrt{\rho E}. \tag{4}$$

Henceforth dots and primes denote differentiation with respect to the variables t and x.

The initial velocity has in nondimensional quantities (2) the form

$$\frac{\partial w_*}{\partial t_*}|_{t=0} = v_0^* \dot{w}|_{t=0},$$

from which follows

$$\dot{w}(x_0, 0) = 1. \tag{5}$$

Boundary conditions are

$$w(0,t) = w(2,t) = M(0,t) = M(2,t) = 0. \tag{6}$$

Let us denote by e and σ_* deformation and stress in some point of the beam. According to the hyphoteses of Kirchoff we have

$$e = -z_* \frac{\partial^2 w_*}{\partial x_*^2}.$$

Passing to the nondimensional quantities (2), we obtain

$$\frac{E}{\sigma_s} e = -\frac{\gamma}{8} z w'' \qquad (z = \frac{2}{h} z_*). \tag{7}$$

Nondimensional bending moment M can be calculated from the formula

$$M = 2 \int_0^1 \sigma z dz \qquad (\sigma = \frac{\sigma_*}{\sigma_s}). \tag{8}$$

We shall confine us to elastic-plastic material without strain-hardening. We have three possibilities for evaluating the nondimensional stresses σ.

(i) Deformation is elastic and

$$\sigma = -(1/8)\gamma z w''. \tag{9}$$

(ii) Plastic deformation for which $\sigma = \pm 1$.

(iii) Elastic unloading (e_m and σ_m are the deformation and stress from which the unloading begins):

$$\sigma - \sigma_m = \frac{E}{\sigma_s}(e - e_m).$$

On account of (7) the latter equation can be put into the form

$$\sigma - \sigma_m = -(1/8)\gamma z(w'' - w''_m). \tag{10}$$

The method of solution is as follows. We shall assume, that all quantities are known at the instants $t - \Delta t, t$. The solution for the next instant $t + \Delta t$ we shall find according to the following scheme:

Step 1: We shall calculate the quantities $\dot{w}$ and w from the formulae of central differencies

$$\begin{aligned} \dot{w}(x, t + \Delta t) &= 2\ddot{w}(x, t)\Delta t + \dot{w}(x, t - \Delta t), \\ w(x, t + \Delta t) &= \ddot{w}(x, t)\Delta t^2 + 2w(x, t) - w(x, t - \Delta t). \end{aligned} \tag{11}$$

Step 2: By numerical differentiation we shall find $w''(x, t+\Delta t)$ and calculate the nondimensional stress $\sigma(x, z, t + \Delta t)$ from formulae (9)-(10).

Step 3: By evaluating numerically the integral (8) we find the bending moment $M(x, t + \Delta t)$.

Step 4: Next we shall evaluate $M''(x, t + \Delta t)$.

Step 5: Equation (3) gives us nondimensional acceleration $\ddot{w}(x, t + \Delta t)$.

Step 6: We shall increase the time t by Δt and return to Step 1.

For starting this procedure we must know the initial values at the instants $t = 0$ and $t = \Delta t$. Here we shall assume that time increment Δt is so small that the beam's response for $t \leq \Delta t$ is purely elastic and shall use the solution, presented in the next Section.

In the computations the beam was segmented into 20 parts: followingly $\Delta x = 0.1$. For calculating the derivatives w'' and M'' five grid points have been taken; outside the interval $x \in [0, 2]$ the quantities w, M were continued to odd functions. Time increment Δt was determined from numerical tests; in the following it was taken $\Delta t = 0.001$. The integral (8) was evaluated by eight-point Gaussian quadrature.

The proposed method of solution is less computer time consuming than the ordinary FEM methods. It should be emphasized that the results depend only upon a single beam and material parameter γ. The values of this parameter as a function of the initial velocity v_0^* for some materials are (the material properties have been taken from Table 1 of the paper [5]):

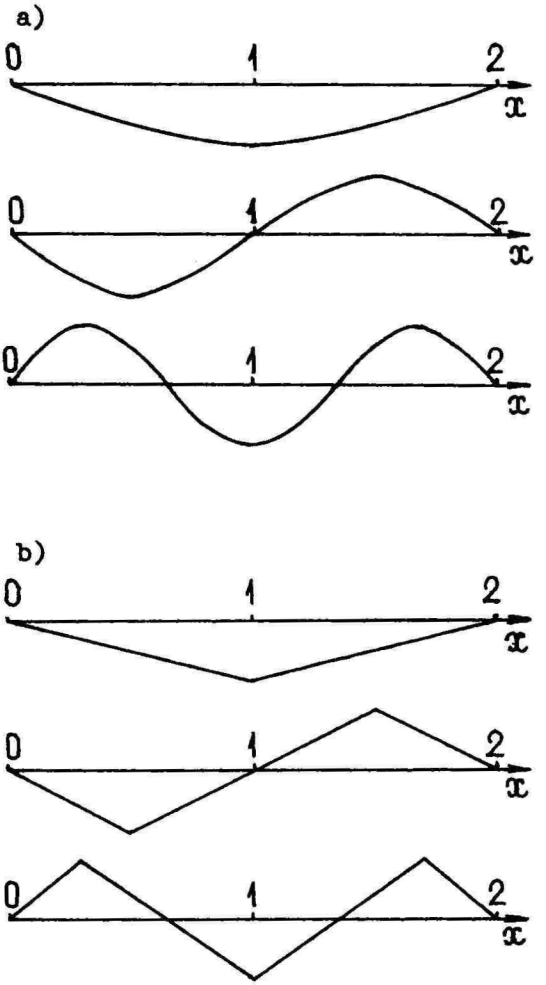

Figure 1: Three first modal forms a) for an elastic beam, b) for a rigid-plastic beam

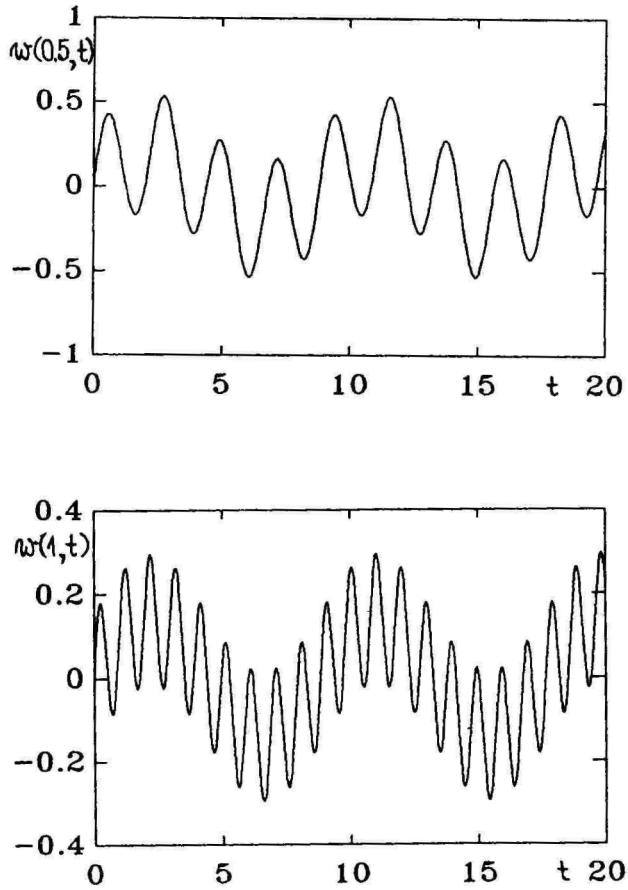

Figure 2: Deflection histories for the elastic beam in the cases where second or third mode was excited

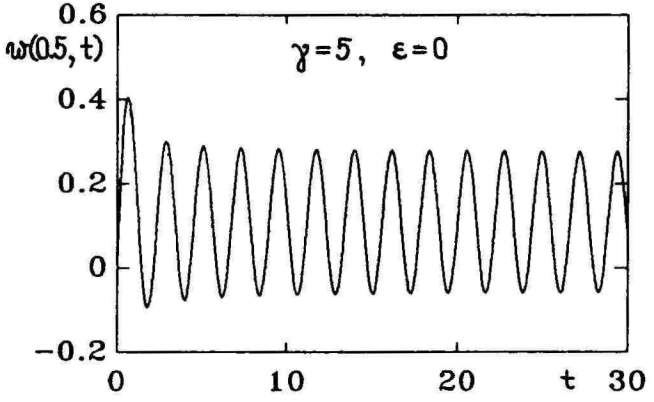
0.6
w(0.5, t)
γ=5, ε=0
0.4
0.2
0
−0.2
0
10
20
t
30

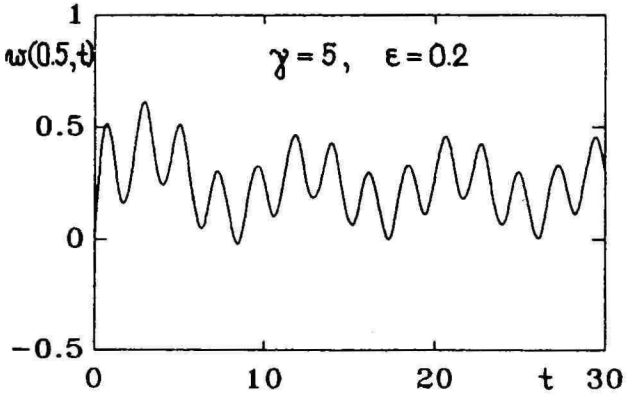
1
w(0.5,t)
γ=5, ε=0.2
0.5
0
−0.5
0
10
20
t
30

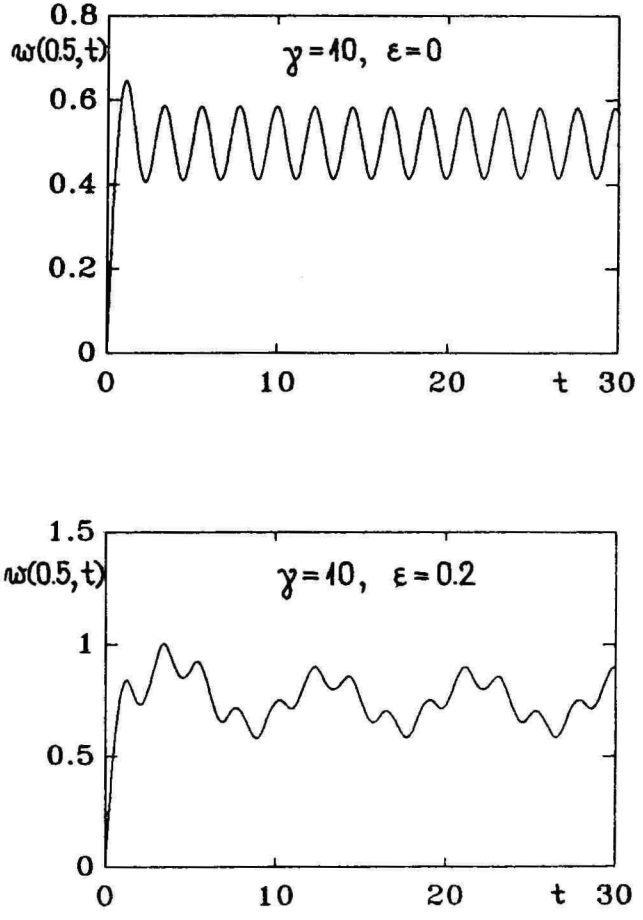

Figure 3: Deflection histories for elastic-plastic beams; second mode is induced

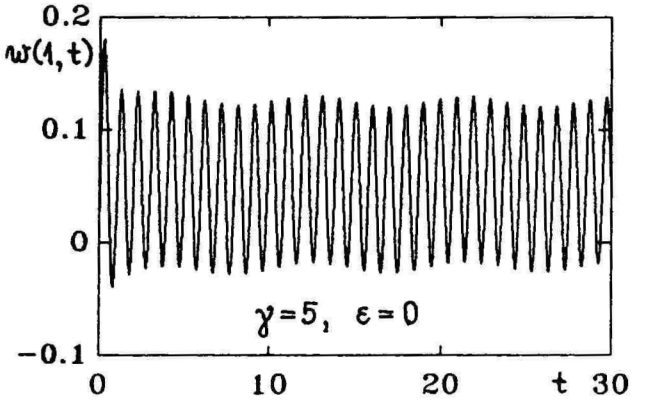
0.2
w(1, t)
0.1
0
−0.1
γ=5, ε=0
0
10
20
t 30

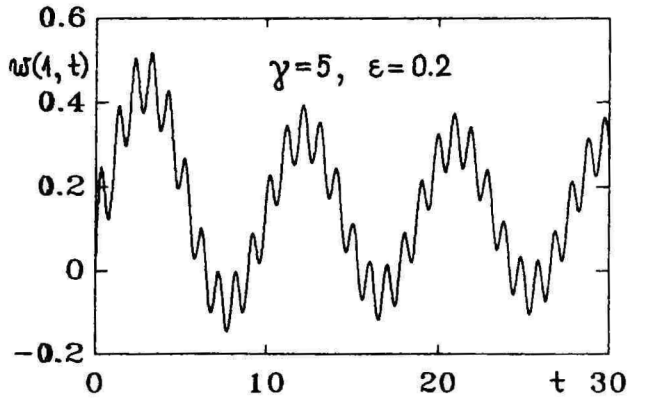
0.6
w(1, t)
γ=5, ε=0.2
0.4
0.2
0
−0.2
0
10
20
t 30

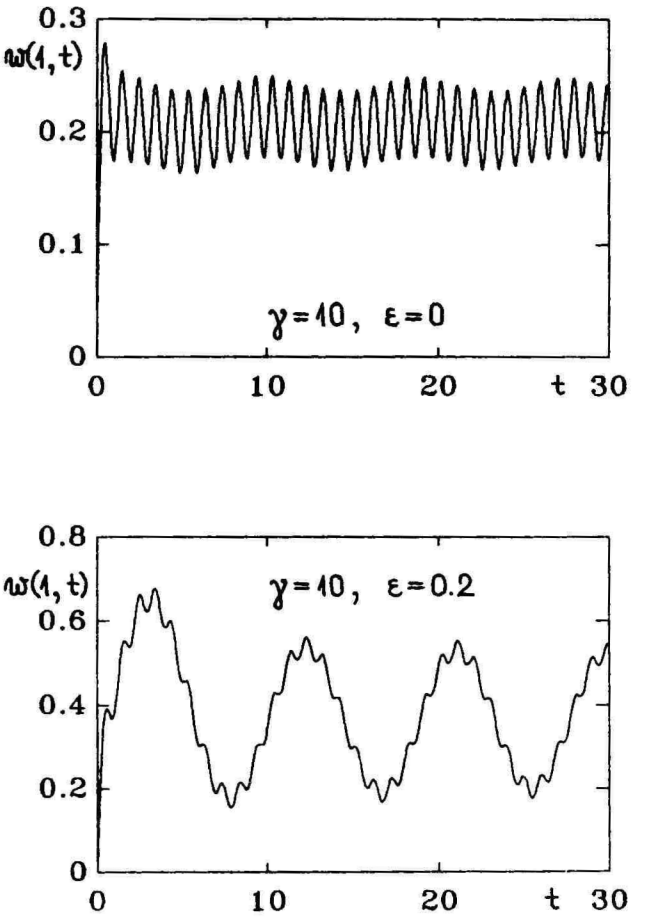

Figure 4: Deflection histories for elastic-plastic beams; third mode is induced

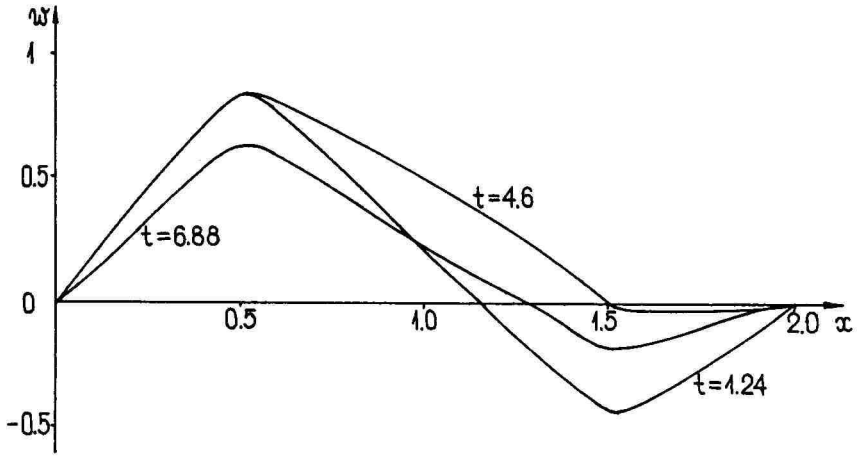

Figure 5: Deflection curves versus beam length for $\gamma = 10$, $\varepsilon = 0.2$; second mode is induced

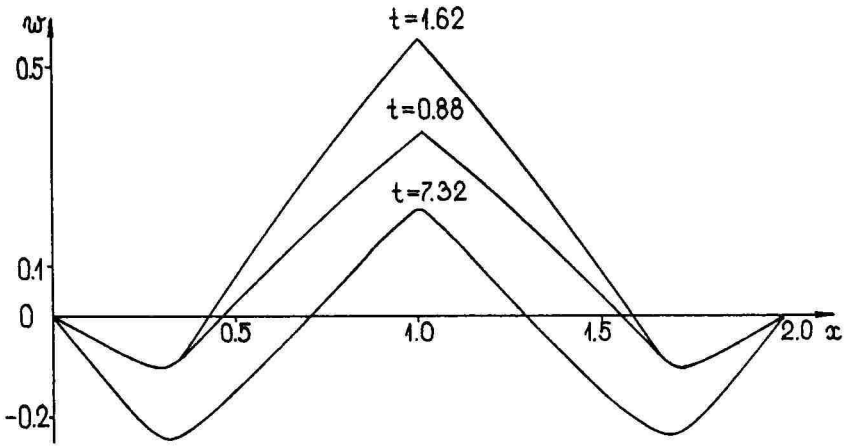

Figure 6: Deflection curves versus beam length for $\gamma = 10$, $\varepsilon = 0.2$; third mode is induced

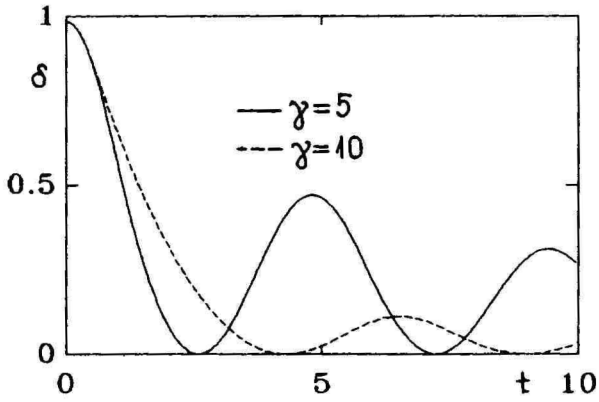
1
δ
0.5
0
γ=5
γ=10
0
5
t
10

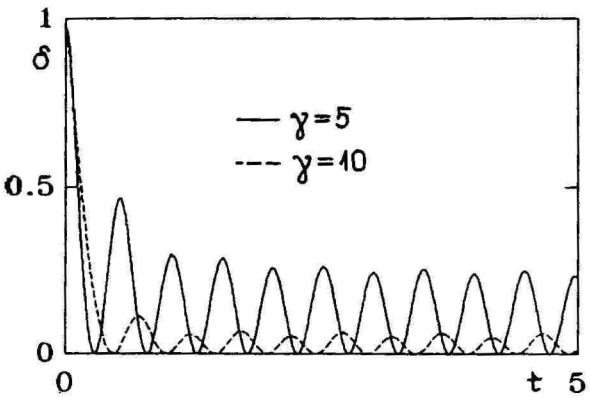
1
δ
0.5
0
γ=5
γ=10
0
t
5

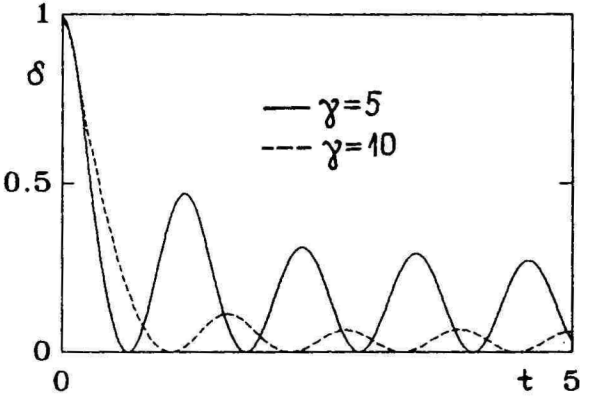

Figure 7: Ratio of the kinetic energy of the beam to the initial kinetic energy versus time of motion

(i) Mild steel 0.23% C	$\gamma = 0.765 v_0^*$;
(ii) Titanium Al-4V	$\gamma = 0.099 v_0^*$;
(iii) Aluminium 7075-T6	$\gamma = 0.099 v_0^*$;
(iv) Aluminium 6061-T651	$\gamma = 0.190 v_0^*$.

3 The elastic solution

First we shall assume that the response of the beam is wholly elastic. It follows from (8)-(9) that

$$M = -(\gamma/12)w''$$

and the equation of motion (3) obtains the form

$$w^{IV} = -12\ddot{w}. \tag{12}$$

This equation can be solved by the method of separation of variables; the solution has the form

$$w = \sum_{k=1}^{\infty} a_k \, sin\mu_k \, t \, sink\frac{\pi}{2}x, \tag{13}$$

where

$$\mu_k = \frac{k^2\pi^2}{8\sqrt{3}}. \tag{14}$$

The coefficients a_k we shall determine from the prescribed initial velocity field which we shall take in the form

$$v(x) = A \, sin\pi x + B \, sin\frac{3}{2}\pi x + \varepsilon \, sin\frac{\pi}{2}x. \tag{15}$$

The meaning of this equation is as follows. If $A = 1, B = \varepsilon = 0$ the second mode of motion is induced; similarly the case $B = 1, A = \varepsilon = 0$ brings us to the third mode (Fig.1a). The last term of equation (15) characterizes perturbation in the form of the first mode (ε is a prescribed parameter). For comparison in Fig. 1b also the first three modes for the rigid-plastic beam are presented.

Further on we shall examine two cases:

(i) Initial velocity corresponds to the second mode (with perturbation). Here it follows from equations (13) and (15) that

$$a_1 = \frac{\varepsilon}{\mu_1}, \qquad a_2 = \frac{1}{\mu_2}, \qquad a_3 = 0. \tag{16}$$

(ii) If the initial velocity is induced according to the third mode, we have

$$a_1 = \frac{\varepsilon}{\mu_1}, \qquad a_2 = 0, \qquad a_3 = \frac{1}{\mu_3}. \tag{17}$$

It follows from these results that if $\varepsilon = 0$ (undisturbed motion) the second (or third) mode maintain their form during the whole motion. If $\varepsilon \neq 0$, then taking into account the fact that $\mu_2 = 4\mu_1$ and $\mu_3 = 9\mu_1$, we can state that the effect of perturbation is in case of the third mode is more significant than for the second mode. All in all we have here the sum of two harmonic vibrations and no transition to the fundamental mode, as it was shown in [4] for rigid-plastic beams, does not take place. This is demonstrated also in Fig. 2 where deflection histories for the cases, where second and third mode have been excited are shown; the perturbation parameter ε has the value $\varepsilon = 0.2$.

4 Elastic-plastic case

In the case of elastic-plastic deformations calculations were carried out for two values of the parameter $\gamma = 5$ and $\gamma = 10$. Both undisturbed motion ($\varepsilon = 0$) and disturbed motion with $\varepsilon = 0.2$ were considered. Deflection history diagrams are presented in Figs. 3-4; in the case of Fig. 3 the second mode of initial motion was induced, for Fig. 4 - the third mode. It follows from these calculations that plastic deformations occur only in the beginning of the motion, after that elastic vibrations take place. By increasing the parameter γ the amplitude of the elastic vibrations decreases and for sufficiently high values of γ turns to zero (this case corresponds to the model of a rigid-plastic material). As to the disturbed motion $\varepsilon \neq 0$ the long-term motion maintains its periodical character, but now the vibrations have a morre complicated form as for the undisturbed motion $\varepsilon = 0$.

Deflection curves versus beam coordinate x for the parameters $\gamma = 10$ and $\varepsilon = 0.2$ are demonstrated in Figs. 5-6. These curves are calculated for three characteristic instants (these instants were chosen so that the velocity in the section $x = 0.5$ or correspondingly in $x = 1$ was zero). From these Figs. a tendency of the disturbed motion to go over to the fundamental mode catches attention; by increasing the parameter γ this tendency becomes stronger, which is in accordance with the results of the paper [4]. It also follows from Figs. 5-6 that the vertexes of these curves are more sharp-edged than in the case of elastic solutions; this circumstance indicates also the transition from elastic modes to rigid-plastic modes (compare Fig. 1a and 1b). So we can state that by increasing the parameter γ the beam's response continuously transfers to that which was predicted by the rigid-plastic model and for sufficiently high values of γ the application of such a material is wholly justified.

Now let us say a few words about using higher modes in the energy-absorbing devices. First we can estimate energy absorbation by calculating the peak deflection w_{max} (i.e. maximal deflection at the instant where the deflection rate at some characteristic section for the first time turns zero). These values for undisturbed motion $\varepsilon = 0$ are presented in Table 1. It follows from this table, that the values w_{max} for the second and third mode from motion are significantly smaller than in the case of the first mode being induced. This is in complete accordance with the results of the paper [2].

In the case of elastic-plastic beams another quantity for estimating the

Table 1:

	v_{max}		σ_1		σ_4	
	$\gamma = 5$	$\gamma = 10$	$\gamma = 5$	$\gamma = 10$	$\gamma = 5$	$\gamma = 10$
First mode	1.61	2.60	0.469	0.277	0.110	0.060
Second mode	0.40	0.64	0.470	0.277	0.109	0.064
Third mode	0.18	0.28	0.448	0.272	0.108	0.060

amount of absorbed energy is important - it is the maximal kinetic energy in the long-term motion. Let us denote by σ the ratio of the kinetic energy of the beam to the initial kinetic energy. This quantity versus time for $\varepsilon = 0$ is presented in Fig. 7 for the cases where a first, second or third form motion was induced; the solid and dotted lines correspond to the cases $\gamma = 5$ and $\gamma = 10$, respectively. The first and fourth maxima of $\sigma(t)$ are presented also in the Table 1. It follows from the Fig. 7 and from this table that the maxima of δ practically do not depend upon the number of the mode. So if we have in view the amount of the kinetic energy in the long-term motion then the use of higher modes as energy-absorbers does not give any effect.

Acknowledgement

The author wishes to express his appreciation to Professor Norman Jones for reading the manuscript and for his valuable comments.

References

[1] Martin, J.B and Symonds,P.S, Mode approximations for impulsively loaded rigid-plastic structures. *J. Eng. Mech. Div., Proc. ASCE*, 1966, 92, 43-66.

[2] Jones, N. and Wierzbicki, T., A study of the higher modal dynamic plastic response of beams. *Int. J. Mech. Sci.*, 1976, 18, 525-596.

[3] Jones, N. and Soares, C. G., Higher modal dynamic plastic behavior of beams loaded impulsively. *Int. J. Mech. Sci.*, 1978, 20, 135-147.

[4] Lepik, Ü, On the dynamic response of rigid-plastic beams. *J. Struct. Mech.*, 1980, 8(3), 227-235.

[5] Symonds, P. S., Finite elastic and plastic deformations of pulse loaded structures by an extended mode technique. *Int. J. Mech. Sci.*, 1980, 22, 597-605.

Высшие моды в динамике упруго-пластических балок

Юло Лепик

Резюме

Проблема высших мод в динамике жестко-пластических балок была исследована в [2–4]. В данной работе предлагается решение этой задачи для упруго-пластических балок. Это решение зависит лишь от одного параметра γ. Показано, что с увеличением параметра γ решение упруго-пластической задачи непрерывно переходит в решение для жестко-пластической балки. Обсуждается возможность применения высших мод как поглотитель энергии.

Optimal design of rigid-plastic conical shells of piece-wise constant thickness

JAAN LELLEP and ELLA PUMAN

Tartu University

Abstract Conical shells loaded by the rigid central boss are considered. The minimum weight designs of the shells of piece-wise constant thickness are established under the condition that the load carrying capacities of the optimized shell and of the reference shell of constant thickness, respectively, coincide. The material of the shells is assumed to be an ideal rigid-plastic one obeying the Tresca yield condition and associated flow law. Simple approximations of the exact yield surface are used.

1 Introduction

The problems of load carrying capacity of conical shells subjected to the distributed or concentrated loads have been investigated by Hodge [1], Jones and Ich [2], Kuech and Lee [3], Lance and Lee [4], Onat [7], Onat and Lance [8] and others.

However, very little attention has been paid to the optimal design of rigid-plastic conical shells. Previous studies related to the optimization of plastic plates and shallow spherical shells [5,6] show that more than 10% of the material might be saved by the use of the shell of piece-wise constant thickness.

In the present paper an optimal design technique is suggested for rigid-plastic conical shells loaded by the central rigid boss. It is assumed preliminarily that the thickness of the shell is piece-wise constant.

2 Formulation of the problem

Let us consider a conical shell loaded by the central boss (Fig. 1). The central boss is absolutely rigid; it is loaded by the vertical load P.

It is assumed that the shell wall is of piece-wise constant thickness. We are looking for the design of the shell for which the load carrying capacity is given but the material volume (weight) of the shell attains the minimal value.

Let the thickness be

$$h = \begin{cases} h_0, & a \le r \le b, \\ h_1, & b \le r \le R, \end{cases} \tag{1}$$

where h_0, h_1, b are previously unknown parameters. Thus, the material volume of the shell wall can be expressed as

$$V = \frac{\pi}{\cos\varphi}\Big(h_0(b^2 - a^2) + h_1(R^2 - b^2)\Big). \tag{2}$$

When minimizing (2), one has to take into account the basic equations of the theory of plastic axisymmetric shells.

3 Basic equations and assumptions

The equilibrium equations for a shell element have the form

$$\begin{aligned} \frac{d}{dr}\big(rN_1\big) - N_2 &= 0, \\ \frac{d}{dr}\big(rM_1\big) - M_2 &- rN_1\frac{\sin\varphi}{\cos^2\varphi} + \frac{P}{2\pi\cos^2\varphi} = 0, \end{aligned} \tag{3}$$

where φ is the angle of inclination of the generator of the shell. Here N_1, N_2 stand for the membrane forces and M_1, M_2 for the bending moments, respectively, whilst r is the current radius.

The strain rate components corresponding to the theory with small strains and displacements can be presented as

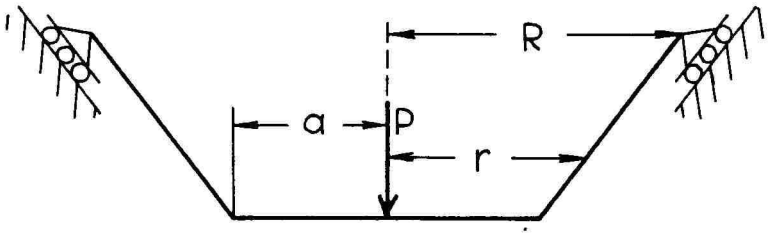

Figure 1: Shell geometry

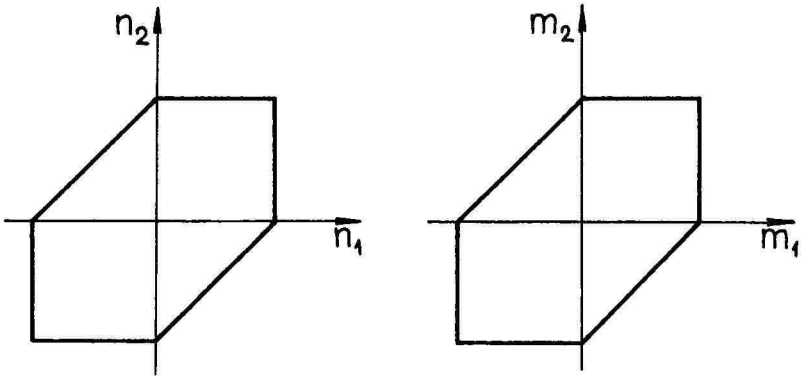

Figure 2: Two moment limited interaction yield surface

$$\dot{\varepsilon}_1 = \frac{d\dot{U}}{dr}\cos\varphi, \qquad \dot{\kappa}_1 = -\frac{M_0}{N_0}\cos^2\varphi\frac{d^2\dot{W}}{dr^2},$$
$$\dot{\varepsilon}_2 = \frac{1}{r}(\dot{U}\cos\varphi + \dot{W}\sin\varphi), \qquad \dot{\kappa}_2 = -\frac{M_0}{N_0}\frac{1}{r}\cos^2\varphi\frac{d\dot{W}}{dr}, \tag{4}$$

where $\dot{W}$ and $\dot{U}$ stand for the displacement rates in the normal and tangential directions, respectively. The quantities M_0 and N_0 denote the limit moment and limit force. Evidently , $M_0 = \sigma_0 h^2/4$, $N_0 = \sigma_0 h$, where σ_0 is the yield stress.

Assume that the material of the shell is ideally rigid-plastic and obeys the Tresca's yield condition. The two-moment limited interaction yield surface suggested by Hodge [1] will be used in the present study. This yield surface is presented by the hexagons on the planes of membrane forces and moments, respectively (Fig. 2). The hexagons will be approximated with the squares (Fig. 3) and diamonds (Fig. 4). It was shown by Jones and Ich [2] that the generalized square and diamond yield conditions lead to the predictions of the load carrying capacity which are quite close to those obtained by the use of the hexagons of Tresca.

It will be convenient to use the following non-dimensional quantities:

$$\sigma = \frac{r}{R}, \quad \alpha = \frac{a}{R}, \quad \beta = \frac{b}{R}, \quad \delta = \frac{h_0}{h_*}, \quad v = \frac{h}{h_*},$$
$$\gamma = \frac{h_1}{h_*}, \quad w = \frac{W}{R}, \quad u = \frac{U}{R}, \quad n_{1,2} = \frac{N_{1,2}}{N_*}, \tag{5}$$
$$m_{1,2} = \frac{M_{1,2}}{M_*}, \quad k = \frac{M_*\cos^2\varphi}{RN_*\sin\varphi}, \quad q = \frac{P}{2\pi RN_*\sin\varphi} - \frac{M_*\cos^2\varphi}{RN_*\sin\varphi},$$

where h_* is the thickness of the reference shell of constant thickness and $M_* = \sigma_0 h_*^2/4$, $N_* = \sigma_0 h_*$.

Making use of (5) the equilibrium equations (3) could be presented as

$$(\varrho n_1)' - n_2 = 0,$$
$$k[(\varrho m_1)' - m_2 + 1] - \varrho n_1 + q = 0, \tag{6}$$

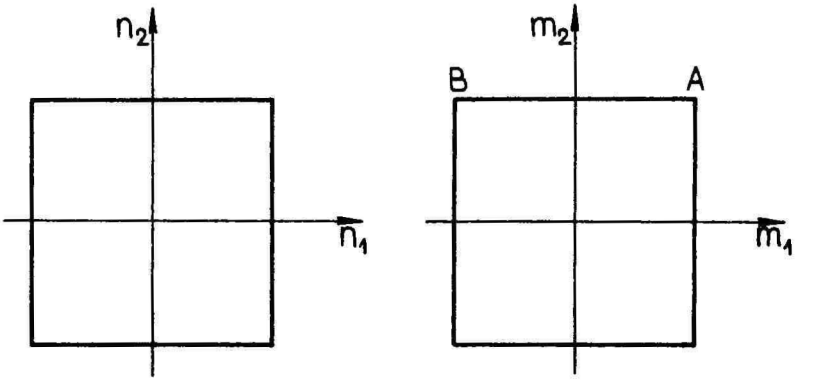

Figure 3: Generalized square yield condition

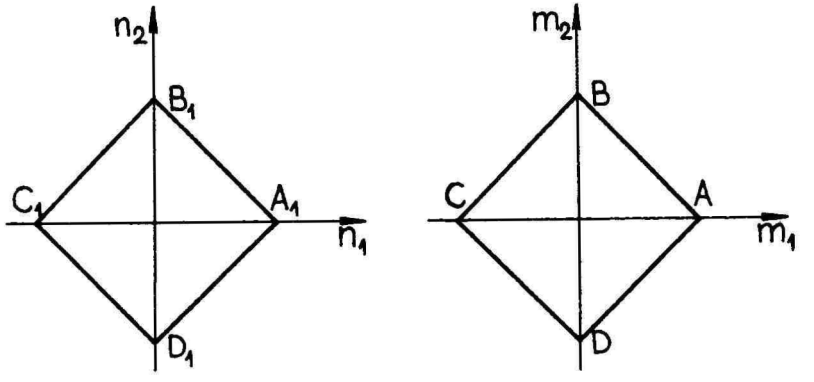

Figure 4: Generalized diamond yield condition

4

where the primes denote the differentiation with respect to ϱ.

The strain rate components (4) take the form

$$\begin{aligned} \dot{\varepsilon}_1 &= \dot{u}' \cos\varphi, & \dot{\kappa}_1 &= -k\dot{w}'' \sin\varphi, \\ \dot{\varepsilon}_2 &= \frac{1}{\varrho}(\dot{u}\cos\varphi + \dot{w}\sin\varphi), & \dot{\kappa}_2 &= -\frac{k}{\varrho}\dot{w}' \sin\varphi. \end{aligned} \tag{7}$$

The statical boundary conditions for the considered shell turn to be

$$m_1(\alpha) = \delta^2, \qquad m_1(1) = 0 \tag{8}$$

for a simply supported shell and

$$m_1(\alpha) = \delta^2, \qquad m_1(1) = -\gamma^2 \tag{9}$$

for a clamped shell.

Two cases of the simply supported edge will be distinguished. In the first case we have a simply supported sliding edge, so that

$$n_1(1) = 0, \tag{10}$$

In the second case the edge is pinned, e.g. $n_1(1) \neq 0$ and

$$\dot{u}(1) = 0. \tag{11}$$

However, (11) will not be considered in this paper. In both cases

$$\dot{w}(1) = 0, \qquad \dot{u}(\alpha) = 0. \tag{12}$$

4 Load carrying capacity of the shell of constant thickness

Let us consider the reference shell of constant thickness (Fig. 1). Thus, $h = h_*$, e.g., $v \equiv 1$, $\gamma = \delta = 1$. It appeared that the exact load carrying capacity corresponding to the Tresca material is of quite complicated nature. The exact solution of the limit analysis problem includes several different yield regimes corresponding to the sides of yield hexagons even when the two

moment limited interaction yield surface is used (Fig. 2). However, we are looking for simpler predictions of the limit load. For this purpose generalized square (Fig. 3) and diamond (Fig. 4) yield conditions will be applied.

4.1 Exact solution for the diamond yield condition

First consider the case of the diamond yield condition (Fig. 4). Let us assume that the stress state of the shell corresponds to the sides AB and D_1A_1 of the diamonds depicted in Fig. 4. Thus,

$$n_2 = n_1 - 1 \tag{13}$$

and

$$m_2 = 1 - m_1. \tag{14}$$

When substituting (14) in the first equation of (6) after integration one obtains

$$n_1 = \ln \frac{C}{\varrho} \tag{15}$$

For determination of the constant of intergration the condition $n_1(1) = 0$ can be used. Thus, (15) yields

$$n_1 = -\ln \varrho. \tag{16}$$

Inserting (14) and (16) into (6) leads to the equation

$$m_1' + \frac{2}{\varrho} m_1 = -\frac{1}{k}\left(\ln \varrho + \frac{q}{\varrho}\right) \tag{17}$$

The general solution for (17) could be presented as

$$m_1 = \frac{B}{\varrho^2} - \frac{\varrho}{9k}\left(3 \ln \varrho - 1\right) - \frac{q}{2k}, \tag{18}$$

where B is a constant of integration.

For determination of the constant B and the limit load q we have boundary conditions (9) which yield together with (18)

$$B = \frac{q}{2k} - \frac{1}{9k} \tag{19}$$

and

$$q = \frac{2}{9(1-\alpha^2)}\Big(1 + 9k\alpha^2 + \alpha^3(3\ln\alpha - 1)\Big). \tag{20}$$

Let us study now the kinematical admissibility of the solution established above. According to the associated flow law the strain rate vector with components (7) must be directed along the external normal to the yield surface. It is seen from Fig. 4 that

$$\dot{\varepsilon}_1 = -\dot{\varepsilon}_2 \tag{21}$$

and

$$\dot{\kappa}_1 = \dot{\kappa}_2. \tag{22}$$

It follows from (22) by the use of (9) that the deflection rate is given as

$$\dot{w} = B\ln\varrho, \tag{23}$$

where (12) has been taken into account and B is an integration constant. Making use of (23), (7) and (12) one obtains from (21)

$$\dot{u} = B\tan\varphi\Big(1 - \ln\varrho + \frac{\alpha}{\varrho}(\ln\alpha - 1)\Big). \tag{24}$$

Thus, the solution is statically and kinematically admissible, e.g. exact within the framework of the current concept.

4.2 Lower bound predictions for the square yield condition

It appears that simple lower bound predictions of the exact solution can be obtained under the assumption that

$$n_1 = n_2 = 0 \tag{25}$$

In this case the first equation in set (6) is satisfied spontaneously.

Let us assume that the stress state of the shell corresponds to the side AB in Fig. 3. Thus,

$$m_2 = 1 \tag{26}$$

When substituting (25), (26) into (6) after integration,

$$m_1 = \frac{q}{k}\left(\frac{1}{\varrho} - 1\right) \tag{27}$$

and

$$q = \frac{k\alpha}{1-\alpha} \tag{28}$$

Note that the stress distribution (27) is statically admissible not only for the generalized square yield condition (Fig. 3) but also for the limited interaction yield condition (Fig. 2). Thus, the lower bound prediction (28) holds good for the yield conditions presented in Fig. 2 and Fig. 3.

Similarly, for the shell built in at the edge, one has the load carrying capacity

$$q = \frac{k\,(1+\alpha)}{1-\alpha} \tag{29}$$

Evidently, (29) holds good only for the square yield condition.

5 Shells of piece-wise constant thickness

5.1 Exact solution for the diamond yield condition

Consider a simply supported shell, the material of which corresponds to the generalized diamond yield condition (Fig. 4). Let us assume that the stress state of the shell is such that $m_1 \geq 0$, $m_2 \geq 0$, $n_1 \geq 0$, $n_2 \leq 0$. Thus, it can be expected that

$$n_2 = \begin{cases} n_1 - \delta, & \varrho \in (\alpha, \beta), \\ n_1 - \gamma, & \varrho \in (\beta, 1) \end{cases} \tag{30}$$

and

$$m_2 = \begin{cases} \delta^2 - m_1, & \varrho \in (\alpha, \beta), \\ \gamma^2 - m_1, & \varrho \in (\beta, 1). \end{cases} \tag{31}$$

Substituting (30) in the first equilibrium equation (7) and integrating the equation one obtains

$$n_1 = \begin{cases} -\delta \ln \varrho + (\delta - \gamma) \ln \beta, & \varrho \in (\alpha, \beta), \\ -\gamma \ln \varrho, & \varrho \in (\beta, 1). \end{cases} \tag{32}$$

Note that the quantity n_1 satisfies the boundary requirement (10) and the condition of continuity imposed at the point $\varrho = \beta$.

When inserting (31), (32) in the second equation of the set (7) after integration the solution can be presented as

$$m_1 = \begin{cases} \dfrac{C_1}{\varrho^2} + \dfrac{1}{2}(\delta^2 - 1) - \dfrac{\delta\varrho}{9k}(3 \ln \varrho - 1) - \dfrac{q}{2k} + \dfrac{\varrho(\delta - \gamma) \ln \beta}{3k}, & \varrho \in (\alpha, \beta), \\ \dfrac{C_2}{\varrho^2} + \dfrac{1}{2}(\gamma^2 - 1) - \dfrac{\gamma\varrho}{9k}(3 \ln \varrho - 1) - \dfrac{q}{2k}, & \varrho \in (\beta, 1). \end{cases} \tag{33}$$

For determination of the integration constants C_1, C_2 in (33) the boundary conditions (8) can be employed. The latter yield

$$\begin{aligned} C_1 &= \frac{\alpha^2}{2}(\delta^2 + 1) + \frac{\delta\alpha^3}{9k}(3 \ln \alpha - 1) + \frac{q\alpha^2}{2k} - \frac{\alpha^3(\delta - \gamma) \ln \beta}{3k}, \\ C_2 &= \frac{1}{2}(1 - \gamma^2) - \frac{\gamma}{9k} + \frac{q}{2k}. \end{aligned} \tag{34}$$

The bending moment m_1 must be continuous everywhere. Thus, $m_1(\beta-) = m_1(\beta+)$ and it follows from (33), (34) that

$$\begin{aligned} q &= \frac{1}{\alpha^2 - 1}\Big\{k\left[(1 - \gamma^2)(1 - \beta^2) - \alpha^2(1 + \delta^2) + \beta^2(1 - \delta^2)\right] - \\ &- \frac{2}{9}\delta\left[3\alpha^3(\ln \alpha - \ln \beta) + \beta^3 - \alpha^3\right] + \frac{2}{9}\gamma\left[\beta^3 - 1 - 3\alpha^3 \ln \beta\right]\Big\}. \end{aligned} \tag{35}$$

Note that the plastic regimes used herein are the same as those corresponding to the shell of constant thickness. Thus, the kinematical relations (21)-(24) also hold good in the present case.

5.2 Lower bound solutions

At first let us consider the case of the diamond yield condition. Let us assume that the thickness is a piece-wise constant but (25) and (31) hold good. Integrating the equilibrium equations (7) under these assumptions yields

$$m_1 = \begin{cases} \dfrac{B_1}{\varrho^2} - \frac{1}{2}(1 - \delta^2 + \dfrac{q}{k}), & \varrho \in (\alpha, \beta), \\ \dfrac{B_2}{\varrho^2} - \frac{1}{2}(1 - \gamma^2 + \dfrac{q}{k}), & \varrho \in (\beta, 1), \end{cases} \tag{36}$$

where B_1, B_2 are arbitrary constants. Making use of (8), (9) one can determine

$$\begin{aligned} B_1 &= \frac{\alpha^2}{2}(1 + \delta^2 + \frac{q}{k}), \\ B_2 &= \frac{1}{2}(1 - \gamma^2 + \frac{q}{k}). \end{aligned} \tag{37}$$

Finally, due to the continuity of m_1 it follows from (36), (37) that the limit load can be expressed as

$$q = \frac{k}{\alpha^2 - 1}\Big((\beta^2 - 1)(\gamma^2 - 1) - \delta^2(\alpha^2 + \beta^2) + \beta^2 - \alpha^2\Big). \tag{38}$$

Similarly in the case of the generalized square yield condition (Fig. 3) one obtains

$$q = \frac{k}{\alpha - 1}\Big(1 - \alpha - \gamma^2 + \beta(\gamma^2 - \delta^2)\Big). \tag{39}$$

whereas

$$m_2 = \begin{cases} \delta^2, & \varrho \in (\alpha, \beta), \\ \gamma^2, & \varrho \in (\beta, 1). \end{cases} \tag{40}$$

Note that (39), (40) are valid in the case of Tresca's hexagons (Fig. 2).

For the shell built in at both edges the lower bound of the load carrying capacity corresponding to the gneralized square yield condition turns into

$$q = \frac{k}{\alpha - 1}\Big(1 - \alpha - 2\gamma^2 + \beta(\gamma^2 - \delta^2)\Big), \tag{41}$$

6 Optimal design of the shell of piece-wise constant thickness

Let us consider a simply supported shell in the case of which (30)-(35) are valid. We are looking for a shell design whose volume (weight) (2) attains a minimal value. Making use of (5), the cost function can be put into the form

$$I = \delta\,(\beta^2 - \alpha^2) + \gamma\,(1 - \beta^2), \tag{42}$$

where $I = V\cos\varphi/(\pi h_* R^2)$.

When minimizing (42) one has to take into account that the bending moment (34) must meet the requirements

$$\gamma^2 \le m_1 \le \delta^2 \tag{43}$$

for $\varrho \in (\alpha, \beta)$ and

$$0 \le m_1 \le \gamma^2 \tag{44}$$

for $\varrho \in (\beta, 1)$. At the same time

$$n_* \le n_1 \le \delta \tag{45}$$

for $\varrho \in (\alpha, \beta)$ and

$$0 \le n_1 \le n_* \tag{46}$$

for $\varrho \in (\beta, 1)$, where $n_* \in (0, \gamma)$, if $\gamma \le \delta$.

It is reasonable to assume that the material resources will be utilized in the most efficient manner if $m_1(\beta) = \gamma^2$. This leads to the relation

$$\frac{1}{2\beta^2}(1 - \beta^2)(1 - \gamma^2 + \frac{q}{2k}) + \frac{\gamma}{9k\beta^2}\Big(\beta^3(1 - 3\ln\beta) - 1\Big) - \gamma^2 = 0, \tag{47}$$

which holds good for the optimal values of the quantities β and γ. Thus one has to minimize the cost function (42) taking (35) and (47) into account.

In order to define the constrained minimum of (42) let us introduce the Lagrangian function

$$
\begin{aligned}
I_* &= \delta\,(\beta^2-\alpha^2)+\gamma\,(1-\beta^2)+\lambda_1\Big\{q-\frac{1}{\alpha^2-1}\Big[k\,(1-\gamma^2)(1-\beta^2)- \\
&- k\alpha^2(1+\delta^2)+k\beta^2(1-\delta^2)-\frac{2}{9}\delta\left(3\alpha^3(\ln\alpha-\ln\beta)-\alpha^3+\beta^3\right)+ \\
&+ \frac{2}{9}\gamma\left(\beta^3-1-3\alpha^3\ln\beta\right)\Big]\Big\}+\lambda_2\Big\{\frac{1}{2\beta^2}(1-\beta^2)(1-\gamma^2+\frac{q}{2k})+ \\
&+ \frac{\gamma}{9k\beta^2}\Big(\beta^3(1-3\ln\beta)-1\Big)-\gamma^2\Big\} \qquad (48)
\end{aligned}
$$

where λ_1, λ_2 are certain Lagrangian multipliers.

Necessary conditions for extremum of (48) can be written as

$$
\frac{\partial I_*}{\partial\delta}=0, \qquad \frac{\partial I_*}{\partial\gamma}=0, \qquad \frac{\partial I_*}{\partial\beta}=0. \qquad (49)
$$

The set (49) is to be solved (35) and (47) with respect to β, γ, δ, λ_1, λ_2. At the same time one has to check if the constraints (43)-(46) are satisfied.

Note that (43)-(46) impose certain restrictions on the applicability of the solution of the set (35), (47), (49) for fixed values of the load parameter q.

7 Numerical results

The set of equations has been solved numerically for different values of the external load q and the geometrical parameter k. The results of calculations are presented in Tables 1-2. Tables 1,2 correspond to the cases if $k = 0.9$; and $k = 0.3$; respectively. Tables 1,2 show that the optimal values of the geometrical parameters are not very sensitive with respect to the parameter k. However, the corresponding limit loads differ several times.

Economy of the design might be evaluated with the help of the coefficient $e = V/V_*$, where V_* is the volume of the reference shell of constant thickness h_*. Thus,

Table 1: Optimal parameters for k=0.9

q	α	β	δ	γ	V_*	V	e
0.227	0.05	0.7577	1.2491	0.5664	0.9975	0.9552	0.9576
0.264	0.15	0.7239	1.2669	0.6152	0.9775	0.9283	0.9496
0.338	0.25	0.6880	1.2650	0.6758	0.9375	0.8756	0.9340
0.459	0.35	0.6994	1.2194	0.6961	0.8775	0.8027	0.9148
0.649	0.45	0.7393	1.1652	0.6924	0.7975	0.7142	0.8963
0.951	0.55	0.7870	1.1176	0.6830	0.6975	0.6141	0.8805
1.459	0.65	0.8361	1.0788	0.6742	0.5775	0.5012	0.8679
2.423	0.75	0.8845	1.0481	0.6679	0.4375	0.3758	0.8589
4.756	0.85	0.9317	1.0244	0.6648	0.2775	0.2368	0.8535
16.686	0.95	0.9776	1.0068	0.6652	0.0975	0.0830	0.8516

$$V_* = \frac{\pi h_*}{\cos\varphi}(R^2 - a^2). \tag{50}$$

Making use of (2), (5) and (50) one can establish

$$e = \frac{1}{1-\alpha^2}\Big(\delta\,(\beta^2 - \alpha^2) + \gamma\,(1-\beta^2)\Big). \tag{51}$$

The values of the economy coefficient (51) have accommodated in the last columns of Tables 1,2.

The calculations carried out show that the greater is the load carrying capacity of the reference shell the greater is the eventual material saving. For instance, in case $k = 0.9$; $p = 16.686$ one can economize 14.5% of the material if a shell of piece-wise constant thickness is used. Approximately the same amount of the material could be saved in the case $k = 0.3$.

The limit load (20) is presented in Fig. 5 for different values of the parameter k. The solid lines corresponds to $k = 0.9$ whereas the dotted and dashed lines are associated with $k = 0.5$ and $k = 0.3$, respectively.

Table 2: Optimal parameters for k=0.3

q	α	β	δ	γ	V_*	V	e
0.224	0.05	0.8653	1.1553	0.4862	0.9975	0.9843	0.9868
0.236	0.15	0.8111	1.1986	0.5786	0.9775	0.9595	0.9816
0.258	0.25	0.6640	1.2680	0.7649	0.9375	0.9074	0.9679
0.292	0.35	0.6849	1.2229	0.7690	0.8775	0.8321	0.9483
0.345	0.45	0.7356	1.1730	0.7454	0.7975	0.7392	0.9270
0.431	0.55	0.7868	1.1279	0.7207	0.6975	0.6316	0.9056
0.582	0.65	0.8366	1.0882	0.6986	0.5775	0.5115	0.8857
0.880	0.75	0.8848	1.0542	0.6811	0.4375	0.380291	0.8691
1.631	0.85	0.9318	1.0270	0.6698	0.2775	0.2379	0.8575
5.578	0.95	0.9776	1.0071	0.6658	0.0975	0.0831	0.8520

The bending moment m_1 is presented in Fig. 6. In Fig.6 the solid lines correspond to the optimal design and dashed lines are associated with the reference shell of constant thickness. The curves labeled with 1 correspond to the case $\alpha = 0.1$ whereas curves with label two are associated with $\alpha = 0.2$. Corresponding loading parameters are equal to $q_1 = 0.241$ and $q_2 = 0.296$. It is seen from Fig.6 that the bending moment in the shell of piece-wise constant thickness exceeds the moment corresponding to the reference shell of constant thickness.

Note that the discontinuities in the slopes of the moment distributions (solid lines in Fig.6) are admissible since the shear force is continuous at $\varrho = \beta$.

The same procedure might be applied in the case of the lower bound. The results of the corresponding calculations are presented in Tables 3,4. Table 3 corresponds to the diamond yield condition, whereas Table 4 is associated with the generalized square yield condition.

Calculations carried out show that the optimal values of the parameters β, γ and δ but weakly depend on the value of the external load q. Especially non-sensitive is the parameter γ in the case of the lower bound solution and the diamond yield condition.

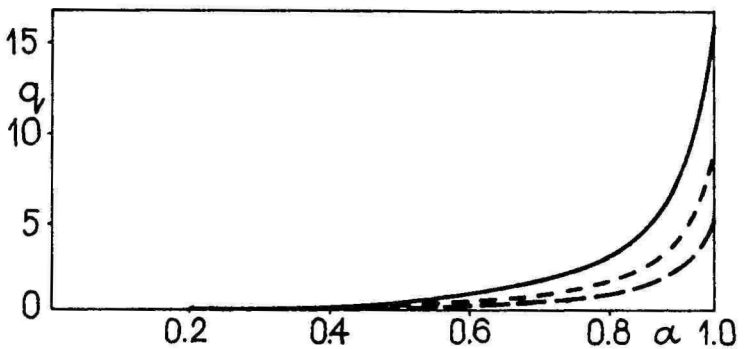

Figure 5: Load carrying capacity for the diamond yield condition

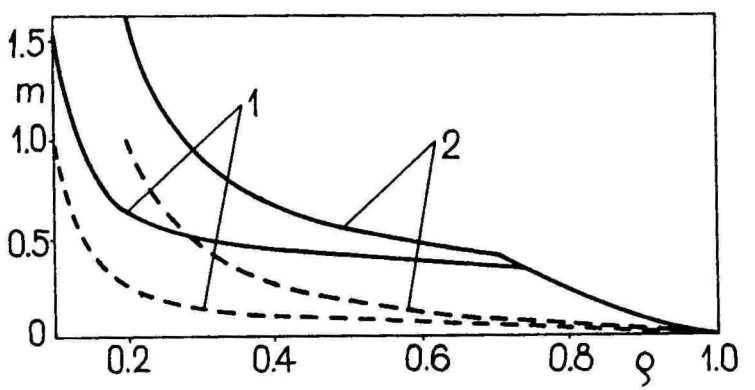

Figure 6: Bending moment

Table 3: Optimal parameters for the diamond yield condition

q/k	α	β	δ	γ	V_*	V	e
0.053	0.05	0.6170	1.1707	0.6350	0.9975	0.8360	0.8381
0.176	0.15	0.6527	1.1466	0.6392	0.9775	0.8296	0.8487
0.333	0.25	0.6876	1.1248	0.6454	0.9375	0.8017	0.8552
0.538	0.35	0.7237	1.1043	0.6520	0.8775	0.7536	0.8588
0.818	0.45	0.7619	1.0850	0.6579	0.7975	0.6861	0.8604
1.222	0.55	0.8025	1.0668	0.6625	0.6975	0.6002	0.8605
1.857	0.65	0.8450	1.0499	0.6655	0.5775	0.4964	0.8595
3.000	0.75	0.8887	1.0342	0.6672	0.4375	0.3753	0.8579
5.667	0.85	0.9331	1.0197	0.6677	0.2775	0.2375	0.8557
19.000	0.95	0.9777	1.0063	0.6672	0.0970	0.0832	0.8532

Table 4: Optimal parameters for the generalized square yield condition

q/k	α	β	δ	γ	V_*	V	e
0.005	0.05	0.0791	1.3600	0.9962	0.9975	0.9951	0.9976
0.046	0.15	0.2293	1.3183	0.9703	0.9775	0.9590	0.9810
0.133	0.25	0.3623	1.2576	0.9329	0.9375	0.8969	0.9567
0.279	0.35	0.4783	1.1970	0.8960	0.8775	0.8183	0.9325
0.508	0.45	0.5804	1.1445	0.8648	0.7975	0.7273	0.9120
0.867	0.55	0.6717	1.1018	0.8403	0.6975	0.6250	0.8961
1.463	0.65	0.7547	1.0681	0.8219	0.5775	0.5109	0.8846
2.571	0.75	0.8310	1.0419	0.8086	0.4375	0.3836	0.8769
5.207	0.85	0.9018	1.0217	0.7994	0.2775	0.2420	0.8721
18.513	0.95	0.9682	1.0063	0.7933	0.0975	0.0848	0.8698

References

[1] Hodge, P.G., Limit analysis of rotationally symmetric plates and shells. *Prentice Hall*, 1963.

[2] Jones, N. and Ich, N.T., The load carrying capacities of symmetrically loaded shallow shells. *Int. J. Solids and Struct.*, 1972, 8, $N°12$, 1339-1351.

[3] Kuech, R.W. and Lee, S.L., Limit analysis of simply supported conical shells subjected to uniform internal pressure. *J. Franklin Inst.*, 1965, 280, $N°1$, 71-87.

[4] Lance, R.H. and Lee, C.-H., The yield point load of a conical shell. *Int. J. Mech. Sci.*, 1969, 11, $N°1$, 129-143.

[5] Lellep, J., Optimization of plastic structures. *Tartu*, 1991.

[6] Lellep, J. and Hein, H., Optimization of rigid-plastic shallow spherical shells of piece-wise constant thickness. *Struct. Optim.*, 1993, 5, $N°3$, 197-203.

[7] Onat, E.T., Plastic analysis of shallow conical shells. *J. Eng. Mech. Div. Proc. Amer. Soc. Civ. Eng.*, 1960, 86, $N°6$, 1-12.

[8] Onat, E.T. and Lance, R., Analysis of plastic shallow conical shells. *Trans. ASME. J. Appl. Mech.*, 1963, 30, $N°2$, 199-210.

Оптимальное проектирование жесткопластических конических оболочек кусочно-постоянной толщины

Ян Леллеп и Элла Пуман

Резюме

Рассматриваются конические оболочки с центральной жесткой шайбой Предполагается, что стенка оболочки кусочно постоянная. Найдены проекты минимального веса при условии, что несущая способность оболочки кусочно-постоянной толщины совпадает с несущей способностью сравниваемой оболочки постоянной толщины. Материал оболочки считается идеально жесткопластическим, подчиняющимся условию пластичности Треска. Рассматриваются разные варианты аппроксимации поверхности текучести.

Optimal design of a fiber-reinforced cylindrical shell

JAAN LELLEP and ELMAR SAKKOV

Tartu University

Abstract Optimal design of cylindrical shells of piece-wise constant thickness is studied. The shells under consideration are subjected to the impulsive loading whereas they are composed of a rigid-plastic composite material. An approximation of the yield surface suggested by Lance and Robinson is employed.

1 Introduction

Problems of optimal design of reinforced rigid-plastic beams were studied in [1,4]. In [5] these results were generalized for the case of an arbitrary number of reinforcement layers.

However, only very little attention is paid to the optimization of plastic shells subjected to dynamic loading. Lepik [6] has studied circular cylindrical shells of piece-wise constant thickness. Herein, an attempt is made to define an optimal shape of a rigid-plastic circular cylindrical shell subjected to the impulsive loading. A simple approximation of the yield surface for fiber-reinforced plastic shells, suggested by Lance and Robinson [2,3] is used.

2 Formulation of the problem and basic equations

We consider a cylindrical shell of piece-wise constant thickness $h(x)$, length 2ℓ and radius R (Fig.1). Both edges of the shell are assumed to be hinged. The shell is composed of a fiber reinforced composite material. The model

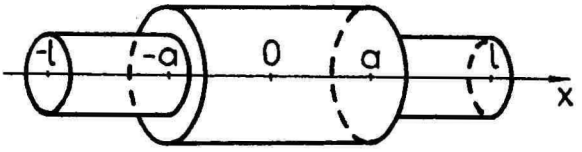

Figure 1: Shell geometry

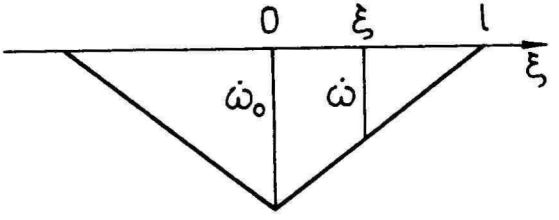

Figure 2: Velocity distribution

of a composite material can be considered as a system of stiff strong fibers embedded uniformly in a relatively less stiff and generally ductile metallic matrix.

The shell is assumed to deform under an impulsive loading given in the form of the initial kinetic energy K_0.

The parameters $\alpha = \frac{a}{\ell}$ and $\gamma = \frac{h_1}{h_0} < 1$ are sought for under the requirement that the maximum residual deflection at midpoint of the shell generator attains the minimum value for a given structural weight.

The equilibrium equations for a shell are

$$\frac{\partial^2 M}{\partial x^2} - \frac{N}{R} + P = \varrho \frac{\partial^2 W}{\partial t^2} \cdot \begin{cases} h_0; & x \in [0, a] \\ h_1; & x \in [a, \ell], \end{cases} \tag{1}$$

where M is the longitudinal bending moment, N is the circumferential membrane force and P is the internal pressure. The transverse deflection of the shell is denoted by $W(x,t)$ and the density of the shell material by ϱ.

Let us introduce the following notations:

$$\xi = \frac{x}{\ell}, \qquad \alpha = \frac{a}{\ell}, \qquad \gamma = \frac{h_1}{h_0}.$$

The yield moment M_0 and yield force N_0 are constants to be calculated as

$$M_0 = \frac{\sigma_0 h^2}{4}, \qquad N_0 = \sigma_0 h,$$

σ_0 being the yield stress of the material in the axial direction. For $h = h_0$ let us denote

$$M_* = \frac{\sigma_0 h_0^2}{4}, \qquad N_* = \sigma_0 h_0.$$

One can present (1) as

$$m'' + \omega(p - n) = \ddot{w} \begin{cases} 1; & \varrho \in [0, \alpha] \\ \gamma; & \varrho \in [\alpha, 1], \end{cases} \tag{2}$$

where the following dimensionless quantities are defined:

$$m = \frac{M}{M_*}, \qquad n = \frac{N}{N_*}$$
$$p = \frac{PR}{N_*}, \qquad \omega = \frac{N_*\ell^2}{M_*R}$$

and the dot denotes differentiation with respect to dimensionless time τ and the prime denotes differentiation with respect to ξ.

Plastic behaviour of cylindrical shells made of a ductile composite material has been studied by Lance and Robinson [2,3] who suggested a simple approximation of the exact yield surface for a fiber-reinforced shell. In the present study we shall assume that the ductile matrix is reinforced either circumferentially or longitudinally with ductile fibers and that the material can be considered as an homogenous anisotropic plastic material obeying the piece-wise linear yield surface presented by Lance and Robinson [2,3]. Following the ideas of Lance and Robinson we have

$$n = \pm\nu \begin{cases} 1; & \varrho \in [0, \alpha] \\ \gamma; & \varrho \in [\alpha, 1], \end{cases}$$

$$m = \begin{cases} 1; & \varrho \in [0, \alpha] \\ \gamma; & \varrho \in [\alpha, 1], \end{cases}$$

where $\nu = \frac{\sigma_1}{\sigma_0}$, σ_1 being the yield stress of the material in the circumferential direction.

Let us take $p = 0$ (impulsive loading), so the equation to be integrated takes the form

$$m'' = (\omega\nu + \ddot{w}) \begin{cases} 1; & \varrho \in [0, \alpha] \\ \gamma; & \varrho \in [\alpha, 1], \end{cases} \tag{3}$$

3 Integration of the basic equations

Integration of the equations (3) will be carried out using the approximate mode-form technique [6] according to which the rate of the shell deflection is given by (Fig.2)

$$\dot{w}(\xi,\tau) = \dot{w}_0(1-\xi). \tag{4}$$

After calculating the acceleration of deflections from (4) and substituting into (3) we have

$$m'' = [\omega\nu + \ddot{w}_0(1-\xi)] \begin{cases} 1; & \varrho \in [0,\alpha] \\ \gamma; & \varrho \in [\alpha,1], \end{cases} \tag{5}$$

Let us integrate now the equations (5) with respect to ξ, satisfying the following boundary and continuity conditions:

$$\begin{aligned} m'(0) &= 0, & m'(\alpha+0) &= m'(\alpha-0), \\ m(0) &= 1, & m(\alpha+0) &= m(\alpha-0), \end{aligned}$$

This leads to the relation

$$m = \begin{cases} \omega\nu\frac{\xi^2}{2} + \ddot{w}_0(\frac{\xi^2}{2} - \frac{\xi^3}{6}) + 1, \\ \omega\nu\gamma\frac{(\xi-\alpha)^2}{2} + \gamma\ddot{w}_0\Big[\frac{(\xi-\alpha)^2}{2} - \frac{\xi^3}{6} + \frac{\alpha^3}{6} + \frac{\alpha^2}{2}(\xi-\alpha)\Big] + \\ +\Big[\omega\nu\alpha + \ddot{w}_0(\alpha - \frac{\alpha^2}{2})\Big](\xi-\alpha) + \omega\nu\frac{\alpha^2}{2} + \ddot{w}_0(\frac{\alpha^2}{2} - \frac{\alpha^3}{6}) + 1 \end{cases}$$

Taking into account the following conditions

$$m(1) = 0, \qquad m(\alpha) = \gamma^2,$$

one eventually obtains

$$\frac{\omega\nu\alpha^2 - 2\gamma + 2}{\alpha^2(3-\alpha)} - \frac{1}{2}\frac{\omega\nu\gamma(1-\alpha)^2 + \omega\nu\alpha(2-\alpha) + 2}{\gamma(1-\alpha)^3 + \alpha(\alpha^2 - 3\alpha + 3)} = 0. \tag{6}$$

In (6) ω and ν are given parameters and α as well as γ the parameters to be determined.

4 Determination of the optimal parameters. Numerical example

Let us assume that the total volume of the shell is given. Thus

$$V_0 = h_0 \ell[\alpha + \gamma(1-\alpha)].$$

Let us denote

$$V = \frac{V_0}{h_0 \ell} = \alpha + \gamma(1-\alpha). \tag{7}$$

From (7) one obtains

$$\gamma = \frac{V-\alpha}{1-\alpha}. \tag{8}$$

After substituting (8) into (6) we reach the equation for determination of optimal parameters:

$$\begin{aligned} &\omega\nu(1-V)\alpha^5 - [\omega\nu(2-V)+2]\alpha^4 + [\omega\nu(1+V)+8]\alpha^3 - \\ &-(4V^2+\omega\nu V - 8V + 10)\alpha^2 - 8(1-V)^2 + 4V(1-V) = 0\,. \end{aligned} \tag{9}$$

Some results of the computational analysis are presented in Table 1. Here $e = w(0,\tau_f)/w_0$ is the "economic coefficient", where w_0 is the residual deflection of the uniform shell with the same volume V as the corresponding optimal shell.

Table 1: Optimal parameters for the case $\omega\nu = 10$

V	α	γ	e
0.4	0.25	0.20	0.92
0.5	0.26	0.32	0.87
0.6	0.29	0.44	0.90
0.7	0.30	0.57	0.91

References

[1] Aunin, U., Lellep, J. and Sakkov, E., Optimal design of plastic reinforced beams under impulsive loading. *Mech. of Comp. Mater.*, 1986, $N°$ 2, 293-301 (in Russian).

[2] Lance, R.H. and Robinson, D.N., A maximum shear stress theory of plastic failure of fiber-reinforced material. *J. Mech. and Phys. Solids*, 1971, 19, $N°$ 2, 49-60.

[3] Lance, R.H. and Robinson, D.N., Plastic analysis of filled, reinforced circular cylindrical shells. *Int. J. Mech. Sci.*, 1973, 15,$N°$ 1, 65-79.

[4] Lellep, J. and Sakkov, E., On optimization of a reinforced beam subjected to dynamic loading. *Trans. Tartu Univ.*, 1985,$N°$ 721,7-15 (in Russian).

[5] Lellep, J. and Sakkov, E., Optimum design of a reinforced beam under dynamic loading. *Mech. of Comp. Mater.*, 1993, 29, $N°$ 6,811-815.

[6] Lepik, Ü., Optimal design of inelastic structures under dynamic loading. *Tallinn, Valgus*, 1982 (in Russian).

Оптимальное проектирование армированной цилиндрической оболочки

Яан Леллеп и Эльмар Сакков

Резюме

Рассматриваются цилиндрические оболочки кусочно постоянной толщины изготовленные из композитного материала.

Оболочки подвержены действию динамической нагрузки. Найдены проекты оболочек кусочно постоянной толщины заданного веса при которых максимальный прогиб достигает минимального значения.

Optimal design of rigid-plastic annular plates with piece-wise constant thickness

HELLE HEIN

Tartu University

Abstract The minimum weight problem is studied in the case of annular plates with piece-wise constant thickness. Geometrical nonlinearity is taken into account. The yield line method proposed by Sawczuk is applied.

1 Introduction

Optimal design problems of plastic plates in limit state have been considered by many authors [4, 9, 11, 12]. The post-yield behaviour of circular and annular plates has been studied in several papers [1, 2, 5, 7, 10]. Lellep and Majak [8] found optimal design of annular plates material of which was obeying von Mises yield criterion. In [3] and [5] an approximate method has been developed for studying plates with piece-wise constant thickness. An optimal design technique in the post-yield range has been developed for shallow spherical shells by Lellep and Hein [6]. In the present paper optimal design of annular plates with piece-wise constant thickness will be discussed. Moderately large deflections are taken into account.

2 Formulation of the problem

Let us consider a simply supported annular plate of inner radius a and outer radius A. The plate is subjected to the uniformly distributed pressure loading

of intensity P. All characteristics of the plate depend only on the radial coordinate r. It is assumed that the plate is axisymmetric and has been divided into $n+1$ rings of the constant thickness

$$h = h_i, \quad r \in D_i, i = 0, \ldots, n \tag{1}$$

where D_i stands for an interval $(a_i, a_{i+1}), a_0 = a, a_{n+1} = A$. The geometrical parameters a, A, the number of rings and the load intensity will be considered as the given constants.

We are looking for a design of the annular plate for which the material volume

$$V_u = \sum_{i=0}^{n} h_i(a_{i+1}^2 - a_i^2) \tag{2}$$

attains the minimal value under the condition that the deflections of the plate of piece-wise constant thickness and of the reference plate of constant thickness, respectively, coincide. By minimizing (2) one has to take into account the configuration variations.

3 Governing relations and basic assumptions

The equilibrium equations have the form

$$\begin{aligned} (\varrho n_1)' &= n_2, \\ \{(\varrho m_1)' &- m_2 + \varrho n_1 w'\}' + 2p\varrho = 0 \end{aligned} \tag{3}$$

whereas the deformation components coupled with the stress components can be written as

$$\begin{aligned} \varepsilon_1 &= \frac{M_*^2}{A^2 N_*^2}(u' + \frac{1}{2}w'^2), & \kappa_1 &= -\frac{M_*}{A^2 N_*}w'', \\ \varepsilon_2 &= \frac{M_*^2}{A^2 N_*^2}\frac{u}{\varrho}, & \kappa_2 &= -\frac{M_*}{A^2 N_*}\frac{w'}{\varrho} \end{aligned} \tag{4}$$

In (3) and (4) the primes denote the differentiation with respect to the nondimensional coordinate ϱ. Dimensional and nondimensional quantities are related by

$$\varrho = \frac{r}{A}, \quad n_{1,2} = \frac{N_{r,\varphi}}{N_*}, \quad m_{1,2} = \frac{M_{r,\varphi}}{M_*}, \quad \gamma_j = \frac{h_j}{h_*},$$
$$w = \frac{N_* W}{M_*}, \quad u = \frac{A N_*^2 U}{M_*^2}, \quad p = \frac{A^2 P}{2M_*}, \quad \alpha_j = \frac{a_j}{A}, \quad j = 0, \dots n. \quad (5)$$

Here N_r, N_φ denote the membrane forces, M_r, M_φ - the bending moments, U, W - radial and normal displacements, h_* - thickness of te plate with constant thickness and $N_* = \sigma_0 h_*, M_* = \sigma_0 h_*^2/4$, σ_0 - yield stress.

The boundary requirements for variables (5) are:

1) on the inner side

$$m_1(\alpha) = n_1(\alpha) = q(\alpha) = 0, \quad w(\alpha) = w_0 \quad (6)$$

where $\alpha = \alpha_0$ and q stand for the shear force;

2) on the outer side

$$m_1(1) = w(1) = u(1) = 0. \quad (7)$$

The material of the plate is assumed to be rigid, perfectly plastic obeying the Tresca yield condition. The effects of elastic strains and strain-hardening are neglected.

The approximation of the exact yield surface can be presented as (Fig.1)

$$n_s^2 + \mid m_s \mid \leq \gamma_j^2, s = 1, 2 \quad (8)$$

for the region $D_j, j = 0, \dots, n$.

The deformation type theory of plasticity is employed according to which the vector of strain components (4) is orthogonal to the yield surface (8).

4 Necessary optimality conditions

Let us assume that $p \geq p_0$ where p_0 stands for the load carrying capacity of the plate. For $p < p_0$ the plate remains rigid, but from $p = p_0$ the plastic flow starts and the annular regions are in different plastic stage. Suppose that in (8) the plastic behaviour of the plate corresponds to the following flow regime: $\mid n_1 \mid \leq \gamma_j, \mid m_1 \mid \leq \gamma_j^2, n_2^2 + \mid m_2 \mid = \gamma_j^2$ for each $\varrho \in D_j$.

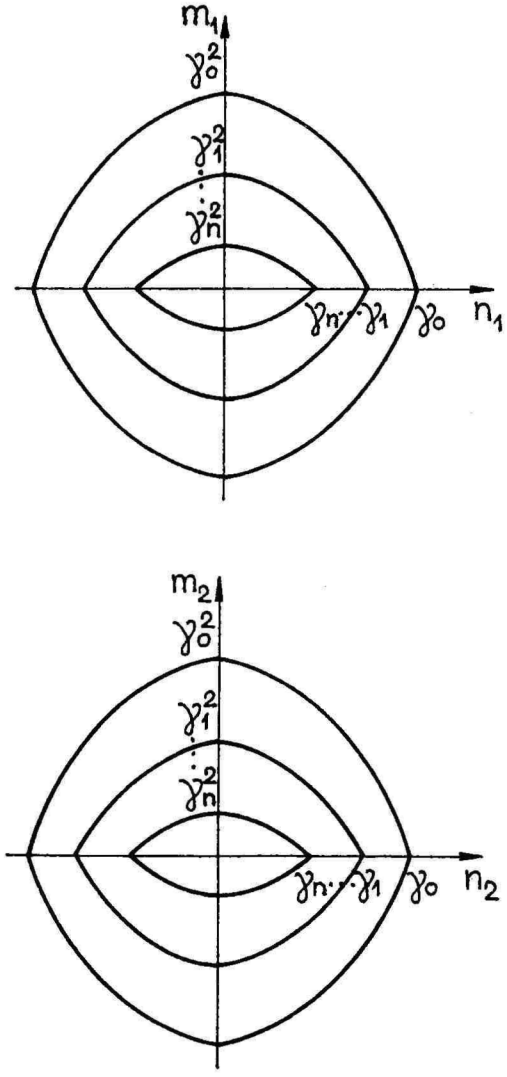

Figure 1: Yield curves

Applying the same technique as in [5] and [6] the equilibrium equations could be presented as

$$n_1' = -\frac{n_1}{\varrho} + \frac{\varphi_j}{4\varrho}(\varrho - \alpha_{j+1}) + \frac{1}{\varrho}R_j, \tag{9}$$

$$m_1' = -\frac{m_1}{\varrho} - n_1\varphi_j - p\varrho + \frac{1}{\varrho}p\alpha^2 + \frac{1}{\varrho}\{\gamma_j^2 - \frac{\varphi_j^2}{16}(\varrho - \alpha_{j+1})^2 - \\ - \frac{\varphi_j}{2}R_j(\varrho - \alpha_{j+1}) - R_j^2\}, \qquad \varrho \in D_j, j = 0, \ldots, n, \tag{10}$$

where

$$\varphi_j = \frac{w_{j+1} - w_j}{\alpha_{j+1} - \alpha_j}, \qquad j = 0, \ldots, n, \tag{11}$$

$$R_j = \frac{1}{4\varphi_j}\sum_{i=j+1}^{n}\varphi_i^2(\alpha_i - \alpha_{i+1}), \qquad j = 0, \ldots, n-1,$$

$$R_n = 0. \tag{12}$$

The quantities w_j denote deflections at $\varrho = \alpha_j; w(\alpha_j) = w_j$. The optimization problem consists in minimization of (2) under the condition that the optimal solution satisfies differential conditions (9) and (10), algebraic conditions (8) and boundary conditions (6) and (7).

Let us introduce the augmented functional

$$V_* = V + \sum_{i=0}^{n}\int_{D_i}(\Psi_1 n_1' + \Psi_2 m_1' - L_i)d\varrho + \sum_{j=1}^{n}\eta_j(n_1^2(\alpha_j) + m_1(\alpha_j) - \gamma_j^2 + \xi_j^2), \tag{13}$$

where Ψ_1, Ψ_2 are the adjoint variables, η_i - the unknown constants and V stands for the material volume in nondimensional form. The quantities L_i are introduced as follows:

$$L_i = \Psi_1\Big\{-\frac{n_1}{\varrho} + \frac{\varphi_i}{4\varrho}(\varrho - \alpha_{i+1}) + \frac{1}{\varrho}R_i\Big\} + \\ + \Psi_2\Big\{-\frac{m_1}{\varrho} - n_1\varphi_i - p\varrho + \frac{1}{\varrho}p\alpha^2 + \frac{1}{\varrho}\{\gamma_i^2 - \frac{\varphi_i^2}{16}(\varrho - \alpha_{i+1})^2 - \\ - \frac{\varphi_i R_i}{2}(\varrho - \alpha_{i+1}) - R_i^2\}\Big\} \qquad i = 0, \ldots, n. \tag{14}$$

The variables n_1, m_1 will be considered as state variables, the quantities α_j, γ_i, $\varphi_i (j = 1, \ldots, n, i = 0, \ldots, n)$ as preliminary unknown constant parameters.

Equalizing the total variation of the functional (13) to zero one obtains

$$\begin{aligned}
\sum_{i=0}^{n} \Big\{ & \frac{\partial V}{\partial \gamma_i} \Delta\gamma_i \int_{D_i} \{\Psi_1' \delta n_1 + \Psi_2' \delta m_1 + \frac{\partial L_i}{\partial n_1} \delta n_1 + \frac{\partial L_i}{\partial m_1} \delta m_1 + \\
+ & \sum_{s=0}^{n} \frac{\partial L_i}{\partial \gamma_s} \Delta\gamma_s + + \sum_{s=1}^{n} \{(\frac{\partial L_i}{\partial w_s} \Delta w_s) + \frac{\partial L_i}{\partial \alpha_s} \Delta\alpha_s)\}\Big\} d\varrho - \\
- & (\Psi_1 \delta n_1 + \Psi_2 \delta m_1)|_{\alpha_s}^{\alpha_s+1} + \frac{\partial V}{\partial \alpha_s} \Delta\alpha_s + \eta_s \{2n_1(\alpha_s)\Delta n_1(\alpha_s) + \\
+ & \Delta m_1(\alpha_s) - -2\gamma_s \Delta\gamma_s + 2\xi_s \Delta\xi_s\} = 0. \qquad (15)
\end{aligned}$$

The adjoint set and the transversality conditions take the form

$$\begin{aligned}
\Psi_1' &= \frac{\Psi_1}{\varrho} + \Psi_2 \varphi_i, \\
\Psi_2' &= \frac{\Psi_2}{\varrho}, \quad \varrho \in D_i, i = 0, \ldots, n \qquad (16)
\end{aligned}$$

and

$$\Psi_1(1) = 0. \qquad (17)$$

Bearing in mind that the quantities $\Delta\gamma_i, \Delta\xi_j$ and Δw_j are the independent variations, from (15) follow the equations

$$\alpha_{i+1}^2 - \alpha_i^2 - 2\eta_i\gamma_i - 2\int_{D_i} \frac{\Psi_2 \gamma_i}{\varrho} d\varrho, \qquad i = 0, \ldots n \qquad (18)$$

and

$$\xi_j \eta_j = 0, \qquad \sum_{i=0}^{n} \int_{D_i} \frac{\partial L_i}{\partial w_j} d\varrho = 0, \qquad j = 0, \ldots n. \qquad (19)$$

In (18), for the shake of brevity, $\eta_0 = 0$. Substituting into (15) the ordinary first-order variations $\delta n_1(\alpha_j \pm), \delta m_1(\alpha_j \pm)$ with the total variations and taking into account that $\Delta n_1(\alpha_j)$, $\Delta m_1(\alpha_j)$ are arbitrary, one obtains

$$[\Psi_1(\alpha_j)] - 2\eta_j n_1(\alpha_j) = 0, \tag{20}$$
$$[\Psi_2(\alpha_j)] - \eta_j = 0, \qquad j = 1, \ldots, n. \tag{21}$$

Similarly $\Delta\alpha_j$ are arbitrary constants. Therefore one has

$$2\alpha_j(\gamma_{j-1} - \gamma_j) - \sum_{i=0}^{n} \int_{D_i} \frac{\partial L_i}{\partial \alpha_j} d\varrho + L_j(\alpha_j) - L_{j-1}(\alpha_j) = 0. \tag{22}$$

5 Optimal solution

In choosing the optimal design of the plate one should bear in mind that the constraints (6), (7), (9) - (12) and relations (16) - (22) are to be satisfied. Let us assume that the optimal design corresponds to the case $\xi_j = 0$ in (19). It means that the plastic hinge circles will form at the positions $\varrho = \alpha_j, (j = 1, \ldots, n)$ between two parts of constant cross section. Among these hinges the plate deforms into the truncated cones.

The system of equations (16) may be integrated to give

$$\begin{aligned} \Psi_1 &= \Psi_{1i}\varrho + \Psi_{2i}\varrho^2\varphi_i, \\ \Psi_2 &= \Psi_{2i}\varrho, \varrho \in D_i, \qquad i = 0, \ldots, n. \end{aligned} \tag{23}$$

In (23) Ψ_{1i} and Ψ_{2i} stand for integration constants which may be expressed by means of (20), (21)

$$\begin{aligned} \Psi_{1n} &= -\Psi_{2n}\varphi_n, \\ \Psi_{1j-1} &= \Psi_{1j} + \eta_j(\varphi_j - \frac{2n_1(\alpha_j)}{\alpha_j}), \\ \Psi_{2j-1} &= \Psi_{2j} - \frac{\alpha_j}{\eta_j}, \qquad j = n, n-1, \ldots, 1. \end{aligned} \tag{24}$$

Integration of (9) yields

$$n_1 = \frac{\varphi_j}{4}(\frac{\varrho}{2} - \alpha_{j+1}) + R_j + \frac{1}{\varrho}B_j \tag{25}$$

where the integration constants B_j may be presented in the form

$$\begin{aligned} B_0 &= -\frac{\varphi_0\alpha}{4}(\frac{\alpha}{2}-\alpha_1)-\alpha R_0, \\ B_j &= B_{j-1}-\frac{\alpha_j^2}{8}(\varphi_j-\varphi_{j-1})+\frac{\varphi_j}{4}\alpha_j\alpha_{j+1}+\alpha_j(R_{j-1}-R_j), \\ & \qquad j=1,\ldots,n \end{aligned} \tag{26}$$

Performing the integration in (10), one obtains

$$\begin{aligned} m_1 &= \gamma_j^2-\frac{1}{48\varrho}\varphi_j^2(\varrho-\alpha_{j+1})^3-\frac{1}{4\varrho}\varphi_j R_j(\varrho-\alpha_{j+1})^2- \\ &- \frac{1}{8}\varphi_j^2\varrho(\frac{\varrho}{3}-\alpha_{j+1})-R_j^2-\frac{1}{2}R_j\varphi_j\varrho^2+p\alpha^2-B_j\varphi_j+\frac{1}{\varrho}E_j, \\ & \qquad \varrho\in D_j. \end{aligned} \tag{27}$$

Satisfying the boundary conditions (6) as well as the continuity requirements of the quantity m_1 one obtains the integration constants E_j as

$$\begin{aligned} E_0 &= -\alpha\gamma_0^2+\frac{1}{48}\varphi_0^2(\alpha-\alpha_1)^3+\frac{1}{4}\varphi_0 R_0(\alpha-\alpha_1)^2+ \\ &+ \frac{1}{8}\varphi_0^2\alpha^2(\frac{\alpha}{3}-\alpha_1)+R_0^2\alpha+\frac{1}{2}\varphi_0 R_0\alpha^2-\frac{2}{3}p\alpha^3+\varphi_0 B_0\alpha, \\ E_j &= E_{j-1}-\frac{1}{12}\varphi_{j-1}^2\alpha_j^3+\frac{1}{2}\alpha_j^2(\varphi_j R_j-\varphi_{j-1}R_{j-1})+ \\ &+ \alpha_j(\varphi_j B_j-\varphi_{j-1}B_{j-1})+\alpha_j(\gamma_{j-1}^2-\gamma_j^2)+\alpha_j(R_j^2-R_{j-1}^2)+ \\ &+ \frac{1}{8}\varphi_j^2\alpha_j^2(\frac{\alpha_j}{3}-\alpha_{j-1})+\frac{1}{48}\varphi_j^2(\alpha_j-\alpha_{j-1})^3+ \\ &+ \frac{1}{4}\varphi_j R_j(\alpha_j-\alpha_{j+1})^2, \qquad j=1,\ldots,n. \end{aligned} \tag{28}$$

Combining (7), (12) and (27) yields

$$\gamma_n^2+\frac{1}{12}\varphi_n^2-\frac{p}{3}+p\alpha^2-B_n\varphi_n+E_n=0 \tag{29}$$

Table 1: $\alpha_0 = 0.2$

w_0	p	α_1	γ_0	γ_1	w_1	e
0.0	2.6785	0.7361	1.1145	0.7132	0.0000	0.9229
0.5	2.7204	0.3501	1.3516	0.8895	0.3048	0.8921
1.0	2.8460	0.3120	1.3699	0.9095	0.4850	0.8995
1.5	3.0552	0.2899	1.3034	0.9371	0.6966	0.9158
2.0	3.3482	0.2821	1.1761	0.9689	0.9911	0.9384

Finally, it results from (8),(25) and (27) that

$$\begin{aligned}\gamma_{j-1}^2 &- \gamma_j^2 + \frac{1}{12}\varphi_{j-1}^2\alpha_j^2 - R_{j-1}^2 - \frac{1}{2}R_{j-1}\varphi_{j-1}\alpha_j - \frac{1}{3}p\alpha_j^2 + p\alpha^2 - \\ &- B_{j-1}\varphi_{j-1} + \frac{E_{j-1}}{\alpha_j} + (R_{j-1} - \frac{1}{8}\varphi_j\alpha_j + \frac{B_{j-1}}{\alpha_j})^2 = 0 \qquad (30)\end{aligned}$$

where $j = 1, \ldots, n$. Substituting Ψ_1, Ψ_2, n_1, m_1 from (23), (25), (27) into (14) and then the constants φ_i, R_i from (11) and (12) into (23)-(30) and performing the integration in (18), (19) and (22) one obtains the system of algebraic equations for determination of the unknown parameters α_j, γ_i, w_j and constants $\Psi_{1i}, \Psi_{2i}, \eta_j, B_i, E_i$ as well.

6 Discussion

The numerical results for the annular plate with two thicknesses are presented in Table 1 and Figure 2. The optimal parameters γ_0, γ_1, α_1, w_1 corresponding to the load intensity p and deflection w_0 are presented in Table 1. The quantities p and w_0 correspond to the plate with constant thickness. The coefficient of economy could be introduced as the ratio V/V_* where $V_* = 1-\alpha^2$. In Fig.2 the bending moments of the optimal plate (curve 1) and of the plate of constant thickness (curve 2) are presented. The calculations carried out show that the saving of material decreases if the deflections increase.

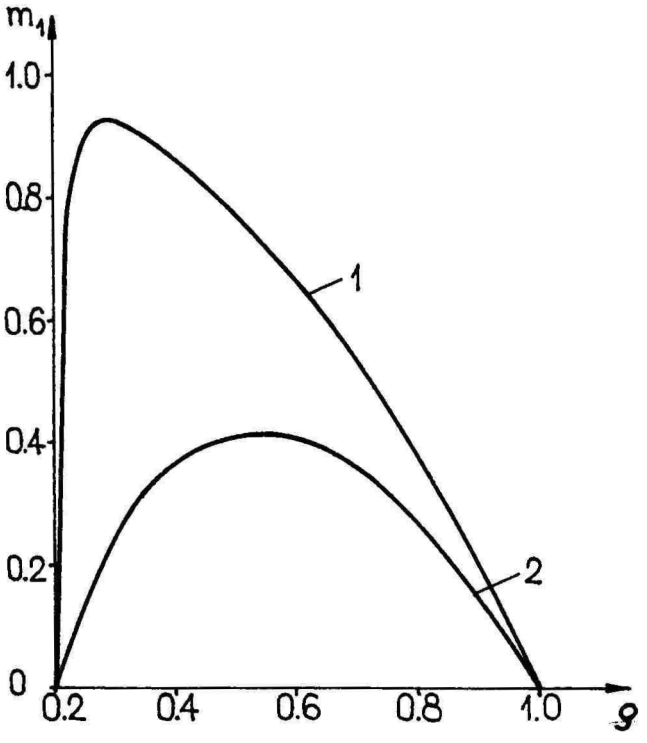

Figure 2: Bending moment

References

[1] Calladine, C.R., Simple ideas in the large deflection plastic theory of plates and slabs. In: *Engineering plasticity, (ed. J. Heyman and F.A. Leckie), Cambridge Univ.Press*, 1968, 93-126.

[2] Erkhov, M.I., Kislova, L.V., Large deflections of rigid-plastic circular plates with hinged edges. In *Issled. po Stroit. Mekh. i Metodam Rascheta.* Moscow, 1981, 4-12 (in Russian).

[3] Hein H.A., Lellep J.A., Optimization of geometrically non-linear rigid-plastic circular plates with piece-wise constant thickness. *Prikl. Mekh. (Soviet Appl. Mech.)*, 1993, 29, 6, 57-63 (in Russian).

[4] Lamblin, D., Cinquini, C., Gerlement, G., Application of linear programming to the optimal plastic design of circular plates subject to technological constraints. *Comput. Meth. Mech. and Eng.*, 1978, 13, $N°2$, 233-243.

[5] Lellep, J., Hein, H., An approximate analysis of large plastic deformations of circular and annular plates. *Tartu Ülik. Toim.*, 1992, 939, 54-69.

[6] Lellep, J., Hein, H., Optimization of rigid-plastic shallow spherical shells of piece-wise constant thickness. *Structural Optimization*, 1993, 6, $N°2$, 134-141.

[7] Lellep J., Majak J., Large deflections of rigid-plastic annular plates. *Tartu Riikl. Ülik. Toim. (Trans. Tartu State Univ.)*, 1987, 772, 33-43 (in Russian).

[8] Lellep, J., Majak, J., Optimal design of plastic annular plates of von Mises material in the range of large deflections. *Structural Optimization*, 1993, 5, $N°3$, 197-203.

[9] Lepik, Ü., Minimum weight design of circular plates with limited thickness. *Int. J. Non-Linear Mech.*, 1972, 7, $N°4$, 353-360.

[10] Onat, E.T., Haythornthwaite, R. M., Load carrying capacity of circular plates at large deflections. *J. Appl. Mech.*, 1956, 23, $N°1$, 49-55.

[11] Salupere, A., Optimal design of rigid-plastic annular plates with piece-wise constant thickness. *Structural Optimization*, 1992, 4, $N°3-4$, 186-191.

[12] Sheu, C.Y., Prager, W., Optimal plastic design of circular and annular sandwich plates with piece-wise constant cross section. *J. Mech. Phys. Solids*, 1969, 17, $N°1$, 11-16.

Оптимальное проектирование жесткопластических кольцевых пластин кусочно-постоянной толщины

Хелле Хейн

Резюме

В работе представлена методика решения задач минимизации веса жесткопластических кольцевых пластин кусочно-постоянной толщины.

Предполагается, что материал пластинок подчиняется условию пластичности Треска. Учитываются умеренно большие прогибы.

Optimal location of additional supports for rigid-plastic circular and annular impulsively loaded plates

GENNADI OLENEV and KALJO SOONETS

Tartu University

Abstract Optimal location of the rigid circular additional support for a rigid-plastic circular or annular plate subjected to the initial transverse impulse is sought for under the condition that the maximal residual deflection of the plate attains a minimal value. The material of the plate is assumed to obey the square yield condition. Different supporting conditions of the plate are considered. The influence of the impulse shape on the optimal location of the additional support is examined. The problem is solved by means of the mode form motions method.

Notation

We use the following nondimensional quantities (the corresponding dimensional quantities are given in the brackets):

$r(\varrho)$	–	radial coordinate;
$a(A)$	–	inner radius of the annular plate;
b, c	–	radii of the stationary hinge circles;
$s(S)$	–	radius of the additional support;
s_0	–	radius of the optimal additional support;
$w(W)$	–	deflection;
w_f	–	maximal residual deflection;
$t(\tau)$	–	time;
T_0, T_1	–	time of the motion ;
$m(M)$, $n(N)$	–	radial and circumferential bending moments, correspondingly;
$q(Q)$	–	shear force;
$u(U)$	–	actual initial velocity;
v	–	spatial mode;
e	–	economy coefficient;
ν	–	surface density;
$U_0 = U \mid_{\varrho=0}$		;
R	–	radius of the circular plate or outer radius of the annular plate;
M_0	–	limit bending moment;

1 Introduction

The stiffness of structures can be increased by applying additional supports, and their locations must be optimally selected. This problem was pointed out by Rozvany [6], Mróz and Rozvany [3], Prager and Rozvany [5]. The reader is also referred to books by Lepik [2], Rozvany [7] and Lellep [1].

The problem of optimal support location of rigid-plastic circular plate under dynamic loading was solved by Olenev [4]. This paper discusses uniform impulse, square yield condition and moving hinges.

In the present paper we find optimal location of rigid additional support for a circular or annular plate supported in several ways. Additional internal support has apriori a circular form and is concentric with the edge of the plate. The plate is loaded impulsively and four different shapes of the initial velocity field are examined. Optimal location of the support is sought for under the condition that maximal residual deflection of the plate attains a

minimal value. The material of the plate is assumed to obey the square yield condition. Equations of motion are integrated approximately by using the method of mode form solutions and different time-modes have been used for different parts of the plate. Finally we compare approximate and exact rigid-plastic solutions.

2 Basic equations and preliminaries

We shall consider a rigid-plastic circular plate of radii 1 and an annular plate of the same outer radii and inner radii a. The rigid concentric with the outer edge additional support of the radii s is supplied to the plate. Inequalities $0 \leq a < s < 1$ are fulfilled. The plate is subjected to an impulsive loading, the concrete forms of the initial impulse will be indicated later. At the initial moment $t = 0$ the plate is not deformed, but all its points have a prescribed transverse speed $u(r)$, $r \neq s$.

The motion equations of the plate have the form

$$\begin{aligned} (rm)' - n &= rq, \\ (rq)' &= 12r\ddot{w}. \end{aligned} \tag{1}$$

The relationships between dimensional and nondimensional quantities are as follows:

$$r = \frac{\varrho}{R}, \qquad a = \frac{A}{R}, \qquad s = \frac{S}{R}, \qquad t = \frac{12M_0}{\nu U_0 R^2}\tau, \qquad u = \frac{U}{U_0},$$

$$w = \frac{12M_0}{\nu U_0 R^2}W, \qquad m = \frac{M}{M_0}, \qquad n = \frac{N}{M_0}, \qquad q = \frac{R}{M_0}Q.$$

Primes and dots denote differentation with respect to r and t.

Initial conditions are as follows:

$$w(r,0) = 0, \qquad \dot{w}(r,0) = u(r).$$

In case of clamped or simply supported outer edge

$$\dot{w}(1,t) = 0,$$

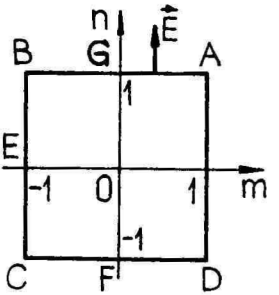

Figure 1: Yield condition

besides

$$\dot{w}(s,t) = 0.$$

We shall use the Johansson yield condition which can be represented by square yield curve (Fig. 1). The displacement-rate vector may be represented in the form

$$\vec{E} = (-\dot{w}'', -\frac{1}{\varrho}\dot{w}').$$

According to the method of mode form motions the modal form solution will be taken in the form

$$\dot{w}(r,t) = \Phi(t) \cdot v(r), \tag{2}$$

where the amplitude-function can be prescribed as the linear function

$$\Phi(t) = -t + T\ ,$$

because in case of a modal motion $\ddot{w} = const < 0$. The mode $v(r)$ must be piecewise-linear function according to the associated deformation law. The deflection-rate field (2) neglects the travelling bending hinges, i.e. only stationary hinges are taken into account.

The intensity of initial impulse is assumed to be high enough to obtain the limit stage of the plate. The following kinds of support will be accepted: in case of a circular plate

1) unsupported edge;

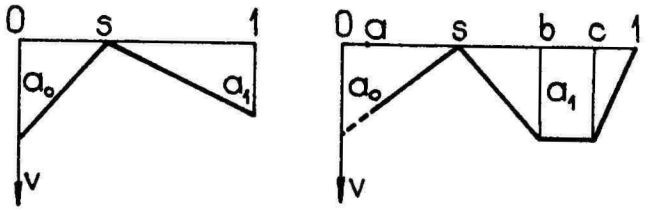

Figure 2: Velocity field: a) Case 1 b) Case 2–4

2) clamped edge;

3) simply supported edge;

in case of annular plate

4) unsupported internal and a) clamped external edge, b) simply supported external edge.

In case of the circular plate the yield hinge appears in the center, in cases 2–4 the circular yield hinges appear at $r = b$ and $r = c$, $s < b < c < 1$ [4]. The radial moment $m(r)$ must be continuous; the shear force $q(r)$ beyond support location $r = s$ is also continuous. At the center of circular plate, the places of circular yield hinges and free edges $q = 0$. The circumferential bending moment n can be discontinuous at the yield hinges (at angle-points of yield curve).

The mode of velocity field will be described as follows (Fig. 2).

The plate with a free external edge (case 1):

$$v(r) = \begin{cases} \frac{a_0}{s-a}(s-r), & 0 \le r \le s, \\ \frac{a_1}{1-s}(r-s), & s \le r \le 1. \end{cases} \tag{3}$$

The plate with a supported external edge (cases 2–4, for cases 2 and 3 $a = 0$):

$$v(r) = \begin{cases} \frac{a_0}{s-a}(s-r), & a \le r \le s, \\ \frac{a_1}{b-s}(r-s), & s \le r \le b, \\ a_1, & b \le r \le c, \\ \frac{a_1}{1-c}(1-r), & c \le r \le 1. \end{cases} \tag{4}$$

Because $\dot{w}'' \equiv 0$, the points of the plate for $r \notin (b, c)$ can be in plastic stage only in regimes AB and CD of the yield curve. Now we get the following regimes:
the plate with free external edge

regime AB, $n = 1$ for $0 \le r < s$;
regime CF, $n = -1$ for $s \le r \le 1$;

the plate with supported external edge

regime AB, $n = 1$ for $a \le r < s$;
regime CD, $n = -1$ for $s \le r \le b$;
regime DA, $n \neq const$, $m \equiv 1$ for $b \le r \le s$;
regime AB or AG, $n = 1$ for $c \le r < 1$;

The clamped edge $r = 1$ is subjected to regime B, the simply supported edge to regime G.

The uniqueness of the hinge b in the interval $s < r < 1$ lead to contradiction if the outer edge of the plate is supported : if $m(b+0) = m(b-0) = 1$, $n(b-0) = -1$, $n(b+0) = 1$ then the first equation of (1) will yield

$$m(b \pm 0) + (b \pm 0)m'(b \pm 0) - n(b \pm 0) = bq(b \pm 0)$$

and by using continuity of function $q(r)$ of $r = b$, we get $m'(b+0) - m'(b-0) = 2/b > 0$ which is in contradiction with inequalities $m'(b-0) \ge 0$ and $m'(b+0) \le 0$. Therefore, in certain segment $[b, c]$ with positive length regime DA takes place and $m \equiv 1$, $v \equiv a_1 = const$.

The bending moment m is subjected to the following boundary conditions:

$m(0) = 1$, $m(a) = 0$ if $a \neq 0$, $m(s) = -1$;

at unsupported or simply supported edge $m(1) = 0$;
at clamped edge $m(1) = -1$;
at yield hinges $m(b) = 1$, $m(c) = -1$.

The determination of the parameter T of the amplitude-function $\Phi(t)$ will be considered later in particular cases.

The plate comes to rest when $\dot{w} = 0$, i.e. at instant $t = T$. The distribution of residual deflections will be calculated by using the equation

$$w(r,T) = \int_0^T v(r)(T-t)dt = \frac{1}{2}T^2 v(r). \tag{5}$$

The location $s = s_0$ of the additional support is assumed to be optimal, when

$$\max_{a \le r \le 1} w(r,T) \to min.$$

3 Solution of basic equations

Now we shall integrate the equations of motion (1), taking into account that $\ddot{w} = -v(r)$ and expressions (3)-(4). In case of the plate with free external edge the integration is carried out in two intervals, otherwise in four intervals. Making use of continuous and boundary conditions for bending moments m, n and shear force q, we can determine the constants of integration, the parameters a_0 and a_1 of the mode of velocity field, as well the radii of bending yield hinges b and c as functions of the radius s of the additional support.

We shall present some results for particular cases of boundary conditions.

Region $a \le r \le s$. For all cases 1–4 the bending moment can be expressed as follows

$$m(r) = -\frac{a}{r} + 1 + \frac{a_0}{s-a}\left[r^3 - 2sr^2 + 2a^2(3s-2a) + \frac{3a-4s}{r}a^3\right]. \tag{6}$$

The parameter of velocity field is

$$a_0 = \frac{2s-a}{(s+3a)(s-a)^2}. \tag{7}$$

Region $s \le r \le 1$.

1) For the plate with free edge, the distribution of the bending moment can be expressed as follows

$$m(r) = -1 + \frac{1}{r} - \frac{a_1}{1-s}\Big(r^3 - 2sr^2 + 6s - 4 - \frac{4s-3}{r}\Big), \tag{8}$$

the parameter

$$a_1 = \frac{1}{(1-s)^2(3+s)}\,. \tag{9}$$

2) As mentioned above, in case of supported outer edge of the plate segment $b \le r \le c$ is in regime DA, where $m(r) \equiv 1$ and the velocity field may be represented in form (4). Then

$$m'(b) = m'(c) = 0; \qquad n(b) = -1, \qquad n(c) = 1, \qquad n'(r) > 0.$$

By the first equation of system (1)

$$q(b) = \frac{2}{b}, \qquad q(c) = 0.$$

The integration of (1) yields in the region $[s, b]$

$$m(r) = 1 - \frac{a_1}{b-s}\Big[r^2(r-2s) - 2b^2(2b-3s) + \frac{b^3(3b-4s)}{r}\Big], \tag{10}$$

$$a_1 = \frac{2s}{(b-s)^2(3b+s)}; \tag{11}$$

in the region $[b, c]$

$$m(r) \equiv 1, \qquad q(r) = \frac{2(c^2-r^2)}{(c^2-b^2)r}, \qquad n(r) = 1 - rq, \tag{12}$$

$$a_1 = \frac{1}{3(c^2-b^2)}; \tag{13}$$

in the region $[c, 1]$

$$m(r) = \frac{a_1}{1-c}\Big[r^2(r-2) + 2c^2(3-2c) + \frac{4c^3 - 6c^2 + 1)}{r}\Big] + 1 + \frac{m_1 - 1}{r}, \tag{14}$$

where $m_1 = 0$ for simply supported edge, $m_1 = -1$ for clamped edge,

$$a_1 = \frac{1 - m_1}{(1-c)^2(1+3c)}. \tag{15}$$

4 Determination of initial field of modal velocities

We will consider how to connect the actual initial velocities $u(r)$ and modal velocities $\dot{w}(r,0)$. Since the shape function $v(r)$ is prescribed, the problem is reduced to determination of parameter T of amplitude-function. Next we shall determine the magnitude T by the method of Martin and Symonds [8].

For the part remaining both inside and outside of the support we will choose different amplitude-functions

$$\Phi_0(t) = T_0 - t, \qquad \Phi_1(t) = T_1 - t,$$

thus, that the time of motion for parts of the plate may be different.

Parameters T_0 and T_1 are chosen taking into account the Martin and Symonds method

$$T_i = \frac{\int_{S_i} u(r)v(r)rdr}{\int_{S_i} v(r)rdr}, \qquad (i = 0, 1), \tag{16}$$

where $S_0 = [a, s]$ and $S_1 = [s, 1]$.

Denominator N_0 of fraction (16) for a region S_0 is

$$N_0 = \frac{1}{12}a_0^2(s-a)(s+3a).$$

For a region S_1 denominator N_1 is

$$N_1 = \frac{a_1^2}{12}(1-s)(3+s),$$

if the outer edge is simply supported and

$$N_1 = \frac{a_1^2}{12}\left[1 - s^2 - b(2s+3b) + c(2+3s)\right],$$

if the outer edge is clamped.

The numerator of fraction (16) depends on velocity field $u(r)$. We consider the following four cases of actual initial velocity field. Note, that $u(0) = 1$.

1) Uniform loading $u(r) \equiv 1$:

$$\begin{aligned} T_0 &= \frac{a_0}{6N_0}(s-a)(s+2a), \\ T_1 &= \frac{a_1}{6N_1}(1-s)(s+2), \\ T_1 &= \frac{a_1}{6N_1}(1+c+c^2-b^2-bs-s^2) \end{aligned}$$

for free and clamped outer edge, respectively.

Next we shall concentrate an a particular case of the circular plate where $a = 0$.

2) Linear loading $u(r) = 1 - r$:

$$\begin{aligned} T_0 &= \frac{a_0}{12N_0}s^2(2-s), \\ T_1 &= \frac{a_1}{12N_1}(1-s)^2(1+s), \\ T_1 &= \frac{a_1}{12N_1}\Big[b^3-(2-s)b^2+(s^2-2s)b+s^3-2s^2- \\ &- c^3+c^2+c+1\Big] \end{aligned}$$

for free and clamped outer edge, respectively.

3) Parabolic loading $u(r) = 1 - r^2$:

$$\begin{aligned} T_0 &= \frac{a_0}{60N_0}s^2(10-3s^2), \\ T_1 &= \frac{a_1}{60N_1}(1-s)^2(3s^2+9s+8), \\ T_1 &= \frac{a_1}{60N_1}\Big[3b^3(b+s)-(b^2+sb+s^2)(10-3s^2)- \\ &- 3c^3(1+c)+7(1+c+c^2)\Big] \end{aligned}$$

for free and clamped outer edge, respectively.

4) Sine-type loading $u(r) = \cos(\pi r/2)$:

$$
\begin{aligned}
T_0 &= \frac{4a_0}{\pi^3 s N_0}\left[4\sin\frac{\pi s}{2} - \pi s(\cos\frac{\pi s}{2}+1)\right], \\
T_1 &= \frac{2a_1}{\pi^3 N_1}\left[\pi(\pi - s) + 8\sin\frac{\pi s}{2} - 2\pi s\cos\frac{\pi s}{2} - 8\right], \\
T_1 &= \frac{4a_1}{\pi^3 N_1}\left[\frac{1}{b-s}\Big(4\sin\frac{\pi s}{2} - 4\sin\frac{\pi b}{2} - \pi s\cos\frac{\pi s}{2} + \pi b\cos\frac{\pi b}{2}\Big) + \right. \\
&+ \left. \frac{1}{1-c}\Big(4 - 4\sin\frac{\pi c}{2} + \pi c\cos\frac{\pi c}{2}\Big)\right]
\end{aligned}
$$

for free and clamped outer edge, respectively.

5 Optimal location of additional support

Now we shall determine the optimal radius of additional support.

Motion of inner and outer parts of the plate is determined by (16) and modifications of (16) are presented in the previous paragraph. Final deflection $w_f(r, T_i)$, $i = 0, 1$, attains maximum w_i at $r = a$ if $i = 0$ and at $r = 1$ or $r = b$ for simply supported and clamped edge, respectively, if $i = 1$, thus $w_i = a_i T_i^2/2, i = 0, 1$.

The optimal value $s = s_0$ is determined by the condition

$$\max_{a \le s \le 1}\{w_0, w_1\} \to min. \tag{17}$$

The maximal values of the mid-span deflections are functions of s, where $w_0(s)$ increase and $w_1(s)$ decrease, therefore condition (17) is equivalent to equality $a_0 T_0^2 = a_1 T_1^2$ and values of a_0, a_1, T_0, T_1 in corresponding cases may be calculated by formulae (7), (9), (11), (12), (14) et. al.

6 Discussion of numerical results

Here we shall present the same results for differently supported plates under varying impulsive loading.

Table 1 contains the numerical results for a circular plate with the free edge. In four cases of initial velocity $u(r)$, the optimal location of additional

Table 1:

$u(r)$	s_0	w_f	T_0	T_1	e
1	0.66305	0.43963	0.43963	0.60470	2.0325
$1-r$	0.29440	0.06303	0.07391	0.45472	2.2322
$1-r^2$	0.37242	0.12740	0.13293	0.58174	1.8550
$\cos(\pi r/2)$	0.34875	0.11127	0.11621	0.56008	1.8620

Table 2:

	s_0	b	c	w_f	T_0	T_1
simply supported	0.44145	0.70532	0.75123	0.19487	0.19487	0.27999
clamped	0.40171	0.63640	0.67662	0.16137	0.16137	0.22612

support s_0, maximal residual deflection w_f of plate for $s = s_0$, time of motion T_0 and T_1 for inner and outer parts of plates, respectively, and the economy coeffifient

$$e = \frac{\max\limits_{0 \le r \le 1} w(r, 1/2)}{w_f}$$

are calculated.

Table 3:

r	s_0	b	c
0.2	0.49606	0.74133	0.77753
0.4	0.59822	0.80360	0.82530
0.6	0.72395	0.87232	0.88197
0.8	0.85978	0.93866	0.94102

Table 4:

r	s_0	b	c
0.2	0.46281	0.68156	0.71255
0.4	0.57520	0.75842	0.77648
0.6	0.70984	0.84217	0.85004
0.8	0.85316	0.92350	0.92540

Optimal locations of additional supports and hinges coordinates for some examples for annular plates with free inner edges are presented in Table 3 (simply supported outer edge) and in Table 4 (clamped outer edge). Paper [4] presents analogous results for uniformly loaded circular plate in condition that we take into account the moving hinges ("exact" solution): $s_0 =$

0.7042, $w_f = 0.3824$, $T_0 = 0.496$, $T_1 = 0.505$, $e = 2$. In case of modal solution, the difference in location of additional support is 6%, of residual deflection – 15%, of time of motion 10% and 20% respectively.

Table 2 for $u(r) = 1$ in addition to the analogous values s_0, w_f, T_0, T_1 present values of the radii of stationary hinges b and c. For the simply supported edge the "exact" solution [4] gives $s_0 = 0.46667$, $w_f = 0.1634$ and for the clamped edge $s_0 = 0.4257$, $w_f = 0.1355$.

References

[1] Lellep, J., Optimization of plastic structures. *Tartu University Press*, 1991.

[2] Lepik, Ü., Optimal design of inelastic structures under dynamic loading. *Tallinn, Valgus*, 1982 (in Russian).

[3] Mróz, Z., Rozvany, G.I.N., Optimal design of plastic structures with variable support conditions. *J. Optimiz. Theory and Appl.*, 1975, $N°15$, 85-101.

[4] Olenev, G., Optimal location of additional supports for rigid-plastic circular plates in the case of impulsive loading. *Tartu Riikl. Ülik. Toim.*, 1983, $N°659$, 30-41 (in Russian).

[5] Prager, W., Rozvany, G.I.N., Plastic design of beams: optimal locations of supports and steps in yield moment. *Int. J. Mech. Sci.*, 1975, $N°17$, 627-631.

[6] Rozvany, G.I.N., Analytical treatment of some extended problems in structural optimization. *J. Struct. Mech.*, 1974-1975, 3, $N°3$ 359-385.

[7] Rozvany, G.I.N., Structural design via optimality criteria. *Dordrecht, Kluwer*, 1989.

[8] Symonds, P., Dynamics of nonelastic structures. *Moscow, Mir Publishers* 1982 (in Russian).

Оптимальное положение дополнительных опор к жесткопластическим круговой и кольцевой пластинкам при импульсном нагружении

Геннадий Оленев, Кальё Соонетс

Резюме

В работе изучаеця поведение импульсивно нагруженных идеально жёсткопластических круглых и кольцевых пластинок и находится оптимальное расположение дополнительных опор к ним. Материал пластинки удовлетворяет условию текучести в виде квадрата.

Рассматриваются следующие виды закрепление пласитнки: 1) круглая пластинка а) со свободно опёртым краем, б) с жёсткой заделкой края, в) со свободным краем и 2) кольцевая пластинка со свободным внутренним и жёстко заделанным внешним краями.

В начальный момент времени недеформированная пластинка имеет определённую скорость непрендикулярно к срединной поверхности пластинки.

Рассматриваются четыре поля действительных начальных скоростей . Задача решается методом модальных движений . При этом мода поля скоростей точек пластинки аппроксимирыется кусочно-линей ной функцией и шарнирные окружности стационарны.

Параметр начальной скорости выбирается согласно критерию, предложенному Дж. Мартином и П. Саймондсом, причём амплитудные функции для частей пластинки, не имеющих подкреплённых точек, различны.

Ставится задача найти оптимальное расположение жесткой дополнительной круговой опоры, при котором максимальный остаточный прогиб для всей пластинки был бы минимален.

On the system of ordinary differential equations with a parameter describing dynamic bending of a plastic cylindrical shell

GENNADI OLENEV

Tartu University

Abstract In the present paper the region of variation of a geometric parameter of the cylindrical shell under blast loading is divided into subdomains of motion.

1 Statement of the problem

The problem of dynamic bending of a clamped at the one end and free at the other end ideal rigid-plastic cylindrical shell in the case of uniform impulse loading is reduced to solution of systems of ordinary differential equations. The system, describing the motion of the shell takes in the initial phase the following form [2]:

$$\begin{cases} \dot{\eta} = \dfrac{f(\eta)}{2\eta(1-\eta)\varphi}, \\ \dot{u} = -c^2 - \dfrac{6}{(1-\eta)^2} + \dfrac{(v-u)f(\eta)}{2\eta(1-\eta)^2\varphi}, \\ \dot{v} = -c^2 + \dfrac{6}{(1-\eta)^2}, \end{cases} \tag{1}$$

where

$$\begin{aligned} f(\eta) &= c^2\eta^2(1-\eta)^2 + 12(1-2\eta), \\ \varphi &= u - v\eta, \end{aligned}$$

c^2 is a positive constant (see note at the end of the present paper) and $\dot{()} = d()/d\tau$.

To the system (1) belong the initial conditions

$$\eta(0) = 0,\ u(0) = 1,\ v(0) = 1. \tag{2}$$

Note that from (1) follows the differential equation

$$\eta f(\eta)\ddot{\eta} + 3(1-\eta)^2(c^2\eta^2 - 4)\dot{\eta}^2 = 0,$$

which, as shown by making use of *REDUCE*, does not have an analytical solution.

From (1) and (2) follow the conditions:

$$\eta(0)\dot{\eta}(0) = 6,\ \dot{u}(0) = -c^2 - 6,\ \dot{v}(0) = -c^2 + 6, \tag{3}$$

where

$$\eta(0) := \lim_{\tau \to 0+} \eta(\tau)$$

etc.

Let's consider the maximal interval $(0; T)$ where the solution of the initial problem (1),(2) exists and satisfies the condition $\eta(\tau) > 0$. Then the inequality $\dot{\eta}(\tau) > 0$ follows from (1) and (3), if $f(\eta(\tau)) \neq 0$.

As $\varphi(0) = 1$ and

$$\dot{\varphi} = -\frac{c^2}{2}(2-\eta) - \frac{6(1-\eta+\eta^2)}{\eta(1-\eta)^2} < -0.5(c^2+36),$$

then $T < +\infty$.

Let's mark by η^* the unique root of equation $f(\eta) = 0$ for the interval $(0; 1)$.

In the given problem the condition for the permissible axial bending moment is represented in the form $c^2\eta^2 \leq 12$. The circumferencial hinge with the coordinate η disappers, if φ vanishes.

Let's pose the question: when is the first phase of the shell motion is terminated?

The answer depends on the value of the dimensionless geometric parameter c^2, which in the case of real tubes may have the value of ten thousands.

2 Investigation of the system

There are four essential possibilities for terminating the first phase of motion, associated with the system (1), initial conditions (2) and (3), which retain the continuity the right parts, and namely:

1) transverse velocity u of the hinge with coordinate η becomes equal zero;

2) transverse velocity v of the free end of the shell vanishes;

3) the hinge η reaches the free end of the shell;

4) the hinge η disappears or a new hinge with a coordinate η_1 [2] appears in the clamped end of the shell.

It is clear that $\eta \neq 1$, if it had not previously assumed the value η^*. Function $u \neq 0$ and more over $v \neq 0$ before φ has vanished, because, considering the definition of φ the equality $u = v$ could have been only earlier (or no later) than $v = 0$, if $u > 0$. However, u cannot be equal to v earlier than φ equals 0, because, on the one hand, at the instant $\tau = \tau_0$, when $u(\tau_0) = v(\tau_0)$, we have $\dot{u}(\tau_0) \geq \dot{v}(\tau_0)$, on the other hand, from (1) follows

$$\dot{u}(\tau_0) - \dot{v}(\tau_0) = -\frac{12}{[1 - \eta(\tau_0)]^2} < 0,$$

which is contradictory. Consequently, the cases 1) and 2) cannot take place.

Further let's prove that $\eta < \eta^*$ before $\varphi = 0$. Otherwise exists the instant $\tau = \tau^*$ such that $f(\eta(\tau^*)) = 0$ but $\varphi(\tau*) > 0$, if $0 \leq \tau \leq \tau^*$. Then it follows from (1) that

$$\lim_{\tau \to \tau^*} \dot{\eta}(\tau) = \lim_{\tau \to \tau^*} f(\eta(\tau^*)) = 0.$$

Therefore, using the L'Hospital rule

$$\lim_{\tau \to \tau^*} \frac{\dot{\eta}}{f(\eta)} = \lim_{\tau \to \tau^*} \frac{\ddot{\eta}}{f'(\eta)\dot{\eta}}$$

and also considering the first equation of the system (1), for calculating $\ddot{\eta}$ in the second limit, we conclude that $\dot{\varphi}(\tau^*) = 0$.

On the other hand, using (1), it is easy to show that

$$\dot{\varphi}(\tau^*) = -c^2(1-\eta*) - \frac{6(1+\eta^*)}{(1-\eta^*)^2} < 0.$$

This contradiction concludes our proof.

Finally we shall demonstrate that existence of the instant $\tau = \overline{\tau}$, where $\varphi(\overline{\tau}) = 0$, but $c^2\eta^2(\tau) \leq 12$ and $\eta(\tau) < \eta^*$ for $\tau \in [0;\overline{\tau}]$, leads also to contradiction.

In this case it follows from the first equation of the system (1) that

$$\lim_{\tau \to \overline{\tau}-} \dot{\eta}(\tau) = +\infty.$$

From the equality obtained by using the L'Hospital rule

$$\lim_{\tau \to \overline{\tau}-} (\varphi\dot{\eta} + \frac{\varphi^2\ddot{\eta}}{\dot{\varphi}}) = 0$$

follows that

$$g(\eta(\overline{\tau})) = 0, \tag{4}$$

where

$$g(\eta) = [c^2\eta^2(1-\eta)^2 + 12(2\eta-1)](2\eta-1) + 24\eta(1-\eta).$$

However, in the case $0.5 \leq \eta \leq 1$ we have $g(\eta) > 0$; for the case $0 < \eta < 0.5$, considering the condition $c^2\eta^2 \leq 12$, we conclude that

$$g(\eta) \geq 12\eta(2\eta^2 - 3\eta + 2) > 0.$$

Since $g(0) > 0$, then the polynom $g(\eta)$ has no roots in the segment $[0;1]$, what conflicts with (4).

From the above discussion we conclude that there are only two possibilities:

A) an instant $\tau = \tau_1$ exists, such that $\varphi(\tau_1) = f(\eta(\tau_1)) = 0$ and $c^2\eta^2(\tau) \leq 12$ if $0 \leq \tau \leq \tau_1$;

B) there exists the instant $\tau = \tau_2$, where $c^2\eta^2(\tau_2) = 12$, but $\varphi(\tau) < 0$ and $\eta(\tau) < \eta^*$ for $0 \leq \tau \leq \tau_2$.

The case A) takes place if $c^2(\eta^*)^2 \leq 12$. Taking into account the condition $f(\eta^*) = 0$ this inequality is equivalent to $\eta^* \leq \sqrt{2}/(1+\sqrt{2})$ or $c^2 \leq 6(3+2\sqrt{2})$. The case B) is realized if $c^2 > 6(3+2\sqrt{2})$.

Note. There is a mistake in the system of equations (2.13) in [2]: instead of ψ there should be ψ^2. Therefore numerical solution of this system of differential equations shows that, indeed, $v(\tau_{32}) > 0$ in accordance with the assumption made in [2].

An analogous problem was solved in the paper [1] where the authors consider rectangular uniform loading. But the solution is found only for comparatively small values of loads and for parameter $c^2 = 4\ell^2/(hR)$, where ℓ, h and R are the length, thickness and radius of the shell respectively.

References

[1] Kolesnikov, S.M., Kostrik, V.K., Behavior of rigid-plastic cylindrical shell subjected to internal impulsive pressure. *Prikl. Mech. (Soviet Appl. Mech.)*, 1975, 11(21), N°7, 63-69.

[2] Olenev, G., On optimal location of additional support for rigid-plastic cylindrical shell under impulsive loading. *Tartu Riikl. Ülik. Toim.*, 1983, N°659, 42-51 (in Russian).

О системе обыкновенных дифференциальных уравнений с параметром, описывающей динамический изгиб пластической цилиндрической оболочки

Геннадий Оленев

Резюме

В данной статье область изменения геометрического параметра цилиндрической оболочки, подверженной равномерной импульсной нагрузке, разбивается на подобласти, в каждой из которых движение оболочки полностью определено в рамках идеально жесткопластической модели.

Radial deflections in circular cylindrical shells under local loading

TOOMAS LEPIKULT

Tartu University

Abstract The results of computing of the displacements of cylindrical shells under local loading are presented. The loading is assumed to be perpendicular to the shell axis and distributed along the line of intersection of elliptic cylinder. The method of series expansion of solution is applied. A comparison with the results presented in [1] is carried out.

Notation

x, y, z	– rectangular coordinates;
r, h, ℓ	– radius, thickness, and length of the shell;
$\xi = x/\ell, \varphi$	– cylindrical coordinates;
$\xi', \varphi', \xi_0, \varphi_0$	– coordinates of the fixed point;
ψ	– polar angle (used for the description of loading contour);
a, b	– semi-axis of the ellipse in direction of x- and y-axis respectively;
$\rho_1 = a/r, \rho_2 = b/r, \gamma = r/h,$ $\lambda = \ell/r, \epsilon = h^2/(12r^2)$	– dimensionless parameters of the shell;
w'	– radial displacement in direction of internal normal;
$w = w'/r$	– dimensionless displacement;
X, Y, q	– components of the load;
E	– modulus of elasticity;

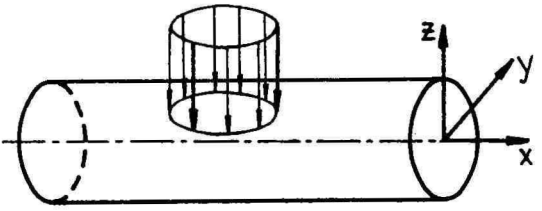

Figure 1: Loading conditions

ν	– Poisson's ratio;
$D = Eh^3/(12(1-\nu^2))$	– cylindrical stiffness of the shell;
δ_{0m}	– Kronecker's symbol;
$\Delta = \partial^2/\partial\xi^2 + \partial^2/\partial\varphi^2$	– Laplace's operator.

1 Statement of the problem

A line-load is applied on a simply supported closed cylindrical shell as shown in Fig. 1. The load is equally distributed along the cross-section of the elliptic cylinder, whose axis intersects the axis of the cylindrical shell investigated. Both axis are assumed to be perpendicular. The load is applied along the intersection line of two cylinders. The objective is to determine the radial displacements of the shell.

2 Method of solution

Next we shall briefly describe the method presented in [1]. The equilibrium equation for the cylindrical shell can be expressed in terms of radial deflections:

$$L(w) = \frac{r^3}{D}[\Delta^2(q) - L_1(X) - L_2(Y)], \tag{1}$$

where

$$L \equiv \Delta^4 + 2\nu\frac{\partial^6}{\partial\xi^6} + 6\frac{\partial^6}{\partial\xi^4\partial\varphi^2} + 2(4-\nu)\frac{\partial^6}{\partial\xi^2\partial\varphi^4} +$$

$$+ \quad 2\frac{\partial^6}{\partial\varphi^6} + \frac{1-\nu^2}{\epsilon}\frac{\partial^4}{\partial\xi^4} + 2(2-\nu)\frac{\partial^4}{\partial\xi^2\partial\varphi^2} + \frac{\partial^4}{\partial\varphi^4};$$

$$L_1 \equiv 2\nu\frac{\partial^3}{\partial\xi^3} - \frac{\partial^3}{\partial\xi\partial\varphi^2} + \epsilon\left(\frac{\partial^5}{\partial\xi\partial\varphi^4} - \frac{\partial^5}{\partial\xi^5}\right);$$

$$L_2 \equiv (2+\nu)\frac{\partial^3}{\partial\xi^2\partial\varphi} + \frac{\partial^3}{\partial\varphi^3} - 2\epsilon\left(\frac{\partial^5}{\partial\xi^4\partial\varphi} + \frac{\partial^5}{\partial\xi^2\partial\varphi^3}\right).$$

Let Φ to be the $2\pi-$ periodical fundamental solution of the operator L, i.e. the solution of the operator equation

$$L(\Phi) = \delta_{2\pi}(\xi - \xi', \varphi - \varphi'), \tag{2}$$

where

$$\delta_{2\pi}(\xi - \xi', \varphi - \varphi') = \sum_{m=-\infty}^{\infty} \delta(\xi - \xi', \varphi - \varphi' - 2\pi m) =$$

$$= \frac{1}{\pi\lambda}\sum_{m=0}^{\infty}\sum_{n=1}^{\infty}(2-\delta_{0m})\cos m(\varphi-\varphi')\sin\frac{n\pi\xi'}{\lambda}\sin\frac{n\pi\xi}{\lambda}, \tag{3}$$

$$\xi' \neq 0, \qquad \xi' \neq \lambda.$$

Then the solution of the equation

$$L(w) = N(\delta_{2\pi}), \tag{4}$$

where N denotes any linear operator is the function

$$w(\xi, \varphi) = N(\Phi). \tag{5}$$

The solution of equation (2) can be expressed as series expansion

$$\Phi(\xi, \varphi, \xi', \varphi') = \frac{1}{\pi\lambda}\sum_{m=0}^{\infty}\sum_{n=1}^{\infty}\Phi_{mn}\cos m(\varphi-\varphi')\sin\frac{n\pi\xi'}{\lambda}\sin\frac{n\pi\xi}{\lambda}, \tag{6}$$

where

$$\Phi_{mn} = \frac{(2-\delta_{0m})\lambda^8}{c_{mn}},$$

$$c_{mn} = a_{mn}^2(a_{mn} - \lambda^2)^2 + \frac{1-\nu}{\epsilon}(\lambda\pi n)^2[(1+\nu)(\lambda\pi n)^2 - 2\epsilon b_{mn}] - (\lambda\pi n)^4,$$

$$a_{mn} = (\lambda m)^2 + (\pi n)^2, \qquad b_{mn} = \lambda^4 m^2(m^2-1) - (\pi n)^4.$$

To solve the equation (1) for any particular case of loading, one can construct the linear operator N and then according to equation (5) to apply that operator to function Φ.

3 Solution of the problem

According to the method described above, the first goal is to determine the linear operator N. Let p_0 to be the intensity of the line-load. Thus, if the load is equally distributed along the ellipse, the canonical equation of which is $(x/a)^2 + (y/b)^2 = 1$ the total load P can be expressed

$$P = p_0 r \ell_0, \tag{7}$$

where

$$\begin{aligned} \ell_0 &= \int_0^{2\pi} (\rho_1^2 \sin^2 t + \rho_2^2 \cos^2 t)^{\frac{1}{2}} dt, \\ \rho_1 &= a/r, \qquad \rho_2 = b/r. \end{aligned}$$

The components of the line load are

$$\begin{aligned} X &= 0, \\ Y(\xi,\varphi) &= \frac{p_0}{r^2} \oint_L \cos^2(\varphi' - \varphi_0) \delta_{2\pi}(\xi - \xi', \varphi - \varphi') dl, \\ q(\xi,\varphi) &= \frac{p_0}{r^2} \oint_L \sin(\varphi' - \varphi_0) \cos(\varphi' - \varphi_0) \delta_{2\pi}(\xi - \xi', \varphi - \varphi') dl, \end{aligned} \tag{8}$$

where L denotes the loading contour, φ' and ξ' – coordinates of the line element dl, φ_0 – rotation of the loading axis.

The parametric equations of the contour of integration are

$$\begin{aligned} x &= r(\rho_1 \cos\psi + \xi_0), \\ y &= r\rho_2 \sin\psi, \\ z &= r(1 - \rho_2^2 \sin^2\psi)^{frac12}, \qquad 0 \le \psi \le 2\pi, \end{aligned} \tag{9}$$

where $r\xi_0$ stands for the $x-$coordinate of the loading axis.

The coordinates φ' and ξ' can be expressed in terms of parameter ψ as follows:

$$\begin{aligned} \varphi' &= \varphi_0 + \arcsin(\rho_2 \sin\psi), \\ \xi' &= \xi_0 + \rho_1 \cos\psi. \end{aligned} \tag{10}$$

Now it is possible to express the contour integrals (8) in terms of definite integrals:

$$\begin{aligned} X &= 0, \\ Y(\xi,\varphi) &= \frac{p_0}{r^2}\int_0^{2\pi} f_1(\rho_2,\psi) f_2(\rho_1,\rho_2,\psi)\delta_{2\pi}(\xi-\xi',\varphi-\varphi')d\psi, \\ q(\xi,\varphi) &= \frac{p_0}{r^2}\int_0^{2\pi} f_3(\rho_2,\psi) f_2(\rho_1,\rho_2,\psi)\delta_{2\pi}(\xi-\xi',\varphi-\varphi')d\psi, \end{aligned} \tag{11}$$

where

$$\begin{aligned} f_1(\rho_2,\psi) &= \rho_2\sin\psi, \\ f_2(\rho_1,\rho_2,\psi) &= (\rho_1^2\sin^2\psi+\rho_2^2\cos^2\psi-\rho_1^2\rho_2^2\sin^4\psi)^{\frac{1}{2}}, \\ f_3(\rho_2,\psi) &= (1-\rho_2^2\sin^2\psi)^{\frac{1}{2}}. \end{aligned} \tag{12}$$

The next step is to use the expressions for load components (11) in equation (1). The linear operator N for equation (4) can be written in the form

$$\begin{aligned} N \equiv \frac{p_0 r^2}{D}\int_0^{2\pi} &[\Delta^2(\cdots) f_3(\rho_2,\psi) f_2(\rho_1,\rho_2,\psi) - \\ &-L_2(\cdots) f_1(\rho_2,\psi) f_2(\rho_1,\rho_2,\psi)]d\psi. \end{aligned} \tag{13}$$

To obtain the residual deflections one can, reply according to (5) that operator to function Φ. The result is

$$w(\xi,\varphi) = \frac{p_0 r^2\lambda^3}{\pi D}\sum_{m=0}^{\infty}\sum_{n=1}^{\infty}(w_{mn}^1\cos m\varphi + w_{mn}^2\sin m\varphi)\sin\frac{n\pi\xi}{\lambda}, \tag{14}$$

where

$$w_{mn}^1 = \frac{(2-\delta_{0m})d_{mn}^1}{c_{mn}}, \qquad w_{mn}^2 = \frac{(2-\delta_{0m})d_{mn}^2}{c_{mn}},$$

$$d_{mn}^1 = \int_0^{2\pi} f_2(\rho_1,\rho f_2,\psi)[f_3^{mn}(\rho_2,\psi)\cos m\varphi' + f_1^{mn}(\rho_2,\psi)\sin m\varphi']\sin\frac{n\pi\xi'}{\lambda}d\psi,$$

$$d_{mn}^2 = \int_0^{2\pi} f_2(\rho_1,\rho_2,\psi)[-f_1^{mn}(\rho_2,\psi)\cos m\varphi' + f_3^{mn}(\rho_2,\psi)\sin m\varphi']\sin\frac{n\pi\xi'}{\lambda}d\psi,$$

$$f_1^{mn}(\rho_2,\psi) = f_1(\rho_2,\psi)[2a_{mn}\epsilon\pi^2 mn^2 + \lambda^2 m(a_{mn} + (1+\nu)\pi^2 n^2],$$

$$f_3^{mn}(\rho_2,\psi) = f_3(\rho_2,\psi)a_{mn}^2.$$

4 Numerical results

In limit process $\rho_1 \to 0$ and $\rho_2 \to 0$ the loading described above tends to the concentrated load in point (ξ_0, φ_0). To compare the results with the ones, presented in [1] the calculations for $\varphi_0 = 0, \xi_0 = \lambda/2, \rho_1 = \rho_2 = 10^{-6}$ were carried out. In tables 1 - 2 the quantities $w_0 = P^{-1}Er^2 w(\varphi_0, \xi_0)$ as well as relational deviations r from the results in [1] are presented.

Table 1:
$\gamma = 100$

λ	w_0	$r(\%)$
1	10897	2.49
3	19665	2.46
5	25952	2.44
7	31248	2.48
9	35806	2.46
11	40497	2.46
13	45457	2.39
15	50140	2.39
17	54059	2.45
19	57108	2.45

Table 2:
$\lambda = 5$

γ	w_0	$r(\%)$
20	747	2.48
25	1210	2.23
33	2221	4.63
50	5582	2.51
100	25952	2.44
200	120158	3.00

Another limit process when only $\rho_1 \to 0$ may approximate the line load along the arc $\xi = const, \varphi_1 \leq \varphi \leq \varphi_2$. The results for $\rho_1 = 10^{-6}, \varphi = \varphi_0 = 0, \xi = \xi_0 = \lambda/2$, and comparison with results in [1] are presented in tables 3 – 5.

Table 3:
$\gamma = 100, \rho_2 = \sin(\pi/10)$

λ	w_0	$r(\%)$
1	3040	3.61
3	9466	3.10
5	15033	3.17
7	20000	3.22
9	24444	3.30
11	29105	3.36
13	34052	3.42
15	38745	3.47
17	42713	3.49
19	45857	3.52

Table 4:
$\lambda = 5, \rho_2 = \sin(\pi/10)$

γ	w_0	$r(\%)$
20	594	4.96
25	931	3.42
33	1631	5.34
50	3793	3.31
100	15033	3.17
200	57309	3.04

Table 5:
$\gamma = 100, \lambda = 5$

ρ_2	w_0	$r(\%)$
$\sin(\pi/4)$	4672	3.34
$\sin(\pi/6)$	8837	3.25
$\sin(\pi/8)$	12367	3.42
$\sin(\pi/10)$	15033	3.17
$\sin(\pi/12)$	17041	2.97
$\sin(\pi/14)$	18563	2.80
$\sin(\pi/16)$	19732	2.57

In all calculations the expansion series were calculated for indexes $m = 0, 1, \ldots, 40$ and $n = 1, 2, \ldots, 81$. The integrals were calculated using the Simpson-method with 41 noddle-points.

References

[1] Zhigalko, J.P., Gurjanov, N.G. Calculation of displacements of simply supported cylindrical shell subjected to concentrated load. *Issl. po teorii plastin i obolochek*, Vol. 3, 1965, 71-80 (in Russian).

Радиальные прогибы круговых цилиндрических оболочек под действием локальной нагрузки

Тоомас Лепикулт

Резюме

Приводятся результаты вычисления малых прогибов круговых цилиндрических оболочек под действием локальной нагрузки. Нагрузка распределена по линии сечения оболочки с эллиптическим цилиндром. Решение строится в виде тригонометрического ряда. Проведено сравнение с результатами работы [1].

Particle deformation during cold pressing of metal powders

JAAN LELLEP and ANDRES LAANSOO

Tartu University and Tallinn Technical University

Abstract The plastic deformations of spherical particles compressed between two rigid plates are considered. An approximate technique of determination of the stress-strain state of the sphere has been developed. The plastic deformations of the flake shape iron powder particles have been successfully studied by the proposed model.

1 Introduction

Cold compaction is an essential operation in the traditional powder metallurgy. During compaction the particles of ductile metals are subjected to plastic deformations to form interparticle contacts and generate internal stresses. For example, spherical particles change their shape by flattening on a more complicated mechanism, which reveals the phenomena of anisotropy electrical, magnetic and mechanical properties of the compacts.

Internal stresses in the ferromagnetic powder particles during compacting decrease the magnetic permeability and increase hysteresis losses of soft magnetic composite materials (magnetodielectrics). The effect of heat treatment of these materials at $450 - 550°C$ and recristallization process depend on the amount of the plastic deformation and the distribution of ferromagnetic particles in the volume.

Changes of geometry of metal particles during pressing can be assesed by combining the individiual behaviour patterns. Mathematical models utilizing uniform spheres [1-3] have provided useful tools allowing to estimate the changes of particle shape, contact areas, density of powder compacts as a

function of compacting pressure.

The theoretical models of behaviour of a spherical particle which will be deformed into a regular dodecahedra or cylindrical metal die are described in [2]. The greatest calculated amount of flattening sphere (cold work) is by B.Wenglinsky 8.6 – 14.5% . This approach was based on the assumption that plastic deformation of the spherical particles will be restricted only to a thin external layer of particles. A geometrical model of the powder material was developed in [3] on the basis of a simple cubic structure of spherical particles. The calculated maximum value of plastic deformation of flattened particles was 46.7 % .

2 Problem formulation and theoretical predictions

Let us consider a sphere of radius R. The material of the sphere is assumed to be ideally plastic with no work-hardening. Elastic deformations have been neglected. The material of the sphere has the yield stress δ_y and shear strength $\tau = \sigma_y/3$ and it will be compressed by force P between two absolutely rigid plates. Assume that the plastic deformations are not very large, the mass forces of particles and deformation of plates are negligible.

The radial and axial strain components can be expressed in the cylindrical coordinate system as:

$$\begin{aligned} \varepsilon_r &= \frac{\partial u}{\partial r}, & \varepsilon_\theta &= \frac{U}{r}, \\ \varepsilon_z &= \frac{\partial w}{\partial z}, & \gamma &= \frac{\partial u}{\partial z} + \frac{\partial w}{\partial z}. \end{aligned} \tag{1}$$

For the rigid-plastic body on the basis of the concept of incompressibility, it can be written

$$\frac{\partial u}{\partial r} + \frac{U}{r} + \frac{\partial w}{\partial z} = 0. \tag{2}$$

Now let us consider only a half of a spherical body pressed between two rigid plates (Fig.1). In the case of Von Mises yield condition, the rates of displacements will follow the potential function $\psi = \psi(r, z)$ taking the form

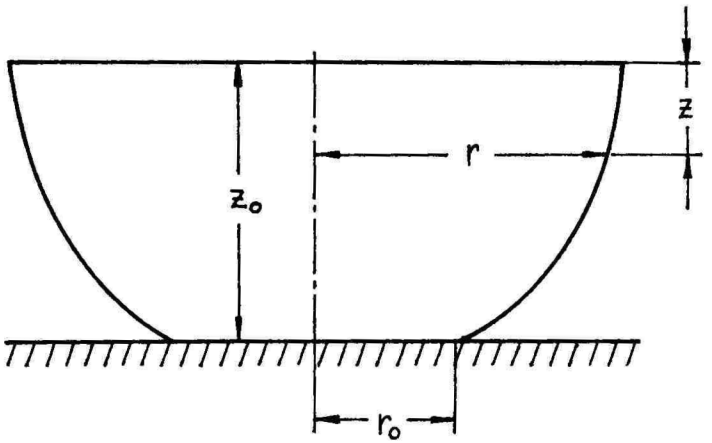

Figure 1: Scematic illustration of half of sphere subjected to pressure

$$u = -\frac{1}{r}\frac{\partial \psi}{\partial z}; \qquad w = \frac{1}{r}\frac{\partial \psi}{\partial r}\ . \tag{3}$$

The kinetic boundary conditions are

$$w|_{z=0} = 0; \qquad w|_{z=z_0} = -w_0; \qquad u|_{r=0} = 0.$$

The statical boundary conditions satisfying this criterion integrally are

$$\begin{aligned} 2\pi \int_0^R \sigma_z|_{z=0} r dr &= -P, \\ 2\pi \int_0^r \sigma_z|_{z=z_0} r dr &= -P, \end{aligned} \tag{4}$$

where $z_0 = R - W_0$.

Assuming that the contact zone is located on a plane and

$$V(z) = \frac{w''}{\sqrt{|z|w'}}, \tag{5}$$

the following equation is obtained

$$V = Az + B. \tag{6}$$

The integrating constants A and B will be determined from the boundary conditions (5). After integration the following relation is eventually obtained

$$w = B \int_0^z e^{\sqrt{3}Az^2} dz, \tag{7}$$

where

$$B = -w_0 \Big(\int_0^{z_0} e^{\sqrt{3}Az^2} dz \Big)^{-1}. \tag{8}$$

The integrating constants A and C_1 will be calculated according to (5) and have the form

$$C_1 = \sigma_T - \frac{2}{R^2} P + A\tau_0 \frac{R^2}{4}, \tag{9}$$

$$A = \frac{2p\big(1 - \frac{r_0}{R^2}\big)}{\tau_0 r_0^2 [z_0^2 + \frac{1}{4}(r_0^2 - R^2)]}. \tag{10}$$

The results for the stress components can be written as

$$\sigma_r = \sigma_T - \frac{2p}{R^2} - \frac{2p\big(1 - \frac{r_0}{R_0}\big)\big(z^2 + \frac{r^2}{2} - \frac{R^2}{4}\big)}{r_0^2 \big[z_0^2 + \frac{1}{4}(r_0^2 - R^2)\big]}, \tag{11}$$

$$\sigma_z = \sigma_r - \sigma_T, \tag{12}$$

$$\tau = A\tau_0 zr. \tag{13}$$

After integrating the following equations are obtained

$$\sigma_0 z_0 - A\tau_0 \Big(\frac{R^3}{12} - r_0^2 \frac{R}{2} \Big) - \frac{2P}{R} = 0, \tag{14}$$

$$r_0 e^{\frac{A}{\sqrt{3}} z_0^2} \Big(1 - \frac{w_0}{2} \Big(\int_0^{z_0} e^{\sqrt{3}Az^2} dz \Big)^{-1} \Big) = R. \tag{15}$$

3 Numerical results

The system of equations (14) and (15) was solved numerically for iron particles with yield stress $\sigma_y = 200MPa$ and the main results are presented in Fig. 2-6.

Figure 2 describes the relation between the displacement w of the sphere with radius 0.1 to 0.9 mm and the compacting pressure. With increasing the diameter of particles the displacement w and ratio W/R , which is characterizing the degree of plastic deformation, is increasing. The components of plastic deformation ϵ_r and γ are more sensitive to changes in the dimensions of particles as to the same changes of displacements. The results of calculations in Fig.4 can be used for approximate calculation of magnetic permeability of powder magnetic materials. It was established that the values of displacements and components of strain practically do not depend on the yield strength of the material.

4 Experiments and discussion

A comparison of the calculated and measured values of plastic deformation of iron particles is given in Fig. 6.

The curves 1, 2 in Fig. 6 are obtained numerically for $R = 0.1$mm and $R = 0.7$mm, respectively. The experimental data are depicted by the curves 3 and 4. Curve 3 corresponds to the iron flake powder with $R = 0.15$ mm. However, curve 4 could be obtained for sponge iron powder with $R = 0.05$ to $R = 0.1$ mm. The average plastic deformation of single iron particles was calculated as the ratio $100W/R$. Experimental results were obtained by the investigation of microstructures of pressed samples on the base of sponge and atomized iron powders. A part of iron powders was cold rolled to get a flake shape and annealed. The powders were covered with 0.8-1.0 % epoxy resin. Compacting pressures 500 to 1100 MPa measured before pressing were employed. The dimensions of regular flattened spherical powders were measured in the horizontal and vertical directions. The approximate value of plastic deformation was calculated as the difference between these dimensions. It was assumed that the particle size in horizontal direction did not change at compacting.

The calculated values of plastic deformation of spherical models and ex-

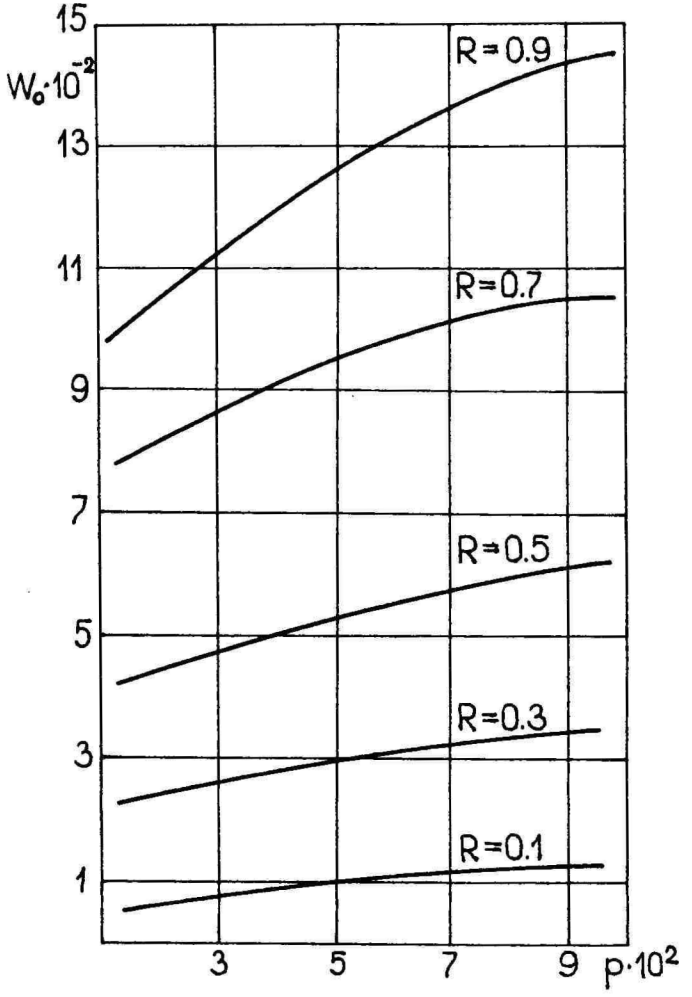

Figure 2: Relation between displacement w and compacting pressure

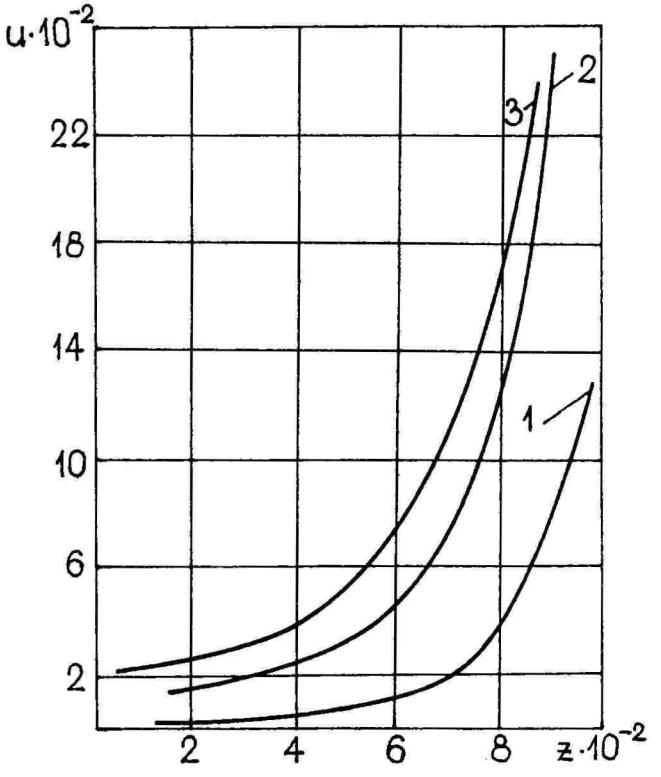

Figure 3: Radial displacement u spheres with radius 0.1mm

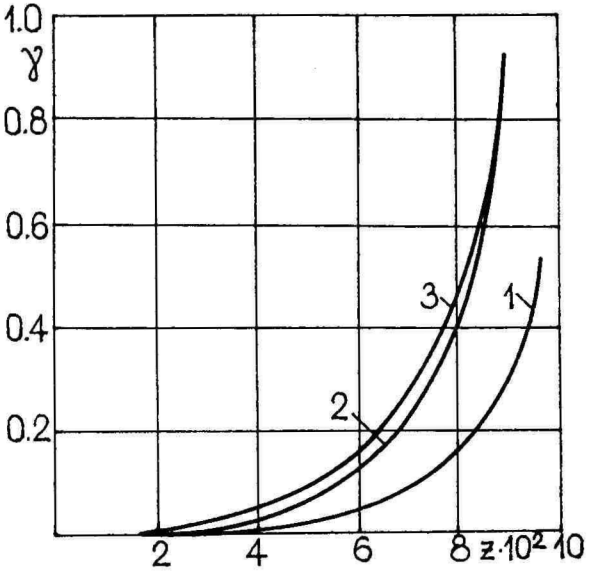

Figure 4: Tangential strain component γ

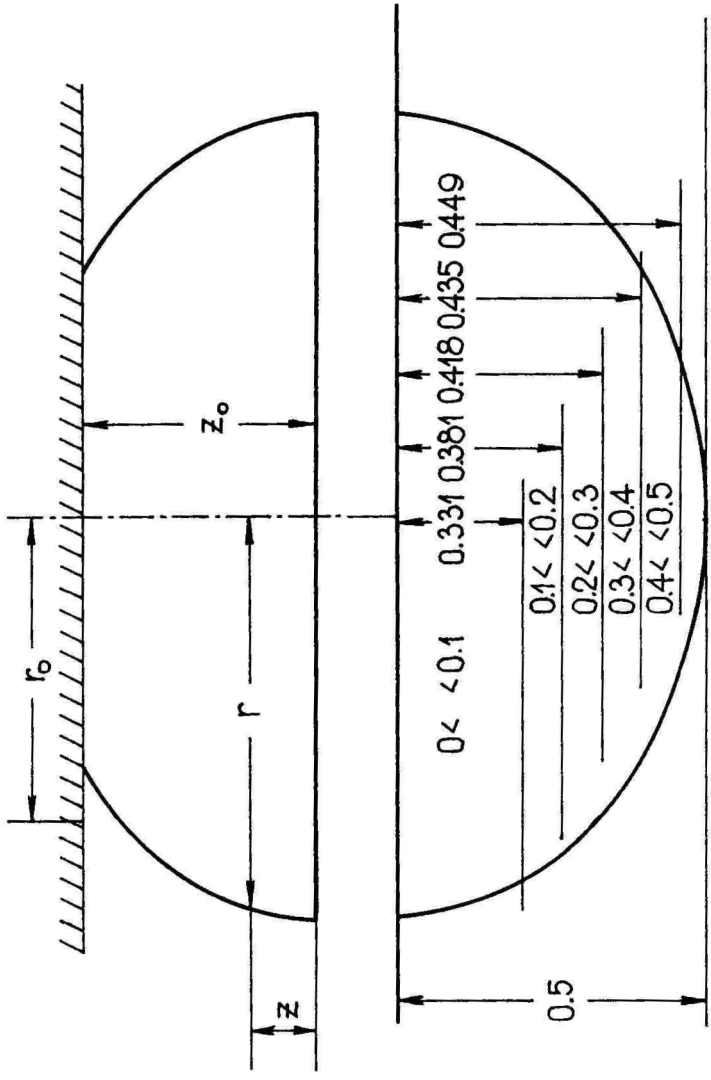

Figure 5: Areas with different strain levels

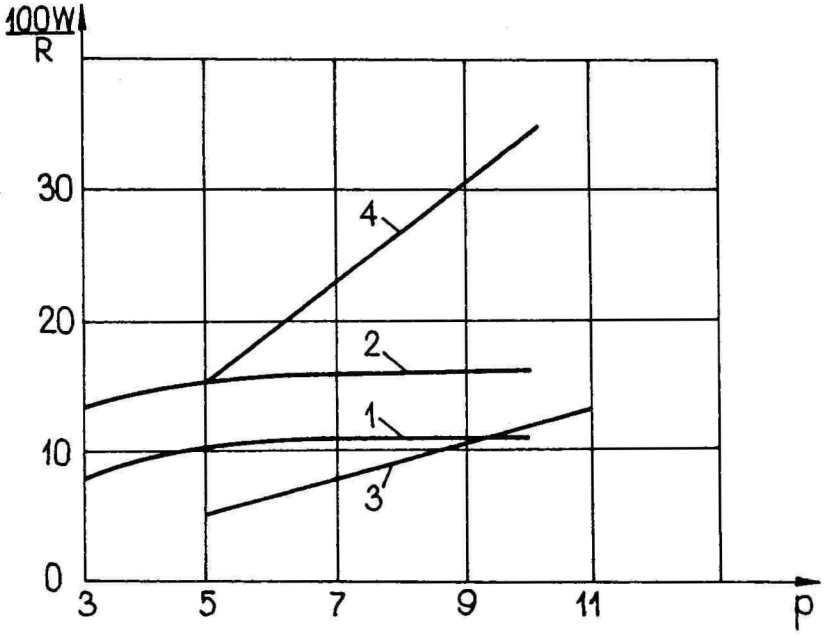

Figure 6: Plastic deformation of iron spheres and powders

perimental results agree for flake shape powder particles and for spherical sponge iron particles in the range of relatively low pressures (less than 500 MPa). The average diameter of flake shape iron particles was 0.3 mm and that of atomized iron 0.9 mm. The results of calculation of plastic deformations on the basis of the spherical models presented in Fig.5, show that the greater part of the sphere is subjected to a relatively small deformation (less than 10 %). Here the compacting pressure was 100 MPa.

Due to several approximations the model suggested and measurements of spherical particles can only give an approximate result. In fact, it was assumed that in the simple cubic packing state the spheres are of equal diameter. In this case the number of interparticle contacts will be 6 (coordination number is 6). However, actually the coordination number is more than six.

The diameter of real powder was within a range of 0.1 to 0.2 mm and the real number of contacts before compacting is more than 6. During pressing the rearrengement and plastic deformation of particles take place and the coordination number is increasing to 8-14.

The results of the experiments and the theoretical predictions are more close each other in the case of the flake iron powder.

References

[1] Moon, I.H. and Kim, K.H.,Relationship between compacting pressure, green density and green strength of copper powder compacts. *Powder Metallurgy*, 1984, 27,$N°$ 2,80-84.

[2] Kordecky, A. and Wenglinsky, B., Theoretical aspects of compaction of dielectromagnetic powder metallurgy parts. *Powder Matallurgy*, 1988, 31, $N°$ 2,113-116.

[3] Laansoo, A. and Käärdi, H., On the deformation of particles of a powder at pressing. *Proc. of Tallinn Politehn. Inst.*, 1986, 628, 66-77(in Russian).

[4] Lellep, J. and Laansoo, A., An approximate solution to the problem of compression of a plastic sphere. *Tartu Riikl. Ülik. Toim.*, 1989, 853, 101-110(in Russian).

Деформирование частиц металлического порошка при холодном прессовании

Яан Леллеп и Андрес Лаансоо

Резюме

Рассматривается поведение металлического порошка при прессовании. Отдельные частицы порошка считаются сферами, материал которых является идеально жесткопластическим. Представлен приближенный метод расчета напряженно-деформированного состояния сферических частиц сжимаемых двумя жесткими плитами.

The periodically equi-strength problem for spherical vessels under harmonic pressures

KALLE HEIN and MATI HEINLOO

Estonian Agricultural University

Abstract The one-dimensional problem of determination of rational distributions of the Young modulus in the radial direction of the spherical vessel, subjected to harmonic pressures on the external and internal radii, is set. These distributions guarantee satisfaction of the Tresca yield criterion simultaneously at all points of the spherical vessel at the moments of time when the harmonic loads reach their limit values. The rational distributions of the Young modulus and connections between limit values of amplitudes of the harmonic pressures are illustrated by graphs.

Notation

$\sigma_r^0, \sigma_\theta^0$	–	radial and hoop stress components;
u^0	–	radial displacement;
p_i, p_e	–	internal and external pressures;
a, b	–	inner and outer radii;
ϱ	–	running radius;
σ^0	–	yield stress;
ν	–	Poisson's ratio;
$E^0(\varrho)$	–	Young's modulus distribution;
γ^0	–	density;
t^0	–	time;
ω^0	–	frequency;
M	–	mass of the sphere;

1 Introduction

The analysis of the structural problems involves the solution of differential equations. It is not always possible to find an exact solution of equations especially when some moduls are functions. Therefore in most of papers these moduls are given in form of power law of variation in order to solve the problem analytically. Of course any function of a variable can be approximated by a polynomial of high accuracy and it justifies such a choice. Some particular types of non-homogeneity for spherical vessels are considered by Ghosh (1963), Chakravorty (1969), De Yudhisthir (1970), Chandra (1977), Mukhopadhyay (1982), Chakraborty (1986) and Mondal (1986). They have been demonstrated that the start of yielding depends on the nature of non-homogeneity. We shall see that yielding may start either at the inner or at the outer surface of a spherical vessel. However, if it starts at an interior point, a plastic region can be formed in between two elastic regions. The formation of more than one plastic zone is also possible as the plastic yielding can start simultaneously at both surfaces depending upon the value of Poisson's ratio and the indices of the power law.

In other studies the distributions of elastic or plastic moduli are found by means of a certain optimal criterion. Klosowisz (1968) determined the piecewise-continuous distribution of Young's modulus which guarantees minimal radial displacement on the outer surface of a spherical vessel. Hein and Heinloo (1985) have examined the equi-strenght stress state and determined the distributions of continuous and piecewise-continuous Young's modulus which guarantee satisfaction of the Tresca yield criterion simultaneously at all points when the quasistatic pressure reaches their limit values.

In this paper the possibility of achieving the above mentioned equi-strength state in the case of spherical vessels under harmonic pressures is studied.

2 Basic equations and formulation of the problem

It is convenient to introduce the following dimensionless quantities

$$\alpha = \frac{a}{b}; \qquad u = \frac{u^0}{b}; \qquad \sigma_r = \frac{\sigma_r^0}{\sigma^0}; \qquad \sigma_\theta = \frac{\sigma_\theta^0}{\sigma^0}; \qquad t = \frac{t^0\omega^0}{2\pi};$$

$$\gamma = \frac{\gamma^0 b^3}{M}; \qquad p_1 = \frac{p_i}{\sigma^0}; \qquad p_2 = \frac{p_e}{\sigma^0}; \qquad r = \frac{\varrho}{b}; \qquad E = \frac{E^0}{\sigma^0}.$$

Let us assume that the spherical vessels are made of an isotropic linearly elastic material which obeys to Tresca yield criterion. Poisson's ratio and the yield stress are constants, whereas Young's modulus is a function of the radial coordinate r. Let us consider spherical vessels under internal and external pressures which we introduce in the following form

$$p_1 = p_{10} + p_{11}\cos 2\pi t, \qquad p_2 = p_{20} + p_{21}\cos 2\pi t. \tag{1}$$

For nonhomogeneous spherical vessels subjected to the harmonic loads (1) the stresses σ_r, σ_θ and radial displacement u must satisfy the equation of motion

$$\sigma_r' + \frac{2}{r}(\sigma_r - \sigma_\theta) = \gamma \frac{\partial^2 u}{\partial t^2} \tag{2}$$

and the compatibility equation

$$m(1+\nu)(\sigma_\theta - \sigma_r) + rm\,[(1-\nu)\sigma_\theta' - \nu\sigma_r'] + rm'[(1-\nu)\sigma_\theta - \nu\sigma_r] = 0, \tag{3}$$

where $m = 1/E(r)$. In eqns (2), (3) and in all other formulae the primes denote differentiation with respect to r in this paper. We consider the vessel under pressures and therefore, the boundary conditions are

$$\sigma_r(\alpha) = -p_1, \qquad \sigma_r(1) = -p_2. \tag{4}$$

As long as the vessel is stressed elastically Hooke's law holds and by using the linear strain-displacement relations we obtain

$$u = rm\,[(1-\nu)\sigma_\theta - \nu\sigma_r], \tag{5}$$

which yields the relation between radial displacement and stress components. The Tresca yield criterion gives

$$|\sigma_\theta - \sigma_r| \leq 1. \tag{6}$$

The condition (6) establishes that all possible stress states lie within or on the Tresca yield surface. If in this condition the sign of equality is valid for

all radial coordinates r, the state lies on the yield surface and the spherical vessel is fully plastic.

Let us suppose now, that in condition (6) the sign of equality will be valid for all radial coordinates r in the moments of time t_n^*, if $|\cos 2\pi t_n^*| = 1$, $n = 1, 2, \ldots$. In this paper the distributions of Young's modulus which guarantee the satisfaction of this assumption, we call rationals and the constructions permitting such change periodically equi-strenth.

3 System of equations

Substituting (5) into equation of motion (2) we obtain

$$\sigma_r' + \frac{2}{r}(\sigma_r - \sigma_\theta) = \gamma m r\Big[(1-\nu)\frac{\partial^2 \sigma_\theta}{\partial t^2} - \nu \frac{\partial^2 \sigma_r}{\partial t^2}\Big]. \tag{7}$$

A solution of the system (3), (7) we shall seek in the form

$$\begin{aligned} \sigma_\theta(r,t) &= \sigma_{\theta 0}(r) + \sigma_{\theta 1}(r)\cos 2\pi t, \\ \sigma_r(r,t) &= \sigma_{r0}(r) + \sigma_{r1}(r)\cos 2\pi t. \end{aligned} \tag{8}$$

The system (3), (7) making use of the relations (8) gives the following system of equations

$$\begin{aligned} \sigma_{r0}' &+ \frac{2}{r}\big(\sigma_{r0} - \sigma_{\theta 0}\big) = 0, \\ \sigma_{r1}' &+ 2\sigma_{r1}\Big(\frac{1}{r} - 2\gamma\pi^2 r m \nu\Big) + 2\sigma_{\theta 1}\Big[2\gamma\pi^2 r m(1-\nu) - \frac{1}{r}\Big] = 0, \\ m(1 &+ \nu)(\sigma_{\theta 0} - \sigma_{r0}) + rm\,[(1-\nu)\sigma_{\theta 0}' - \nu\sigma_{r0}'] + \\ &+ rm'[(1-\nu)\sigma_{\theta 0} - \nu\sigma_{r0}] = 0, \\ m(1 &+ \nu)(\sigma_{\theta 1} - \sigma_{r1}) + rm\,[(1-\nu)\sigma_{\theta 1}' - \nu\sigma_{r1}'] + \\ &+ rm'[(1-\nu)\sigma_{\theta 1} - \nu\sigma_{r1}] = 0. \end{aligned} \tag{9}$$

At moments of time t_n^* taking into account (8) the condition (6) takes the following form

$$\sigma_{\theta 0} - \sigma_{r0} + k\,(\sigma_{\theta 1} - \sigma_{r1}) = \ell, \qquad \forall r \in [\alpha, 1], \tag{10}$$

where $k = \pm 1, \ell = \pm 1$. It is convenient to introduce the unknown function f as

$$\sigma_{\theta 0} - \sigma_{r0} = f. \tag{11}$$

Now, the condition (10) takes the form

$$\sigma_{\theta 1} - \sigma_{r1} = k\,(1 - f). \tag{12}$$

It is not difficult to prove that condition (6) is valid for all moments of time, if

$$0 \le k\ell f \le 1 \tag{13}$$

Excluding from the system (9) $\sigma_{\theta 0}$ and $\sigma_{\theta 1}$, making use of (11) and (12) we obtain the following

$$\begin{aligned} \sigma'_{r0} &= \frac{2}{r} f, \\ \sigma'_{r1} &= s(2\nu - 1)\sigma_{r1} + k\,(1 - f)\Big[\frac{2}{r} - s(1 - \nu)\Big], \\ m' &= mc, \\ f' &= -f\Big(\frac{3}{r} + c\Big) - \frac{1 - 2\nu}{1 - \nu} c\sigma_{r0} \end{aligned} \tag{14}$$

where

$$c = \frac{(1 - 2\nu)\, sr\, [(1 - 2\nu)\sigma_{r1} - k(1 - f)(1 - \nu)] + 3k\ell\,(1 - \nu)}{r\,[(1 - 2\nu)(\sigma_{r1} - k\sigma_{r0}) - k\ell\,(1 - \nu)]}$$

Here $s = 4\gamma\pi^2 rm$.

Now let us consider the boundary conditions for system (14). According to (1), (4) and (8) we get

$$\sigma_{r0}(\alpha) = -p_{10}, \qquad \sigma_{r1}(\alpha) = -p_{11}. \tag{15}$$

The other two boundary conditions for system (14) will be as follows

$$m(\alpha) = m_\alpha, \qquad f(\alpha) = f_\alpha, \tag{16}$$

where f_α – given values chosen in accordance with condition (13).

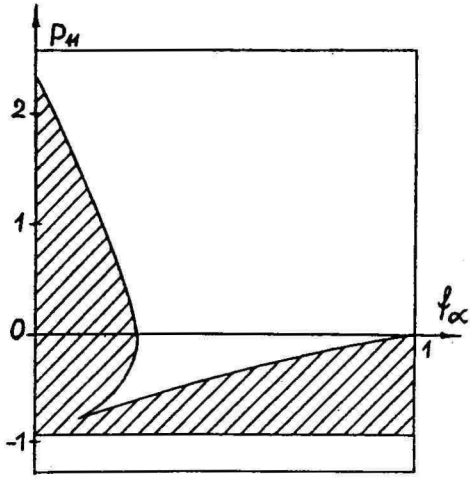

Figure 1:

4 Results of computations

The existence of a solution to the given problem also depends on satisfying of restriction $0 \leq k\ell f \leq 1$. The shaded region in Fig.1 determines the area of non-existence of a solution to the given problem on the $p_{11} - f_\alpha$ plane for $p_{10} = 1.0$, $\ell = 1$, $\nu = 0.3$, $k = 1$.

In Figs. 2-5, the solutions to the given problem are presented. All calculations have been made for $p_{10} = 1.022$, $p_{11} = 0.1$, $m_\alpha = 0.001$, $f_\alpha = -0.1$, $\alpha = 0.6$, $\nu = 0.33$. In Figs.2, 3 the distributions of all stress components have been brought out. The curves 1–4 correspond to σ_{r1}, σ_{r0}, $\sigma_{\theta 1}$, $\sigma_{\theta 0}$ respectively. In Fig.2 $k = 1$ and in Fig.3 $k = -1$ are presented. In Figs.4, 5 one can see the distributions of $f \cdot \ell$ and Young's modulus distributions respectively, whereas curves 1 correspond to the case $k = 1$ and curves 2 to $k = -1$.

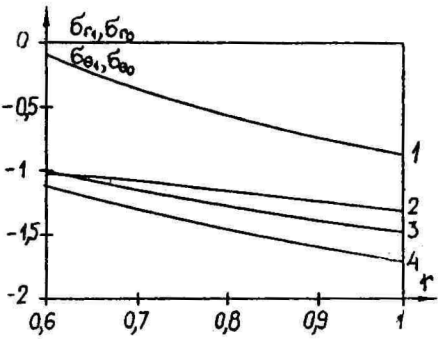

Figure 2:

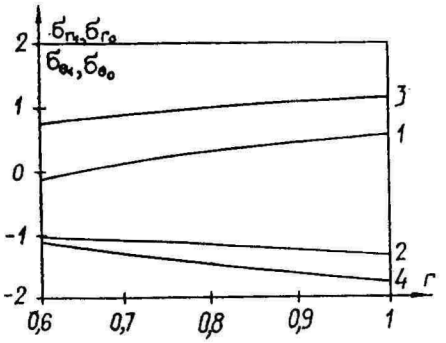

Figure 3:

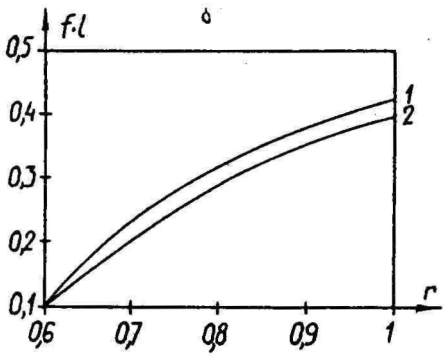

Figure 4:

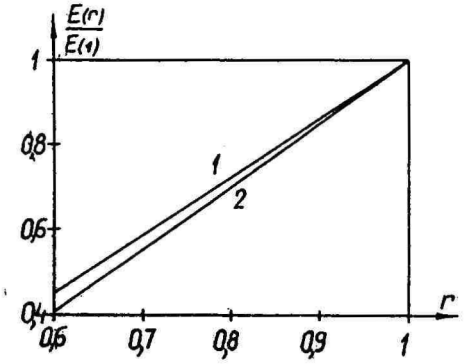

Figure 5:

References

[1] Ghosh,D., Elasto-plastic stresses in a spherical pressure vessel of non-homogeneous material, *J. of Sci. and Engng. Research*, 1963, *N*°7, 308-318.

[2] Chakravorty, J.G., Plastically nonhomogeneous shells under internal pressure, *AIAA J. Techn. Notes*, 1969, *N*°7, 1601-1602.

[3] Yudhisthir, D., Stresses in a non-homogeneous composite spherical pressure vessel, *Fen. Fak. Mech. Istanbul. Univ. Rev. Fac. Sci.*, 1970, *N*°35, 109-113.

[4] Chandra,R.S., Radial deformation of a nonhomogeneous spherically isotropic elastic sphere with a concentric spherical inclusion, *Proc. Ind. Acad. Sci.*, 1977, *N*°85, 338-350.

[5] Mukhopadhyay, J., Effect of non-homogeneity on yield stress in a thick-walled spherical vessel under pressure, *Rev. Roum. Sci. Ser. Mec. Appl.*, 1982, *N*°27, 367-372.

[6] Chowdhury, B., Chakraborty, S. K., Elastic-plastic deformation of non-homogeneous cylindrical and spherical shells, *Proc. Indian Natn. Sci. Acad.*, 1986, *N*°52, 1347-1356.

[7] Mondal, N.C., The effects of nonhomogeneity on the stresses in a gravitating sphere with a rigid core and in a spherical shell under pressure. *Rev. Roum. Sci. Techn. Ser. Mec. Appl.*, 1986, *N*°16, 557-568.

[8] Hein,K., Heinloo, M., Optimal nonhomogeneity of a spherical vessels under pressures. *Tartu Riikl. Ülik. Toim.*, 1985, *N*° 721, 43-51 (in Russian).

Проблема периодической равнопрочности для сферических сосудов под гармонической нагрузкой

Калле Хейн и Мати Хейнлоо

Резюме

Рассматривается одномерная проблема определения рационального распределения модуля Юнга для сферического сосуда под гармонической нагрузкой. Эти распределения гарантируют выполнение условия пластичности Треска в моменты времени, когда гармоническая нагрузка достигает предельного значения. Проводится численное исследование существования решения поставленной задачи. Некоторые рациональные распределения модуля Юнга и зависимости между предельными значениями амплитуд гармонических давлений преставлены в виде графиков.

Comparative analysis of non-associated deformation law

JÜRI KIRS

Tallinn Technical University

Abstract. In this paper the exactness of non-associated deformation law is studied in comparison with Tresca yield condition accompanied by the usual associated deformation law, and also as compared with Mises yield condition

1 Introduction

In [1] a full solution of optimal design of simply supported circular plates considering the hardening of material is presented. The Mises yield condition and the associated deformation law are used. A plate is subjected to uniform dynamic pressure load, which is varying in time according to the law of triangular impulse.

In [2] a similar problem in the case of a clamped circular plates is solved by using two different methods.

In [3] the piecewise-linear yield conditions have been used to solve the problem of optimal design of circular plates considering the hardening of material. Tresca yield condition is accompanied by the non-associated deformation law, the rhombwise yield condition – by the associated deformation law.

In [4] the optimal design of annular plates considering the hardening of material is studied. Tresca yield condition and the associated deformation law are used. A number of particular cases is studied.

2 Formulation of the problem and the basic equations

I. Let us consider a circular plate, hinged by the outer boundary. The radius of the plate is R and thickness $2H$. The plate is subjected to the uniform dynamic pressure load P, which is monotonously decreasing in time according to the law of triangular impulse,

$$P = \begin{cases} P_0\,(1 - \frac{\tau}{\tau_1}); & if \;\; 0 \le \tau \le \tau_1, \\ 0; & if \;\; \tau_1 \le \tau \le \tau_f, \end{cases} \tag{1}$$

where τ –time; P_0 – prescribed constant.

In general the motion of the plate is divided into two phases . During the first phase the plate is loaded with the dynamic pressure load P, which is decreasing in time by the linear law (1) till the moment of time τ_1, when the load P will be equal to zero. A further movement of the plate takes place during the second phase $\tau > \tau_1$ because of inertia. The movement of the plate will stop at the moment $\tau = \tau_f$. However, the movement can already stop during the first phase.

We shall use the cylindrical coordinates r, φ, z. The origin of the coordinates is in the centre of the plate on the median surface. Axis $0z$ is directed downwards. We shall denote $\sigma_r \equiv \sigma_1$ and $\sigma_\varphi \equiv \sigma_2$. We shall take into consideration only plastic deformations and confine ourselves to small deflections. Besides we shall assume that displacement along r-axis is $u_r = 0$.

In [1] the problem of optimal design of such plates is solved considering the isotropic hardening of material. The function of thickness $H(r)$ is determined in such a way, that the residual deflections in the centre of the plate were as small as possible. The method of mode form motions is used. The whole volume of the plate and the lower limit of thickness are prescribed. The Mises yield condition and the associated deformation law are used. But because of the Mises yield condition the equations derived are very complicated and the process of solving them is troublesome.

To avoid all this in [3] linearized yield conditions have been used. The Tresca yield condition for the first time is here accompanied by the non-associated deformation law to solve such kind of problems. By that law the generalized strain rate vector is not perpendicular to the yield surface – to the Tresca hexagon in the above-mentioned case. That method enabled to solve

the problem very simply, but one question remained – the exactness of the method. Therefore the very purpose of this paper is just to estimate the exactness of the non-associated deformation law with Tresca yield condition. In this paper the residual deflections in the centre of the plate are determined by using three different methods: 1) non-associated deformation law with Tresca yield condition; 2) Tresca yield condition and the usual associated deformation law; 3) Mises yield condition with the associated deformation law that the exact solution proceeds from. Let us denote the residual deflections in the centre of the plate for the cases W_N, W_T and W_M correspondingly. Inequality $W_M < W_N$ conveys us not much because we must also know in addition how good is W_T approximation to the exact solution W_M. We have here several possibilities:

1) $W_M < W_T < W_N$ – in this case Tresca yield condition with usual associated deformation law gives a better approximation than non-associated deformation law.

2) $W_M < W_T << W_N$ – in this case the non-associated deformation law must be abandoned because it gives a bad approximation.

3) $W_M < W_N < W_T$ – here the non-associated deformation law should be prefered.

So it is evident that in order to estimate the exactness of that law the comparison nót with just one point, but the segment $[W_M; W_T]$ must be carried out. It is the reason why in this paper exceptionally the hardening of material is not considered – it was proved in [3] that in the case of Tresca yield condition the usual deformation law is not effective (in the model of hardening given there).

Secondly – as the purpose of this paper is not the solving of the problem of optimal design, but only estimation of exactness, the function of thickness $H(r)$ is prescribed. For the purposes of simpleness let us assume that $H = H_0 = const$ in the range of the whole plate.

II. It is convenient to use the following dimensionless quantities:

$$h = \frac{H}{H_0} = 1; \qquad x = \frac{r}{R}; \qquad t = \frac{\tau}{\tau_1};$$

$$w = \frac{W}{H_0}; \qquad m_{1,2} = \frac{M_{1,2}}{\sigma_0 H_0^2}; \qquad q = \frac{PR^2}{\sigma_0 H_0^2}; \tag{2}$$

$$\nu_{1,2} = \frac{\kappa_{1,2}R^2}{H_0\varphi}; \qquad k_{1,2} = \frac{\kappa_{1,2}R^2}{H_0}; \qquad k = \frac{\mu R^2}{\sigma_0 \tau_1^2},$$

where σ_0 – the yield point of material; μ – density; τ_1 – moment of time when the load becomes equal to zero; x – non-dimensional coordinate of the plate; w – non-dimensional deflection of a point of plate; m_1 and m_2 – non-dimensional bending moments in radial and circumferential directions; κ_1 and κ_2 – main curvatures of the plate; ν_1 and ν_2 – non-dimensional generalized main curvatures using the method of mode form motions; k_1 and k_2 – similar curvatures in general case (direct method); k - non-dimensional prescribed plate parameter.

Now the equation of motion takes the form (see [2,3])

$$\frac{d^2}{dx^2}[xm_1] - \frac{dm_2}{dx} + qx = 2khx\frac{\partial^2 w}{\partial t^2}; \tag{3}$$

where non-dimensional load is

$$q = q_0(1-t) \tag{4}$$

and where $h = 1$. In the part of research, where the method of mode form motions is used, the non-dimensional deflection in an optimal point of the plate is

$$w = \varphi(t) \cdot f(x) \tag{5}$$

and therefore the generalized main curvatures are

$$\nu_1 = -f''; \quad \nu_2 = -\frac{f'}{x}. \tag{6}$$

Here and later on an apostrophe (') denotes differentiation with respect to x, dots $(\cdot)$ denote differentiation with respect to non-dimensional time t.

The maximum plastic moment here is $m_S = M_S/\sigma_0 H_0^2 = 1$. In general case by using Mises yield condition the deflection is $w = w(x,t)$. The main curvatures in that case, k_1 and k_2, are presented in paragraph 4.

3 Solution in the case of non-associated deformation law

The equation of motion (3) can be presented in the form

$$(xm_1)' = 1 - 0.5qx^2 + 2k\ddot{\varphi} \int f(x)xdx + C_1, \tag{7}$$

where the formula (5) has been taken into consideration, and also the fact that $h = 1$. Since in the case of Tresca yield condition we use the regime of side AB from Tresca hexagon (see Fig.2), then $m_2 = m_S = 1$. The load q is presented in (4). It remains for us to determine the function $f(x)$. Let us define the function $F(x)$ so, that

$$\nu_1 = F(x)\nu_2. \tag{8}$$

If $F(x)$ were known, the function $f(x)$ could be derived easily from equation (8) considering also formulae (6).

In case of the usual associated deformation law the function $F(x)$ proceeds from the condition of perpendicularity of strain rate vector $\dot{\vec{E}}$ to yield surface (or -curve). Using Mises yield condition this situation is depicted in Figure 1.

Let us abandon now the demand of perpendicularity in case of Tresca yield condition (see Fig.2). How can we define $F(x)$ now? In other words – on the ground of which law does the angle change between the strain rate vector and yield curve ?

The idea presented in [3] lies in a proposition to determine this angle in case of Tresca yield curve (Fig.2) by using the Mises' ellips. Namely – we take the Mises' yield curve and the usual associated deformation law, and determine the dependence of that angle upon the coordinate x. We simply transfer this dependence to the case of Tresca hexagon (see Fig.2). In case of Mises condition

$$m_1^2 + m_2^2 - m_1 m_2 = m_S^2.$$

By means of associated deformation law one obtains

$$\nu_1 \, (2m_2 - m_1) = \nu_2 \, (2m_1 - m_2).$$

Defining now the function $G(x)$ so that $m_1 = G(x)m_S$ and considering (8) one can easily come to the conclusion

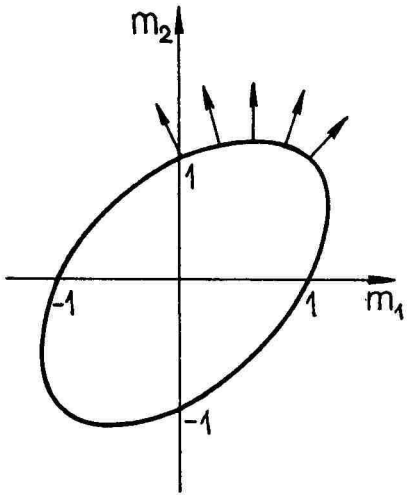

Figure 1: Mises yield condition

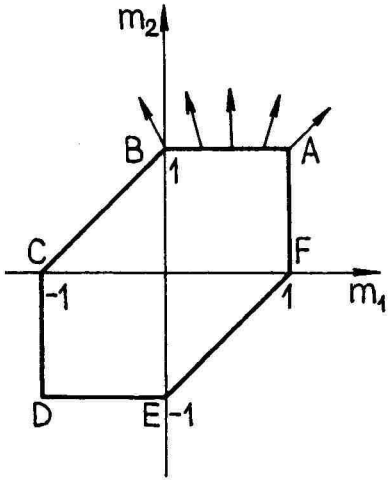

Figure 2: Tresca hexagon

$$F = \frac{2G - 1}{2 - G}. \tag{9}$$

This was used in [3]. However, since the hardening of material is not taken into account here, the situation in this paper is much easier.

As in the case of Mises' condition in the centre of the plate $\nu_1(0) = \nu_2(0)$ then considering (8) one comes to the result $F(0) = 1$. On the outer boundary $x = 1$ we have $\nu_2(1) = -2\nu_1(1)$, therefore $F(1) = -1/2$. It is evident from Figure 1 that $F(x)$ is monotously decreasing from the value $F = 1$ in the centre of the plate up to $F = -1/2$ on the edge of the plate.

Thus the function $f(x)$ must be defined in such a way that the following conditions are satisfied: 1) $f(0) = 1$; 2) $f(1) = 0$; 3) $f'(0) = 0$; 4) $\nu_1(0) = \nu_2(0) \neq 0$; 5) $\nu_2(1) = -2\nu_1(1)$; 6) $F(x)$ is a monotonously decreasing function.

Case A. Let us take the function $f(x)$ as

$$f(x) = a_0 + a_1 x + a_2 x^2 + a_3 x^n, \tag{10}$$

where $n > 2$. After satisfying all six conditions we obtain

$$f(x) = 1 - ax^2 + (a - 1)x^n, \tag{11}$$

where

$$a = \frac{n\,(2n - 1)}{(n - 2)(2n + 3)}. \tag{12}$$

Considering now the formula (11) it is easy to integrate the equation of motion (7) and deduce the expression of bending moment $m_1(x)$. The constants of integration can be determined from conditions $m(0) = 1$ and $m_1'(0) = 0$.

Considering the condition $m_1(1) = 0$ one obtains

$$\ddot{\varphi} = \frac{(q - 6)}{6k\lambda}, \tag{13}$$

where

$$\lambda = \frac{(10 - 3a)}{30} + \frac{2\,(a - 1)}{(n + 2)(n + 3)}. \tag{14}$$

If the movement will stop during the first phase ($t \leq 1$) then

$$t_f = 2\Big(1 - \frac{6}{q_0}\Big); \qquad F_M = w\Big|_{\substack{t=t_f \\ x=0}} = \frac{(q_0 - 6)^3}{9k\lambda q_0^2}, \tag{15}$$

where t_f - final time ;F_M – residual deflection in the centre of the plate.

If the movement of the plate will end during the second phase, then

$$t_f = \frac{q_0}{12}; \qquad F_M = \frac{q_0(q_0 - 8)}{288k\lambda}, \tag{16}$$

where $t_f > 1$.

Here the index of power n remains undetermined. While solving the numerical examples we assign to them many different values and compare the results and also with the exact solution in the case of Mises condition.

Case B. Let us take the function $f(x)$ as

$$f(x) = 1 - ax^2 + bx^3 + cx^4. \tag{17}$$

The above-mentioned 6 conditions are satisfied if

$$a = \frac{15 - 13c}{9}; \qquad b = \frac{6 - 22c}{9}. \tag{18}$$

Here c is a free parameter. After integration of the equation (7) we obtain in this case the formula (13), only here

$$\lambda = \frac{399 + 55c}{1890}. \tag{19}$$

Final time t_f and residual deflection F_M have the same expression as they were in (15) or (16). As we can see by these formulae – the bigger is c the bigger is λ, and the bigger is λ the smaller is F_M. From the condition $\nu_1(0) = \nu_2(0) > 0$ it proceeds that $c < 1.1538$. In the numerical examples we will take $c = 1$.

4 Direct method in the case of Mises condition

In this case we take (3) as basic equation. As regards deflection w we abandon here the method of mode form motions and take simply

$$w = w\,(x,t). \tag{20}$$

From Mises yield condition $m_1^2 + m_2^2 - m_1 m_2 = m_S^2$ we obtain by using associated deformation law that

$$\dot{k}_1(2m_2 - m_1) = \dot{k}_2(2m_1 - m_2), \tag{21}$$

where generalized main curvatures k_1 and k_2 are

$$k_1 = -w''; \qquad k_2 = -\frac{w'}{x}. \tag{22}$$

Equation (21) can be written in the form

$$v'' = \frac{v'(2m_1 - m_2)}{x\,(2m_2 - m_1)}; \qquad v = \dot{w}. \tag{23}$$

Equations (3) and (23) form just the system we have to solve. In addition to that it proceeds from Mises yield condition that

$$m_2 = \frac{1}{2}\Big(m_1 + \sqrt{4 - 3m_1^2}\Big). \tag{24}$$

After necessary alterations the basic system takes the form

$$1)\ xm'' + 1.5m'(1+s) = -q_0(1-t)x + 2kx\dot{v}; \tag{25}$$

$$2)\ xv'' = 1.5v'\Big(s - \frac{1}{3}\Big); \tag{26}$$

$$3)\ s = \frac{m}{\sqrt{4 - 3m^2}}, \tag{27}$$

where (it is simply denoted) $m_1(x,t) \equiv m(x,t)$, since later on the bending moment m_2 will not be mentioned any more.

While solving the system (25-27) one must take into consideration boundary conditions $m(0,t) = 1$, $m'(0,t) = 0$, $m(1,t) = 0$, $w(1,t) = 0$, $v(1,t) =$

$0,\ \dot{v}(1,t) = 0,\ w'(0,t) = 0,\ v'(0,t) = 0,$ and initial conditions $w(x,0) = 0, v(x,0) = 0.$

The study of the equation (25) in the centre $x = 0$ gives the following interrelation which appears to be useful

$$m''\Big|_{x=0} = 0.25\Big\{2k\dot{v}\Big|_{x=0} - q_0(1-t)\Big\}. \tag{28}$$

It is necessary to solve the system differently at the initial moment $t = 0$ since then $v = 0$ in the range of the whole plate. Taking the derivative from both side of the equation (26) we obtain

$$xu'' = 1.5u'(s - \frac{1}{3});\ \ where\ \ \dot{v} = u. \tag{29}$$

Thus, when $t = 0$, then the system we have to solve is (25), (27), (29).

To solve both systems we will substitute the derivatives with finite differences. Let us divide the plate to N parts. We simply denote the steps of variables x and t correspondingly

$$\nabla x \equiv \gamma = \frac{1}{N}; \qquad \nabla t \equiv \beta, \tag{30}$$

at which

$$x_i = i\gamma,\ \ where\ \ i = 0, 1, 2, ..., N. \tag{31}$$

In paragraph 3 we will denote from now on

$$m_{1i}^j \equiv m_i^j \equiv m\ (x_i, t_j). \tag{32}$$

Accelerations u_i^j and deflections w_i^j will be denoted in an analogical way.

Solving the system (25), (29) when $t = 0$, or system (25–26) if $t > 0$ we will attribute to index i all the values from 1 to $N - 1$. If $i = 0$, then we yet cannot solve the systems. Therefore – before we start the values of $m_0^j,\ m_1^j,\ v_0^j$ (or u_0^0), v_1^j (or u_1^0) must be prescribed. If index $i = N - 1$, then $m_N^j \equiv m\ (1, t_j)$ and $v_N^j \equiv v(1, t_j)$ are calculated (or u_N^0 when $t = 0$). So we will learn all the elements of blocks $\{m_i\}$ and $\{v_i\}$, but also the blocks $\{u_i\}$ and $\{w_i\}$. Substituting the derivatives with finite differences we will use formulae with second degree accuracy if $i = 1$ and $i = 2$, but if $i \geq 3$ then the degree of accuracy will be much higher. After the necessary changes we obtain in case of $i = 1$ and $i = 2$:

$$m_{i+1}^j = \frac{1}{(x_i + 0.75A)}\Big\{2x_i m_i^j + m_{i-1}^j(0.75A - x_i) + \\ + x_i\gamma^2(2ku_i^j - q_j)\Big\} \tag{33}$$

$$v_{i+1}^j = \frac{1}{(x_i - 0.75B)}\Big\{2x_i v_i^j + v_{i-1}^j(0.75B + x_i)\Big\}; \tag{34}$$

$$A = \gamma\,(1 + s_i^j); \qquad B = \gamma\,(s_i^j - \frac{1}{3}); \qquad s_i^j = \frac{m_i^j}{\sqrt{4 - 3(m_i^j)^2}};$$

$$q_j = q_0\,(1 - t_j). \tag{35}$$

If $i \geq 3$ then:

$$m_{i+1}^j = \frac{1}{(11x_i + 6A)}\Big\{m_i^j\,(20x_i - 9A) + m_{i-1}^j(18A - 6x_i) - \\ - m_{i-2}^j(4x_i + 3A) + m_{i-3}^j x_i + 24kx_i\gamma^2 u_i^j - 12\gamma^2 q_j x_i\Big\}; \tag{36}$$

$$v_{i+1}^j = \frac{1}{(11x_i - 6B)}\Big\{v_i^j(20x_i + 9B) - v_{i-1}^j(6x_i + 18B) + \\ + v_{i-2}^j(3B - 4x_i) + v_{i-3}^j x_i\Big\}; \tag{37}$$

If $t = 0$ then we will use the same systems, but in equations (34) and (37) the function must be substituted $v(x,t)$ by $u(x,t)$. It remains to give formulae for to calculation of accelerations u_i^j

1) If $t = 0$ $(j = 0)$ then we will take the values of u_i^j simply from the second equation ((34) or (37), using u instead of v).

2) If $j = 1$ then

$$u_i^j = \frac{2v_i^j}{\beta} - u_i^{j-1}. \tag{38}$$

3) If $j = 2$ then

$$u_i^j = \frac{2}{\beta}(v_i^j - v_i^{j-1}) - u_i^{j-1}. \tag{39}$$

4) If $j \leq 3$ then

$$u_i^j = \frac{1}{6\beta}(11v_i^j - 18v_i^{j-1} + 9v_i^{j-2} - 2v_i^{j-3}). \tag{40}$$

Deriving the equation (39) the notion of average acceleration is used. During the interval $t_{j-1} \leq t \leq t_j$ in the arbitrary point x the average acceleration is

$$\lambda_i^{j-1} \equiv (u_i^{j-1,j})_\alpha = 0.5\,(u_i^{j-1} + u_i^j).$$

But as

$$v_i^j = v_i^{j-1} + \beta\lambda_i^{j-1},$$

then we will get the formula (39). Concerning the equation (38) – it has the same origin because $v_i^0 = 0$. Calculation of displacements:

$$\begin{aligned} 1)\ w_i^0 &= 0, \quad where\ \ i = 0, 1, 1, ..., N; \\ 2)\ w_i^1 &= \beta v_i^0 + 0.5\beta^2 u_i^0 = 0.5\beta^2 u_i^0; \qquad (41) \\ 3)\ w_i^j &= w_i^{j-2} + 2\beta v_i^{j-1}, \qquad if\ \ j \geq 2. \qquad (42) \end{aligned}$$

In order to carry out the calculations it is convenient to define the following parameters:

$$\begin{aligned} 1)\ b_j &\equiv u_0^j \equiv \ddot{w}_0^j \equiv \ddot{w}(x = 0, t = t_j), \qquad (43) \\ 2)\ c_j &\equiv -(v'')_0^j \equiv -(\dot{w}'')_0^j, \qquad (44) \\ 3)\ g_j &\equiv -(u'')_0^j \equiv -(\ddot{w}'')_0^j, \qquad (45) \\ 4)\ e_j &\equiv -(m'')_0^j \equiv -m''(x = 0, t = t_j). \qquad (46) \end{aligned}$$

From the second derivative of moment m by the aid of (46)

$$m_1^j = 1 - \frac{\gamma^2 e_j}{2}, \tag{47}$$

where, considering (28)

$$e_j \equiv 0.25\,(q_j - 2kb_j); \qquad m_0^j = 1. \tag{48}$$

In analogical way

$$v_1^j = v_0^j - \frac{\gamma^2 c_j}{2}, \tag{49}$$

$$u_1^j = u_0^j - \frac{\gamma^2 g_j}{2}. \tag{50}$$

Equation (50) will be used only if $j = 0$. We must know the velocity in the centre of the plate. For this purpose the following formulae are used:

$$\begin{aligned}
&1)\ v_0^1 = 0.5\beta\,(b_0 + b_1);\\
&2)\ v_0^2 = 2\beta b_1;\\
&3)\ v_0^3 = \frac{1}{11}(6\beta b_3 + 18 v_0^2 - 9 v_0^1);\\
&4)\ v_0^j = -12\beta b_{j-2} + 8 v_0^{j-1} - 8 v_0^{j-3} + v_0^{j-4}, \quad if\ \ j \geq 4,
\end{aligned} \tag{51}$$

where, as mentioned before, the upper indexis are not power indexis, but they indicate the moment of time t_j.

It is necessary to prescribe the values of parameters b_0 and g_0 if $t = 0$; and b_j, c_j at the other moments $t > 0$. The preliminary estimates for b_0 and g_0 will be obtained by the use of formulae of non-associated deformation law. At other moments:

$$\begin{aligned}
&1)\ b_1 = b_0 - \Delta_0;\\
&2)\ b_2 = 2b_1 - b_0;\\
&3)\ b_3 = 3b_2 - 3b_1 + b_0;\\
&4)\ b_j = 4b_{j-1} - 6b_{j-2} + 4b_{j-3} - b_{j-4}; \quad if\ \ j \geq 4.
\end{aligned} \tag{52}$$

The preliminary estimate for Δ_0 will be also obtained from non-associated deformation law. The parameters c_j can be determined by the use of the following formulae:

$$
\begin{aligned}
&1)\ c_0 = 0;\\
&2)\ c_1 = \frac{2\beta}{\gamma^2}(b_0 - u_1^0);\\
&3)\ c_2 = \frac{2}{\gamma^2}(v_0^2 - v_1^2); \qquad v_0^2 = 2\beta b_1; \qquad v_1^2 = 2\beta u_1^1;\\
&4)\ c_3 = 3c_2 - 3c_1 + c_0;\\
&5)\ c_j = 4c_{j-1} - 6c_{j-2} + 4c_{j-3} - c_{j-4};\ \ if\ \ j \geq 4
\end{aligned}
\tag{53}
$$

It is necessary to mention in this occasion that the formulae (52) and (53) do not guarantee the necessary exactness. During every concrete moment of time it is necessary again and again to do the calculations anew and make the parameters more precise until the necessary exactness is reached.

5 Method of mode form motions in the case of Mises condition

Here again the interrelation (5) be valid, it means

$$w(x,t) = f(x) \cdot \varphi(t). \tag{54}$$

We will integrate the equation of motion (3) considering the formulae (54) and (24). From associated deformation law (23) followed and therefore due to (54)

$$xf'' = 1.5f'(s - \frac{1}{3}), \tag{55}$$

where s is presented by formula (27). In analogical way as in paragraph 4 we denote here also

$$f_i \equiv f(x_i); \qquad \varphi_j \equiv \varphi(t_j). \tag{56}$$

From equation of motion (3) formulae (33) and (36) will follow also in this case, only here

$$u_i^j = f_i\ddot{\varphi}_j = f_i b_j. \tag{57}$$

Instead of equations (34) and (37) we will use the following formulae:

$$1)\ f_{i+1} = \frac{1}{(x_i - 0.75B)}\Big\{2x_i f_i - f_{i-1}(x_i + 0.75B)\Big\}; \quad if\ i = 1,\ i = 2\,, \tag{58}$$

$$2)\ f_{i+1} = \frac{1}{(11x_i - 6B)}\Big\{f_i(20x_i + 9B) - f_{i-1}(6x_i + 18B) + f_{i-2}(3B - 4x_i) + x_i f_{i-3}\Big\};\ \ if\ i \geq 1\,. \tag{59}$$

Here we will define only two assisting parameters:

$$\ddot{\varphi}(t) = b; \qquad f''\Big|_{x=0} = -a. \tag{60}$$

Thus the system we have to solve is (33)+(58) if $i = 1$ and $i = 2$; and (36)+(59) if $i \geq 3$. Solving these systems we will use the following conditions: $f(0) = 1$; $f(1) = 0$; $f'(0) = 0$ and initial conditions $\varphi(0) = 0$ and $\dot{\varphi}(0) = 0$.

Here we must take into consideration that deflection

$$w_i^j = f_i \varphi_j; \qquad w_0^j = \varphi_j \tag{61}$$

and velocity

$$v_i^j = f_i \dot{\varphi}_j; \qquad v_0^j = \dot{\varphi}_j. \tag{62}$$

We will use formulae (47) and (48) also here, as regards the function $f(x)$ we have

$$f_0 = 1; \qquad f_1 = 1 - \frac{a_j \gamma^2}{2}. \tag{63}$$

It is necessary to remind here that the method of mode form motions is an approximate method. The parameter $a = a_j$ should not depend on time t, but due to this approximacy it still does depend on time to some extent. Here one must do a concession and tolerate this because we can get the results that only a little differ from the exact solution (see par. 3). Solving the system and looking for precise values of parameters a_j and b_j is much easier in this case.

The parameters b_j are determined by the use of formulae (52), for the parameters a_j we can put together analogical system. Deflection in the centre of the plate φ_j can be determined on the grounds of the following formulae:

$$\begin{aligned} 1)\ \varphi_0 &= 0; \qquad 2)\ \varphi_1 = 0.5\beta^2 b_0; \\ 3)\ \varphi_2 &= \beta^2(b_0 + b_1); \qquad 4)\ \varphi_3 = 2\varphi_2 - \varphi_1 + \beta^2 b_2; \\ 5)\ \varphi_j &= \frac{1}{11}\Big[12\beta^2 b_{j-1} + 20\varphi_{j-1} - 6\varphi_{j-2} - 4\varphi_{j-3} + \varphi_{j-4}\Big]; \end{aligned} \tag{64}$$

To calculate the rate of deflection (velocity) we will use the formulae:

$$\begin{aligned} 1)\ v_0^0 &= \dot{\varphi}_0 = 0; \qquad 2)\ v_0^1 = \dot{\varphi}_1 = 0.5\beta(b_0 + b_1); \\ 3)\ v_0^j &= \dot{\varphi}_j = 2\beta b_{j-1} + \dot{\varphi}_{j-2};\ \ if\ \ j \geq 2. \end{aligned} \tag{65}$$

6 Numerical examples, remarks and conclusions

I) At first a few words about the solution using Tresca's yield condition and usual associated deformation law. We will use the regime of side AB from Tresca's hexagon (see Fig. 2). Due to associated deformation law

$$f(x) = 1 - x. \tag{66}$$

It is quite easy to integrate the equation of motion (7) and reach equation (13), only in this case $\lambda = 1/6$. Final time t_f and residual deflection in the centre of the plate F_M are determined by the use of formulae (15) or (16), only here $\lambda = 1/6$.

II) Let us solve a few numerical examples using all beforementioned methods, it means – 1) Tresca's yield condition with usual associated deformation law. 2) Tresca's yield condition with non-associated deformation law in two occasions: a) case A with several values of index of power n, b) case B. 3) Mises's yield condition in two occasions: a) direct method, b) method of mode form motions. We will compare the results obtained.

The question is – what is exactness of solution using non-associated deformation law compared with exact solution? What is exactness compared

with Tresca's yield condition accompanied by the usual associated deformation law?

Solving the problem in cases 1 and 2 does not offer any difficulties at all. A few explanations are needed in case 3.

III) Case 3a – Mises's yield condition using direct method. The calculations are performed using formulae from parag. 3. We will begin from moment $t = 0$ when b_0 and g_0 must be prescribed. From non-associated deformation law (par. 2) preliminary estimates can be deduced

$$b_0 \approx \ddot{\varphi}(0) = \frac{q_0 - 6}{6k\lambda}; \qquad g_0 \approx -f''(0)b_0, \tag{67}$$

where λ is determined by the formula (14), $f''(0)$ by (11). After that we will calculate the values of functions u and m in two first points: $u_0^0 = b_0, m_0^0 = 1, u_1^0$ and m_1^0. Now it is easy to solve the main system up to the end when the values of index i varied from 1 to $N - 1$. So we can determine at last summary error

$$D_0 = |m_N^0| + |u_N^0|. \tag{68}$$

In the case of exact solution $m_N^0 = m(_{x=1,t=0}) = 0$ and $u_N^0 = 0$. But the solution obtained with the help of preliminary values of parameters b_0 and g_0 is not suitable because of the error D_0. Then the process of making the parameters more precise will follow. For this we will change the value of parameter b_0 in segment $[b_{01}; b_{0,2}]$ with step Δb, and parameter g_0 in segment $[g_{0,1}; g_{0,2}]$ with step Δg. This process will be repeated again and again, decreasing the steps, until summary error D_0 is suitable for us. Then we take next moment of time $t = t_1$ (it means $j = 1$). Parameters b_1 and c_1 are determined by the formulae (52) and (53) where

$$\Delta_0 \approx |\dot{\ddot{\varphi}}|\Delta t = \frac{q_0\beta}{6k\lambda}. \tag{69}$$

Now m_0^1, m_1^1, v_0^1 and v_1^1 are calculated and then the main system can be solved. Summary error is here

$$D_S = |m_N^j| + |u_N^j|. \tag{70}$$

Now the process of making b_1 and c_1 more exact will follow.

After that a nother moment of time is taken again. Succession of operations will always be the following: 1) determining the parameters b_j and c_j; 2) calculation of m_0^j; m_1^j; v_0^j; v_1^j ; 3) solving the main system and finding the summary error; 4) making the parameters more precise. In the process of precising the following formulae are used:

$$\begin{aligned} 1)\ v_0^j &= v_0^{j-1} + \frac{\beta}{12}(5b_j + 8b_{j-1} - b_{j-2}), \quad if \ \ j = 2; \\ 2)\ v_0^j &= \frac{1}{25}(12\beta b_j + 48v_0^{j-1} - 36v_0^{j-2} + 16v_0^{j-3} - 3v_0^{j-4}); \\ & \qquad if \ \ j \geq 4. \end{aligned} \tag{71}$$

The other formulae are the same as in paragraph 3.

IV) Case 3b – using the method of mode form motions in the case of Mises's yield condition. The calculations are performed using the formulae from paragraph 4. The exact value of the parameter b_0 is almost equal to the corresponding one, determined in case 3a. The preliminary estimate for parameter a is obtained from the non-associated deformation law, considering that $a = -f''(0)$. The process of calculations is very similar to the case 3a, only the main system here includes functions m and f; and the parameters are a_j and b_j. The summary error is in this case

$$D = |m_N^j| + |f_N^j|. \tag{72}$$

It is necessary to mention that the process of finding exact values of parameters a_j and b_j is much simpler than that of finding b_j and c_j in direct method.

V) Numerical examples.

1) Let $k = 1$ and $q = 10$. As we can see from table 1 the closest result to exact solution (Mises direct) will be achieved by non-associated deformation law in case B. Considering the case A – it gives a slightly worse result than in case B, but even then if $n = 3$ the result is much better than in the case of Tresca's yield condition with the usual associated deformation law. In table 1 the values of the parameter a that appears in (11) are also presented.

In table 2 the values of parameters b_j, c_j and a_j in case of Mises's yield condition at many different moments of time are presented.

In table 3 the values of deflection $w(x)$ in various points of the plate using all methods are presented.

Table 1:

#	Method		$w_f(0,t_f)$	t_f	
1	Tresca associated		0.4267	0.800	
	class	n			coeff. a
		3	0.3368	0.800	1.666666
		4	0.3246	0.800	1.272727
	Tresca	5	0.3183	0.800	1.153846
	Non- A	6	0.3145	0.800	1.100000
2	assoc.	8	0.3105	0.800	1.052632
		10	0.3085	0.800	1.032609
		∞	0.3048	0.800	1.000000
	B		0.2960	0.800	
3	Mises direct		0.2502	0.718	
4	Mises modal		0.2317	0.700	

Table 2:

t	Mises	direct	Mises	modal
	c_j	b_j	b_j	a_j
0.00	0.00000	2.8595	2.8580	3.42600
0.10	0.87225	2.0700	2.0505	3.54300
0.20	1.51700	1.2792	1.2310	3.66050
0.30	1.91300	0.4843	0.4036	3.78150
0.40	2.04200	-0.3148	-0.4339	3.90499
0.50	1.87950	-1.1199	-1.2814	4.03099
0.60	1.39900	-1.9360	-2.1368	4.15749
0.70	0.56600	-2.7729	-3.0053	4.29049
t_f	0			

Table 3:

x	Tresca assoc.	Non- n=3	asso n=4	ciated n=8	A n=∞	Non-assoc. B	Mises direct	Mises modal
0.0	0.427	0.337	0.325	0.311	0.305	0.296	0.250	0.232
0.1	0.384	0.331	0.320	0.307	0.302	0.295	0.245	0.227
0.2	0.341	0.316	0.308	0.298	0.293	0.290	0.231	0.213
0.3	0.299	0.292	0.288	0.281	0.277	0.278	0.208	0.192
0.4	0.256	0.261	0.261	0.258	0.256	0.259	0.181	0.167
0.5	0.213	0.225	0.227	0.229	0.229	0.232	0.149	0.139
0.6	0.171	0.183	0.187	0.193	0.195	0.197	0.116	0.111
0.7	0.128	0.139	0.144	0.151	0.155	0.154	0.085	0.082
0.8	0.085	0.093	0.096	0.104	0.110	0.106	0.056	0.054
0.9	0.043	0.046	0.048	0.053	0.058	0.053	0.028	0.026
1.0	0.000	0.000	0.000	0.000	0.000	0.000	0.000	0.000

The graphs of deflection are depicted in figure 3 in four cases. Line 1 corresponds to Tresca's yield condition in case of the usual associated deformation law, line 2 – to non-associated deformation law in case B, line 3 – to Mises's yield condition in direct method, line 4 – to Mises's yield condition using the method of mode form motions.

In case A of non-associated deformation law the graphs are very close to line 2, differing slightly only in the middle of the plate.

2) Let $k = 2$ and $q_0 = 18$. Residual deflections in the centre of the plate using different methods are presented in table 4. As we can see from table 4 – the non-associated deformation law in case A gives a solution equal to exact one if $n = 10$. In case B such coincidence was not achieved, but let us remind you that c was a free parameter. We ascribed to it the value 1. If we reduce the value, the coincidence will be better also in case B.

In figure 4 the graphs of deflection in 3 cases are depicted. Line 1 corresponds to non-associated defomation law in case A if $n = 10$; line 2 – to Mises's yield condition in direct method; line 3 – to Mises's yield condition using the method of mode form motions.

3) Let $k = 5$ and $q_0 = 10$. Residual deflections in the centre of the plate using various methods are as follows :

a) Tresca associated : $w_{0f} = 0.0853$

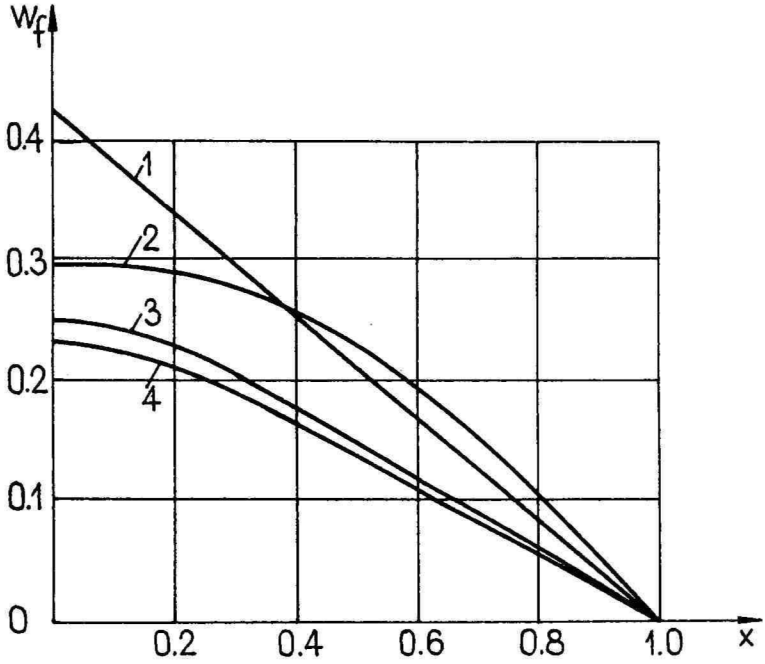

Figure 3: Deflections of the plate

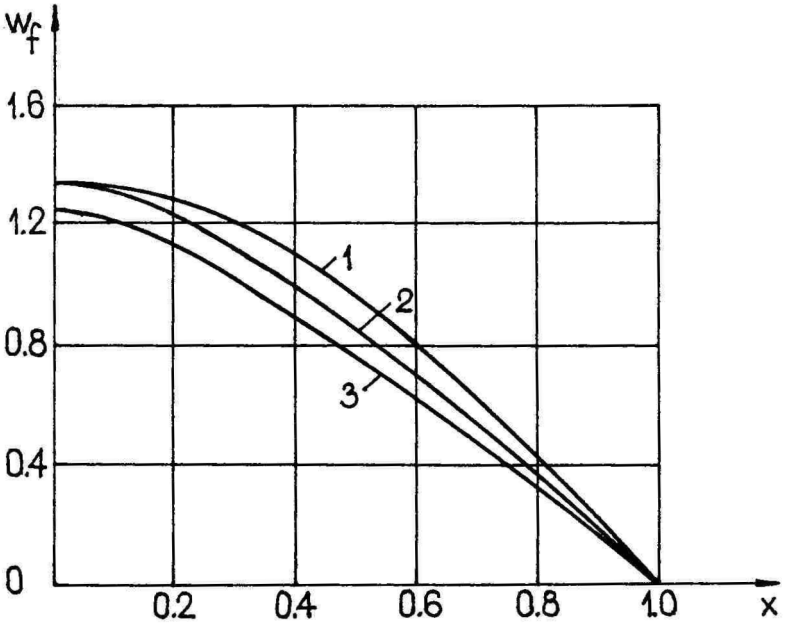

Figure 4: Deflections of the plate

Table 4:

#	Method			$w_f(0,t_f)$	t_f
1	Tresca associated			1.8750	1.500
	class		n		
2	Tresca Non-assoc	A	3	1.4803	1.500
			4	1.4266	1.500
			5	1.3986	1.500
			6	1.3821	1.500
			8	1.3645	1.500
			10	1.3558	1.500
			∞	1.3393	1.500
		B		1.3009	1.500
3	Mises direct			1.3565	1.386
4	Mises modal			1.2540	1.340

b) Non-associated A: n=3 : $w_{0f} = 0.0674$
n=4 : $w_{0f} = 0.0649$
n=6 : $w_{0f} = 0.0629$
n=10 : $w_{0f} = 0.0617$
n=∞ : $w_{0f} = 0.0610$
c) Non-associated B : $w_{0f} = 0.0592$
d) Mises direct : $w_{0f} = 0.0490$
e) Mises mode form : $w_{0f} = 0.0464$

VI) *Several conclusions*:

1) Non-associated deformation law can be used successfully to solve the problems in theory of plasticity. First – it enables to avoid very complicated equations obtained by Mises's yield condition (formulae in case of non-associated deformation law are all very simple). Secondly – it gives results having much better exactness than in case of Tresca's yield condition with the usual associated deformation law.

2) It is necessary to emphasize that the solution obtained by non-associated deformation law is not single because it depends to some extent on the function $f(x)$, chosen beforehand (though we have to admit that the differences are quite small after all). But regardless of concrete form of function $f(x)$

the results obtained are always very much better and more exact that in the case of Tresca's yield condition with usual associated deformation law.

3) Using non-associated deformation law in case of A the results obtained are a little better if the index of power (n) is big enough. If $n = \infty$ the function $f(x)$ has very simple form: $f = 1 - x^2$. As it appeared from the calculations in this case we have the results of quite good exactness. This event ($n = \infty$) can be used in the case we do not solve the problem of optimal design, but are only calculating the residual deflections. But if we still are studying the optimization problem – it is necessary to avoid the case $n = \infty$ as the shape of the plate mostly depends on main curvatures ν_1 and ν_2 . It is easy to see that in this case $\nu_1 = \nu_2 = 2$ in the whole range of the plate. It gives a completely errogneous picture of the distribution of the curvatures ν_1 and ν_2 as compared with exact solution in case of Mises's yield condition.

4) If we do not study deflection-curve $w(x)$, but only the values of function $f(x)$, then non-associated deformation law in case of A gives the best coincidence with Mises's exact solution if:

a) $k = 2$ and $q_0 = 18$ then – $n = 4$ if $t = 0$; and $n \approx 2.5$ if $t = t_f$;

b) $k = 1$ and $q_0 = 10$ then – $n = 3$ if $t = 0$; and $n \approx 2.4$ if $t = t_f$.

Case B appears to yield much worse results. Let it be noted that in the case of Mises's yield condition in direct method the function $f(x)$ was determined by the following formula

$$f(x,t) = \frac{w\,(x,t)}{w\,(0,t)}.$$

5) In the case of Mises's yield condition we can successfully use the method of mode form motions (at least in case if the pressure subjected to the plate is of small or medium quantity).

References

[1] Kirs, J., Optimal shape of a circular plate made of a work-hardening material and subjected to dynamic loading. *Prikl. Probl. Prochn. i Plastichn. Gorkii*, 1988, 72–79 (in Russian).

[2] Kirs, J., Optimal design of built-in circular plates, considering the hardening of material. *Tartu Ülik. Toim.*, 1988, 799, 97–120 (in Russian).

[3] Kirs, J., Optimal design of dynamically loaded circular plates, considering the hardening of material and piece wise linear yield curves. *Tartu Ülik. Toim.*, 1989, 853, 118–136 (in Russian).

[4] Kirs, J., Optimal design of dynamically loaded annular plates, considering the hardening of material. *Tartu Ülik. Toim.*, 1992, 939, 5–19.

Сравнительный анализ неассоцийрованного закона течения

Юри Кирс

Таллинский Технический Университет

Резюме

Шарнирно опертая круглая пластина постоянного профиля нагружена равномерно распределенной динамической нагрузкой. Задача изгиба пластины решается параллельно несколькими способами используя: 1) условие текучести Треска с обычным ассоций рованном законом течения; 2) условие текучести Треска с неассоций рованным законом течения в двух случаях — согласно уравнениям (10) и (17); 3) условие текучести Мизеса как прямым методом так и методом модальных решений. Показано, что неассоцийрованный закон течения можно успешно использовать при решении задач пластичности. С одной стороны, это дает возможность избегать очень сложных уравнений, возникающих при использовании условия текучести Мизеса. С другой стороны, получим решение задачи, точность которого намного лучше, чем при использовании условия текучести Треска с обычным ассоцийрованным законом течения. Основая идея и структура использованного неассоцийрованного закона течения дана в работе [3].

Contents